Abstract

This registration report details the design, construction and software support for a digital torsion meter capable of recording transient twist of any shaft. Graphical results are presented for the delta start transient for an induction motor driven electromechanical rig and compared to results generated by a lumped parameter model for the system. Indications of other tests that will be carried out and improvements to the software and hardware are given. It is projected that the accuracy of this device may be improved to 0.02 degrees and the signal reveal a torsional signature of the states of operation and health of a machine.

The Measurement of Twist of the Shaft of an Electromechanical Rig.

A report of the preliminary work carried out in a project to condition monitor a crankshaft of an internal conbustion engine

Author:- John T. Lenaghan

Supervisor:- G. E. Goodwin

School of Science and Engineering,
Humberside College of Higher Education,
Hull
1988

Preface

This report is written to support the backdating of registration with the CNAA. To this end, it contains details of the work completed to July 1988 and some results obtained since. A little indication is given of the ultimate direction of the work.

John T. Lenaghan
School of Engineering and Science
Humberside College of Higher Education
4th October 1988

Contents

Acknowledgements

Symbols

Chapter 1 Introduction

1.1 Introductory
1.2 Review
1.3 Overall aims
1.4 Application to other systems

Chapter 2 The torsion meter, principle of operation and execution

2.1 Principle of operation
2.2 Mathematical Theory of Operation
2.3 The construction of the discs
2.4 Flexibility in design
2.5 The signal generated and the errors associated
2.6 Driving the optoswitches and signal conditioning
2.7 The microcomputer interface Mark 1, 'User Port'
2.8 Problems and systematic errors
2.8.1 Over Twist
2.8.2 Timer Roll Over
2.8.3 Variable Interrupt Latency
2.9 Limitations of the system (BBC microcomputer)
2.9.1 Frequency of measurements
2.9.2 Accuracy of time measurement
2.10 Improvements - Mark II and beyond
2.10.1 Transfer to a 32 bit RISC microcomputer
2.10.2 Mark II interface
2.11 Data Processing, Daps
getbits {recovery of the data}
daterror {compensation for faults}
process {calculation of the velocity and twist}
ratios {scaling factors for the coding strip}

CHAPTER 3 The Development Rig, Nature and Model

3.1 The Development Rig
3.2 The components of the development rig
3.3 The Model
3.3.1 The induction motor
3.3.2 The transmission chain
3.3.2.1 Motor to Drive Shaft

Chapter 3 continued...

3.3.2.2 Drive Shaft to Pulley
3.3.2.3 The belt transmission
Speed loss
Torque loss
Global slip
Model Equations
3.3.3 DC generator
3.4 The rig model coefficients and parameters
3.5 The Model Equations in Summary
3.6 Computer solution of the model
3.7 The computer control of the rig
3.7.1 Three Phase Supply Control
3.7.2 Generator Load
3.7.3 Software Control

Chapter 4 Outline of experimentation

4.1 The start up transient
4.2 Other tests

Chapter 5 The Results, Graphs from the Meter and Model

5.1 Comparison between the experimental and theoretical
5.2 Errors demonstrated by the time domain graphs
5.2.1 Faithless recording of low speed transients
5.2.2 Zones of doubt and sensitivity
5.2.3 Variable interrupt servicing
5.3 Frequency domain graphs

Chapter 6 Concluding discussion

Appendix 1 Selected Routines in Pascal Code

Figures, Circuits and Graphs

Figure 1, Code disc location
Figure 2, Code disc construction
Figure 3, Light signal
Figure 4, Signal Compensation
Figure 5, Interrupt Servicing
Figure 6, Flow of information
Figure 7, Over twist of the encoder
Figure 8, Photograph of rig
Figure 9, Schematic of rig
Figure 10, Belt and pulleys
Figure 11, Star/delta connection of motor
General flow diagram of acquis
Flow of information

Circuit 1 - Opto-switch to TTL interface
Circuit 2 - Thyristor firing circuit
Circuit 3 - Firing circuit computer interface
Circuit 4 - GTO controlled generator loading
Circuit 5 - GTO computer interface

Graph 1: Velocity - raw data

No error detection and the minimum of calculation to reveal the velocity

Graph 2: Velocity - no timer rollover

The routines for the detection and correction are applied to the data for graph 1

Graph 3: Velocity - as previous and no over-twist

The routines for the detection and correction of over twist are applied to the data

Graph 4: Velocity - as previous and encoding disc compensation

The routine for generating the scaling factors is applied to the data and those factors are used in the subsequent processing

Graph 5: Velocity - Model

The velocity of the rig during the start up over the same period as the measurements

Graph 6: Zones of doubt

The areas of the graphs where interrupt latency interferes with the accuracy of the measurements

Graph 7:Angular Displacement - Raw Data

Graph 8:Angular Displacement - no timer rollover

Graph 9:Angular Displacement - as previous and no over twist

Graph 10:Angular Displacement - as previous and disc compensation

Graph 11:Angular Displacement - Model

Graph 12:Frequency analysis - velocity, of the uniform

Graph 13:Frequency analysis - velocity section twist, uniform velocity section

Graph 14:Verification of model - acceleration, motor, model

Graph 15:Verification of model - acceleration, motor, experiment

Graph 16:Verification of model - velocity, motor, model

Graph 17:Verification of model - velocity, motor, experiment

Graph 18:Verification of model - current, motor, model

Graph 19:Verification of model - current, motor, experiment

Graph 20:Verification of model - current, generator, model

Graph 21:Verification of model - current, generator, experiment

Acknowledgements

In the work to date a number of people have made my task a little lighter to whom I am indebted. I express my thanks to John Evans, the former head of the School of Engineering who had the faith to take me on, Gerry Goodwin who has guided my work with a welcome perspective and George Corfield who has steered this course to registration. I also owe much thanks to the technical staff of the college for building much of the equipment, namely Jim Ashcroft, Peter Hale, John Newdic and Brain Goodare who retired during the course of the work.

This work has been funded by a special initiative grant of the National Advisory Board and carried out within the precincts and under the auspices of Humberside College of Higher Education.

Symbols

a angular acceleration

c compliance of the belt transmission
coefficient of the frictional torque acting on the rotor

D d/dt

E Young's modulus for the belt

f{t} function relating angular displacement to the time after start

f_r function for the r^{th} state variable of lumped parameter model

F tension in the belt arms
Suffices
t taut arm
s slack arm

g{θ} the inverse function of f{t}

G rotational inductance of the generator
intermediate results used for Runge-Kutta algorithm
Suffices
r,n 1=<r=<4, 1=<n=<number of variables

H iteration interval of the Runge-Kutta algorithm

i current in an equivalent circuit of the motor or generator
Suffices
1,...,6 full model of motor
x1,y1 two coil model - stator
x2,y2 - " - - rotor
D,Q D-Q model stator
d,q - " - rotor

{i} current vector for the motor
Suffices
3ph three phase vector
2ph two phase vector

I moment of inertia
Suffices
1 motor rotor, coupling and half shaft
2 coupling and pulley
3 generator and pulley
currents in generator
Suffices
A armature coils
F field coils

k integer count of the number of transitions
scaling factors for the compensation of strips
Suffices
1 for the velocity measurement
2 for the torsion measurement
stiffness
SH shaft
b belt

M mutual inductance between coils of the motor
Suffices
u,v 0<u,v<7, u<>v
full motor model
m D-Q model, mean level

L self inductance of coils
Suffices
1,...,6 full motor model

n_S number of transitions per revolution at which measurements are taken

r resistance of coils
Suffices
1,...,6 full motor model

R resistance of various components
Suffices
L generator load
R rotor bars
S stator coils
radius of pulleys

θ angular displacement
Suffices
1 general
2
MS motor end of shaft
SP pulley end of shaft
G generator

t time elapsed

Suffices

1 interval of encoder period

2 time between transitions at shaft ends

T torque

Suffices

B transmitted by belt

diff loss of torque across the belts

f1 frictional torque on motor

f2 frictional torque on generator

G generator load torque

M motor torque (airgap)

PG torque on the generator due to belt

pre initial tension of belt

v phase voltages across motor

Suffices

1,...,6 full model

angular velocity

x_r r^{th} state variable of lumped parameter model

ω mains supply angular frequency

μ coefficient of friction between belt and pulley

φ angle of contact between belt and pulley

Chapter 1

Introduction

1.1 Introductory

> "The need to measure accurately the torque, or torsion moment, in a shaft, ... has exercised the ingenuity of engineers for many years."[1]

Ford and Douglas wrote this to introduce their paper in 1949, aware of the fifty years of development that had preceded. In the forty years since yet more sensitive and accurate meters applying the currently available technologies have been built. This research is not to develop yet another torque meter, but to monitor the twist by a method that will allow application to a number of rotating structures and generate signals to indicate the states of operation and health.

The research began as a study into the feasibility of condition monitoring a crankshaft while in service, it was taken that the feasibility would be proven by the development of such a technique. This technique would measure the torsion induced in the shaft due to the torque transmitted and be able to pick out transients and characteristic twisting vibrations.

---

[1] Ford, Hugh and Douglas, Alan; "The measurement of torque in shafts"; **Engineering;** 27/5/1949; pp 481 - 484, 505 - 507

There are many uses for such a technique, however, the initial stages are being carried out on an electro-mechanical rig. This is to verify the developed technique against previous results and theory.

1.2 Review

Many methods exist to measure the torque and power output of a prime mover. For example, some monitor a standard section of the transmission system[2]. There are other systems developed more recently that will monitor the torsional vibrations of a rotor by laser techniques[3].

The former usually require access for attachments to the transmission chain or even a standard section to be inserted, changing the characteristics of the measured system. The latter technique can only monitor the velocity at one point from which the torsional vibration

---

[2] Ingham, A. J.; "Torque measuring systems. Measurement Measurement from rotating shafts, associated electronics and calibration methods"; **Industrial Sensors seminar;** Advanced manufacturing techniques, demonstration held at Regional electronics centre, University of Hull; 23/6/88

[3] Eastwood, P. G. and Halliwell, N. A.; "Laser-based measurement of torsional vibration"; **SPIE Optics in Engineering Management 599;** 1985; pp 358 - 366
ibid, "Laser Technology for Condition Monitoring"; **COMADEM 88;** Eds. Raj Rao and Anthony Hope; Conference at Birmingham Polytechnic; 19-21/9/88; pp 154 - 159

has to be deduced.

Recent work from the Hitachi industrial laboratories measure the torque and power output by the mathematical inference from measurement of speed and the theoretical knowledge of the particular prime movers[4]. This technique - state observer - has the limitation that there must be considerable a priori knowledge of the prime mover and the system of which it is a part.

1.3 . Overall aims

It is intended that the monitoring technique described below can give information about the particular system that is as yet not possible to measure, and this measurement may be carried out in a way that does not affect the characteristics of the rig. Also that the observation of the system is independent of knowledge of the system, like the signals obtained from an accelerometer.

The first stage of the project, the stage reported

---

[4]Ohmae, Tsutomu; Matsuda, Toshihiko; Kanno, Minoru; Saito, Keiji and Sukegawa, Takashi; "A Microprocessor-Based Motor Speed regulator Using Fast-Response State Observer for Reduction of Torsion Vibration"; **IEEE Trans. Industry Applications IA-23 (5);** September/October 1987; pp 863 - 871

here, is to develop a monitoring technique. This includes analysis of the technique's limitations and methods of deducing the state of the system from the measurement of torsion (and any prerequisite measurements).

Also reported here is the development of the test rig mathematical model which was used in the first stages to verify the results of the measurement technique.

The principle exploited and tested on this rig is that of described by Pratt[5]. The main difference being the use of the newer microcomputers to carry out the processing and display. This report deals with the development of this on the drive shaft and the necessary computer software to support it.

The ideas that form the basis of the research are, in summary:-

> A version of the angle of twist detector that is supported by a microcomputer to allow sophisticated analysis of its measurements,

---

[5]Pratt, Jr, George W. and McMullin, Paul G.; "Opto-electronic apparatus to generate a pulse modulated signal indicative of the state of health of the mechanical state of a system"; **United States Patent 3871215;** granted 18/3/1975.
Pratt, Jr, George W.; "An Opto-Electronic Torquemeter for Engine Control"; **Society of Automotive Engineers SAE paper 750070;** 2/1976.

A dynamic model of the system that faithfully follows torsion transients.

1.4 Application to other systems

When torque is transmitted through a rotating shaft, then the resulting twist along the shaft may be measured. By the nature of the opto-electronics used the meter is particularly non-invasive, that is it does not require alteration of the system measured other than suitable optical tracks to be attached to the transmission train and access made for the light beam. This system is useful in areas of limited space. By this, it is possible to use the system on any torque transmitting shaft.

CHAPTER 2

The torsion meter, principle of operation and execution

2.1 Principle of operation

When any shaft is transmitting power, the torque twists that shaft. This meter measures this twist by determining the ratio between the time for two marks of known angular displacement at one end of the shaft to pass a reference point and the time between the first mark mentioned above and a similar mark at the other end of the shaft. The first interval is inversely proportional to the angular velocity. The second interval gives a measure of the power if the marks are initially coincident. Hence their ratio reveals the twist.

If this operation is carried out frequently within a revolution and the times are measured accurately then the time history of the velocity, power and twist of the shaft may be displayed in detail. The mathematics supporting this method and its accuracy and sensitivity are worked out below.

A note on terminology; the interval which reveals the velocity is referred to as the 'period', and that which reveals the power, the 'interval'.

2.2 Mathematical Theory of Operation

The period of the signal, t_1, is used to measure the average angular velocity over that particular interval.

$$D\theta = \left(\frac{1}{t_1}\right)\frac{2\pi}{n_S}. \tag{2.1}$$

The displacement between the two code discs is given by

$$(\theta_2 - \theta_1) = \left(\frac{t_2}{t_1}\right)\frac{2\pi}{n_S}, \tag{2.2}$$

The above formulae are necessarily approximations. Usually it is taken that angular displacement is a function of time:

$$\theta = f\{t\} \tag{2.3}$$

and

$$D\theta = Df\{t\}. \tag{2.4}$$

But for the purposes of this analysis it is more convenient to take the inverse function, g say,

$$t = g\{\theta\} \tag{2.5}$$

and

$$^{d}/_{d\theta}\{t\} = g'\{\theta\} = t'. \tag{2.6}$$

This is to allow advantage to be taken of the fixed angle over which the measurements would be taken. But strictly the following analysis is only certain for unidirectional rotation.

The time for one period from one of the coding discs is,

$$t_1 = \int_{2\pi k/n_S}^{2\pi(k+1)/n_S} t' d\theta, \tag{2.7}$$

$$= g\{2\pi(k+1)/n_S\} - g\{2\pi k/n_S\}. \tag{2.8}$$

This gives rise to the Taylor expansion,

$$t_1 = g'\{2\pi k/n_S\}(2\pi/n_S) + {}^1/_2 g''\{2\pi k/n_S\}(2\pi/n_S) + \ldots \tag{2.9}$$

The first term gives the equation (2.1) with

$D\theta = 1/g'$

and and error due to the series truncation of the order of the series' second term (if the series is convergent).

Similarly for the twist, the time between successive leading edges is given by

$$t_2 = \int_0^{2\pi k/n_S} h' d\theta - \int_0^{2\pi k/n_S} g' d\theta, \tag{2.10}$$

where h is the angle function of time for the other end of the shaft. Integrating out and using the following expansion

$$t_2 = h\{2\pi k/n_S\} - g\{2\pi k/n_S\} + g\{0\} - h\{0\}, \tag{2.11}$$

defining g(0),h(0) as 0,

$$h\{2\pi k/n_S\}=g\{2\pi k/n_S\}+g'\{2\pi k/n_S\}(\theta_2-\theta_1) + {}^1/_2 g''\{2\pi k/n_S\}(\theta_2-\theta_1)^2+... \quad (2.12)$$

From (2.11) and (2.12)

$$t_2= g'\{2\pi k/n_S\}(\theta_2-\theta_1). \quad (2.13)$$

From which (2.2) follows and the error due to the approximation is of the order of the third term of (2.12). The value for g' that is used in this evaluation is worked out from equation (2.1). This gives a cumulative error of

$${}^1/_2|g''\{2\pi k/n_S\}|[(2\pi/n_S)^4+(\theta_2-\theta_1)^4]^{1/2}. \quad (2.14)$$

For most measurements the twist is less than $2\pi/n_S$ then the total error has an upper bound of

$${}^1/_2|g''\{2\pi k/n_S\}|(2\pi/n_S)^2. \quad (2.15)$$

This requires an upper bound on the second derivative of time by angle to give an error independent of the functional relationship between time and angle. This derivative may be expressed in terms of angular velocity and acceleration.

If v is the angular velocity and a is the angular acceleration then

$$\frac{d^2t}{d\theta^2} = -\frac{a}{v^3} \quad (2.16)$$

2.3 The construction of the discs

The encoding discs used on this rig are of ABS plastic cut to a circumference of 480mm and mounted on each end coupling of the drive shaft[6]. To the outside edge of each disc is fixed a photographic strip of equally long black and white zones.

Each zone is 12mm long giving a total of twenty black/white transitions at equal angular intervals around the disc. To improve contrast the photographic film is mounted on an aluminium foil tape attached to the disc[7].

2.4 Flexibility in design

The dimensions of the rig and early techniques developed to mark the discs constrained the discs to a circumference of 480 mm. This was to allow them to be constructed easily. However, there is little constraint on the size that they might be in a final apparatus.

The use of photographic techniques allows a shorter strip with finer divisions up to the resolution of the interface system.

---

[6]See Figure 1, Code disc location
[7]See Figure 2, Code disc construction

2.5 The signal generated and the errors associated

The signal processed by the computer is derived from the changes in reflectivity at the discs' edges. Considering the reflectivity at one point above the edge of each of the discs gives a signal[8] which does not follow the perfection of the above equations.

The errors induced into the mathematical analysis by the real system stem from the imperfect nature of the production of the strips. The formulae assume that the transition occur at precisely $2\pi/n_S$ radian intervals about the circumference of the discs. This is not the case. The place of transition may in practice vary from its theoretical location by +/-0.25mm on the surface.

However, any errors in the measurement due to this misalignment of the coding strips will be reflected in the measurements as a periodic variation over each revolution. This periodic variation may be compensated for by the use of scaling factors that are tuned to each zone length between transitions. This is achieved by running the discs at a constant speed and at a constant displacement and comparing the times for each transition with that calculated from the period of one revolution.

---

[8]See Figure 3, Light signal

For the signal that is used for the velocity measurement[9]:

$$t_1^1+t_1^2+ \ldots +t_1^N=T \tag{2.17}$$

where N is the number of transitions in one revolution and T is the period of that revolution

So for each scaling factor K_1^i,

$$K_1^i t_1^i=T/N \tag{2.18}$$

Similarly for the measurement of twist each period of the original signal giving the interval is given by

$$t_2^{i+1}-t_2^i+t_1^i. \tag{2.19}$$

When the appropriate scaling factors are included,

$$K_2^{i+1}t_2^{i+1}-K_2^i t_2^i+K_1^i t_1^i=T/N \tag{2.20}$$

From equation (2.18) this reduces to the ratio,

$$t_2^{i+1}/t_2^i=K_2^i/K_2^{i+1} \tag{2.21}$$

The scaling factors of all times, t_2, bear this ratio to each other. It is then defined that

$$K_2=1 \text{ if } t_2=T/N \tag{2.22}$$

and all other factors are scaled to this. This reduces the fluctuations in the raw data before processing to a residual level which is indistinguishable from other sources of error.

---

[9]See Figure 4, Signal Compensation

2.6 Driving the optoswitches and signal conditioning

This is a description of the Mark 1 interface circuit that drives the reflective opto-switches[10] interfaces the signals to the general interface port of the BBC microcomputer's (including the Archimedes) usually termed the 'User Port'. A diagram of the circuit is displayed in Circuit 1. The signals from the transistor follow the changes in the reflected light intensity from the surface moving beneath it. The rest of the circuit compensates for the ramped change in the signal with a second transistor and conditions it to TTL levels with a chain of Schmitt triggers.

2.7 The microcomputer interface Mark 1, 'User Port'

The information from the rig consists of an electrical signal. The computer has to turn this signal into bytes of information.

The interface and communications from the rig were developed on a BBC microcomputer Master system and upgraded to an Acorn Archimedes. However, this first system employs the 'User Port' of these computers in the

---

[10] RS Reflective Optoswitch part no 307-913; Data sheet 4276 3/3/87

same active way. The algorithm and use of the supporting component of this first interface are discussed.

Some of the draw backs in terms of the limitations and errors in data resulting from the use of this interface are outlined.

A 6522 VIA supports the User PORT. The features that are particularly used by the conversion process are:-

A) The generation of interrupt signals to the system CPU on active edges on signals applied to its control lines and

B) Two general purpose timers which may generate interrupts after a preset time interval

To trace the signal through the computer system and the software developed, let us consider just one transition at the opto-switch. A leading edge appears on one of the control lines to the VIA.

The internal registers of this chip would have been set to allow an interrupt to be sent to the CPU.

The microprocessor detects the interrupt status, leaves its current program and carries out an interrupt

service routine[11], chosen on the basis of the VIA status. The routine for clearing the interrupt due to a leading edge on the control line is chosen. This routine not only clears the interrupt but also reads a timer and passes this value into memory and resets the timer for the next leading edge. Thereby the period of the signal on the control line is turned into bytes.

This mechanism is expanded upon to give the data used by the processing program. The general flow diagrams[12] for the data acquisition routines, 'Acquis' outline the approach in more detail.

Acquis interprets the signals into two groups of bytes by the process above and stores them to an inter-program buffer for use in a processing program, 'Daps' which finally gives the rig velocity and shaft encoders' relative displacement[13].

2.8 Problems and systematic errors

There are two main hardware related errors generated by the interface as set up. One is concerned with the

---

[11] See Figure 5, Interrupt servicing (adapted from Opie, Colin; **Interfacing the BBC Microcomputer**; McGraw-Hill; 1984)

[12] The flow diagrams may be found towards the end of the document

[13] See Figure 6, Flow of information

limit on the displacement measured to an eighteen degree arc and the other is due to the method by which the timers are read.

2.8.1 Over Twist

The encoding discs are given a displacement of between four and nine degrees for the two reasons:-

i)...to allow the recording of twists in the direction reverse to the direction of motion of the shaft,

ii)..to prevent the interrupt due to the start of the period from disc A coinciding with the interrupt for the next leading edge when there is zero or near zero twist.

If the twist on the shaft is more than the length of a black and white zone (or the arc remaining after the displacement mentioned above) then the leading edge of the signal from marking the end of t_2 would come after the next leading edge for the end of the period[14].

The acquisition routines copes with is problem by waiting to measure an interrupt of the correct nature. That is, if it has just processed and interrupt to start the period and interval timers then it will not use another interrupt from that source until it receives one

[14]Figure 7, Over twist of the encoder

that signals the end of the interval. The times transferred to the processing program refer to a double period.

2.8.2 Timer Roll Over

An error arises when reading the 16 bit wide timer eight bits at a time. The timer is not stopped when it is read and it takes a finite time to read even half of the clock. To illustrate that this in certain circumstances is a problem, consider a timer reading at the interrupt, in hexadecimal:-

FD02,

the least significant byte, 02 is read into one of the CPU registers. This takes three microseconds, in which time the timer now reads:-

FCFF

as it counts down. The most significant byte, FC is now read. When the read value of the timer is sent to memory it would be recorded as:-

FC02

precisely 256 (decimal) off the true value at the event. It is not possible for the acquisition program to guard against this. The time is sent as read to Daps, which corrects for these errors.

2.8.3 Variable Interrupt Latency

A final error is due to the microcoding of the CPU used in microcomputers. There is a small variation in the times for the servicing due to the time taken to first detect the signal, the CPU only checks for the IRQ at the end of each machine code instruction the delay in detection may be from zero to two microseconds. This change in delay is reflected in the times read.

2.9 Limitations of the system (BBC microcomputer)

2.9.1 Frequency of measurements

The processing time limits the frequency of interrupts the system can handle hence limits the frequency of the signals. This limitation constrains the number of transitions marked on each of the encoding discs. The processing times for the service routines in Acquis when running on a BBC Master series microcomputer are given in the table below.

	T1	T2	CB1	CB2
O.S	13.0	13.0	13.0	13.0
entry	23.0	25.0	26.0	28.0
service	09.5	20.5	40.5	23.0
other	-	-	28.5	28.5
exit	07.5	07.5	07.5	07.5
TOTAL	53.0	66.0	115.5	72.0

where O.S. refers to the time for the operating system to pass the control to the service routines.

'entry' is the time to decide on the particular service routine.

'service' is the time for clearing the condition and carrying out some specific action.

'other' in the case of the CB1 and 2 routines is the time to send the received data to the main memory.

'exit' the time taken to resume the interrupted activity.

T1, 2 and CB1, 2 refer to the source of the interrupt in the VIA.

The maximum frequency of interrupts that the computer can cope with is given by the sum of the CB1, CB2 service times and time for addition initial detection, that is:

191.5 microseconds.

The maximum frequency that may be dealt with is

10.4 kHz.

Acquis places the data from the interface into the inter-program buffer when the CPU is not otherwise occupied by interrupts. The time required for complete transfer of data collected is

321 microseconds.

The time that must be allowed for processing is

435.25 microseconds.

This leads to the maximum frequency of interrupts for

complete transfer of

2.3 kHz.

A combined frequency 2KHz is the maximum practicable to allow management of the buffers.

2.9.2 Accuracy of time measurement

With the BBC microcomputer the timers are clock at 1Mhz. There is a limit of one clock pulse on the accuracy of measurement of the times. This is a fixed absolute error, particular to the system, of 1 microsecond. As the periods and interval decrease in length with increasing speed the relative error also increases.

Some digital velocimeters employ algorithms to reduce the relative error by the extension of the periods of measurement.[15] This approach is not open to the current approach as it reduces the frequency of measurements. The next section details improvements which reduce this absolute error.

When dealing with a signal from a strip made of 20 black/white zones travelling at 1500 rpm, these residual

---

[15] Bonnert, Richard; "Digital Tachometer with Fast Dynamic Response Implemented by a Microprocessor"; **IEEE Trans Industry Applications IA-19 (6);** November/December 1983; pp 1052 - 1056

errors are: for the Master series computers variation in

latency 0-4 us

clock 1 us

accuracy 0.8% (0.16 degrees)

It should be noted that the latency and clock periods are fixed so the accuracy will improve for a particular system when measuring at a lower velocity and correspondingly worsen at greater velocities.

2.10 Improvements - Mark II and beyond

2.10.1 Transfer to a 32 bit RISC microcomputer

With the introduction of a low cost 32 bit RISC based microcomputer from Acorn, the Archimedes, the opportunity was taken to transfer the developed software to this faster environment. A table above details the processing times for the routines of Acquis. On adapting certain routines the processing times within software have been reduced to one tenth that listed. This left enough time for Daps to operate in real time even though it currently operates in interpreted Basic V.

The 'User Port' supplied with this computer uses timers that are clocked at 2Mhz. This reduces the absolute error in the time measurements to 500 nanoseconds.

To illustrate the limits of the hardware used: when dealing with a signal from a strip made of 20 black/white zones travelling at 1500 rpm, these residual errors are: for the Archimedes variation in

latency	3.5-22.5 processor cycles 2.375 us	
clock	0.5 us	
accuracy	0.3%	(0.04 degrees)

(Compare with the intervals for the Master given in the previous section)

2.10.2 Mark II interface

A large portion of Acquis is devoted to the manipulation of various registers within the VIA to generate the times. It is proposed that most of these algorithms may successfully be transferred to hardwired logic, with the times presented to the CPU directly on its data bus. Circuit 2 is a schematic diagram of part of the circuit.

The advantages of this interface are the elimination of errors in reading due to variable interrupt latency, the reduction in processing time per signal and the reduction of the absolute error in the measurements (by the use of a clock frequency >10MHz).

Using the illustration at the end of the previous

section, the error in measurements of twist will be 0.03% (0.004 degrees)

2.11 Data Processing, Daps

There are four routines that deal with the collection of data, the correction for hardware faults and the final processing to velocity and shaft torsion.

These procedures are named (in this report):-

```
getbits    {recovery of the data}
daterror   {compensation for faults}
process    {calculation of the velocity and twist}
ratios     {scaling factors for the coding strip}
```

Except for ratios, every set of data has to be passed through these routines in turn to be processed. They incorporate the algorithms described above. An interpretation in Pascal is given in Appendix 1.

getbits

This routine recovers the raw data stored by the acquisition program, acquis, in the inter-program buffer convert them to integer times[16]. There are considerable differences between Master and Archimedes versions because of the differences in the memory mapping and routines in Acquis. A Pascal version of this and its

---

[16] A flow diagram for the Master version is given with the flow diagrams

subprocedures are given[17] although in practice machine code is used for speed.

daterror

There are a number of systematic errors introduced into the collected data by the present interface that this routine is designed to detect and correct. These have been detailed in earlier sections.

These errors are detected by this routine in the same way. Four point rolling averages of the periods, t_1, and intervals, t_2, are maintained by another routine process. Against the averages each new set of data is tested.

If there is an error due to the over twist of the shaft during measurement then the period measured would be approximately twice that of immediately before. The period is halved and time lapsed are corrected and processing continues.

If over twist continues more than one period the interval would be much less than the average. If it falls to below one eighth of the previous value it is modified by adding the previous period. The following Pascal code

---

[17]Appendix 1, getbits

illustrates the principle elements of this routine.

```
if sample<oldsample[1]/8 then
     sample:=sample+oldperiod[1];
if (period>1.8*AVperiod) and (period<2.2*AVperiod)
     then
     begin
          period:=period/2;
          runtime:=runtime+period
     end;
```

The ranges on the period are to bracket the differences in the times of the periods due to changes in speed. If the interval measured, the value of sample, is greater than one eighth of the previous measured it is taken as a true reading not subject to errors. By this method no correction is required when the shaft returns to the normal range of measurement.

```
if period>AVperiod+150 then period:=period-256;
if sample>AVsample+150 then sample:=sample-256;
```

These last two conditions of daterror detect the clock rollovers while reading. When either the period or interval (sample) are longer than the previous average by some large figure then they are reduced appropriately. The limit is set at 150 microseconds longer than the previous time because of the variation in speed and the coding disc strips but to allow the detection of the majority of these data faults.

process

This updates the points used in the four point rolling averages and recalculates them. The rig angular velocity and code disc displacement are calculated from equations (4.1) and (4.2). For graphical output the time derived from the accumulated periods is updated. This time represents the time within the sample of data, runtime, and is used to end the iteration loop.

ratios

This routine sets up the values for the scaling factors for the individual zones of the coding discs. Unlike the above mentioned routines this does not lie in the main iteration loop of daps although it does call on their services. To calculate the factors, the routine follows equations (2.18),(2.21),(2.22)[18].

---

[18]See Appendix 1; procedure ratios

CHAPTER 3

The Development Rig, Nature and Model

3.1 The Development Rig

The test rig on which the monitoring technique has been developed is described. It will be used for further work into the nature of transients within induction motor drive systems.

The list of components below is not intended to be exhaustive but describe the principle configuration of the test bed during the stage of the work reported[19].

3.2 The components of the development rig

Induction Motor

Brook Motors Ltd

3 phase induction motor	R10-A31910
Speed	1440 rpm.
Coil Voltage	400/440V
Coil Current	6A
Frequency	50Hz
Output Shaft	1.25" dia.
Number of rotor bars	51
Number of stator teeth	36

Transmission Chain

Bearings	Fenners Ltd	
	RHP 1020-20 Self aligning	
Shaft	Mild Steel	20mm dia.
Pulleys	Fenners Ltd	
	SPZ type	Cat No. 03120243
	Dia.	180mm
	Bush	No.2021
Belt	Fenners Ltd	
	SPZ 1800 680 for	140/140

---

[19] See Figure 8, Photograph of the rig and Figure 9, a schematic diagram of the same.

DC Generator
Higgs Motors of Witton
Model W1033-1
Originally wired in compound mode
Now with
a separately excited field

3.3 The Model

The model consists of a system of first order ordinary differential equations for each part of the rig which are solved by the Runge-Kutta algorithm[20] by computer. Each part of the model is separately discussed.

3.3.1 The induction motor[21]

The standard presentation of the electrical equations for a three phase induction machine involve a six by six matrix connecting the voltages and currents in the three phases for stator and rotor. The elements of the matrix are differential coefficients with time.

$$\begin{Bmatrix} v \\ v^1 \\ v^2 \\ v^3 \\ v^4 \\ v^5 \\ 6 \end{Bmatrix} = \begin{vmatrix} r + DL & DM & DM & DM & DM & DM \\ DM^{1} & r + DL & DM^{13} & DM^{14} & DM^{15} & DM^{16} \\ DM^{21} & DM^{2} & r + DL & DM^{24} & DM^{25} & DM^{26} \\ DM^{31} & DM^{32} & DM^{3} & r + DL & DM^{35} & DM^{36} \\ DM^{41} & DM^{42} & DM^{43} & DM^{4} & r + DL & DM^{46} \\ DM^{51} & DM^{52} & DM^{53} & DM^{54} & DM^{5} & r + DL \\ 61 & 62 & 63 & 64 & 65 & 6 \quad 6 \end{vmatrix} * \begin{Bmatrix} i \\ i^1 \\ i^2 \\ i^3 \\ i^4 \\ i^5 \\ 6 \end{Bmatrix} \quad (3.1)$$

---

[20] Thomas, Benku; "The Runge-Kutta Methods"; **BYTE**; 4/1986; pp 191 - 210.

[21] Jones, Charles V.; **The Unified Theory of Electrical Machines**; Butterworth; 1967

(3.1) may readily be deduced from the equivalent circuit of the induction motor but in this state it is cumbersome to solve. Jones[21] offers transformations that will reduce the number of equations in the special case of balanced supply. It is his model that is adapted for the prime mover.

$$\{i_{3ph}\}=[C_A]\{i_{2ph}\}, \tag{3.2}$$

where $[C_A]$ is the transformation matrix from the three phase currents, $\{i_{3ph}\}$ to the resolved equivalent currents of a two phase machine, $\{i_{2ph}\}$. The transformation is square so the two phase current vector has six components of which two are zero one for the rotor system and the other for the stator. By analysis it is found that the matrix is:

$$[C_A] = \begin{vmatrix} B & 0 \\ 0 & B \end{vmatrix}$$

$$\text{where} \quad B = \begin{vmatrix} (2/3)^{1/2} & 0 & 0 \\ -(1/6)^{1/2} & (1/2)^{1/2} & 0 \\ -(1/6)^{1/2} & -(1/2)^{1/2} & 0 \end{vmatrix}. \tag{3.3}$$

With the transformation:

$$\{Z_{2ph}\}=[C_A]^T\{Z_{3ph}\}, \tag{3.4}$$

and dropping the zero rows and columns one obtains:

$$\begin{Bmatrix} v_{x1} \\ v_{y1} \\ v_{x2} \\ v_{y2} \end{Bmatrix} = \begin{vmatrix} R_1+DL_1 & 0 & MD\cos\theta & MD\sin\theta \\ 0 & R_1+DL_1 & -MD\sin\theta & MD\cos\theta \\ MD\cos\theta & -MD\sin\theta & R_2+DL_2 & 0 \\ MD\sin\theta & MD\cos\theta & 0 & R_2+DL_2 \end{vmatrix} * \{i_{2ph}\}, \tag{3.5}$$

where {v} are the voltages across the stator and rotor of the equivalent two phase machine and M is and equivalent mutual inductance between windings (or bars).

The equations are still non-linear as they contain terms that depend on the angular position of the rotor with respect to the stator, θ which depends on time.

$$[C_B] = \begin{vmatrix} 1 & 0 & 0 & 0 \\ 0 & 1 & 0 & 0 \\ 0 & 0 & \sin\omega t & \cos\omega t \\ 0 & 0 & \cos\omega t & \sin\omega t \end{vmatrix}, \qquad (3.6)$$

where ω is the rotor angular velocity and t the time.

On applying $[C_B]$:

$$\begin{Bmatrix} v_S \\ v_D \\ 0 \\ 0 \end{Bmatrix} = \begin{vmatrix} R_S + L_S D & 0 & 0 & MD \\ 0 & R_S + L_S D & MD & 0 \\ -M\omega & M\dot{\theta} & R_R + L_R D & -L_R\omega \\ MD & M\omega & L_R\omega & R_R + L_R D \end{vmatrix} * \begin{Bmatrix} i_S \\ i_D \\ i_q \\ i_d \end{Bmatrix}, \qquad (3.7)$$

The motor air gap torque is given by:

$$T = (1/2)\{i\}^T (d/d\theta)[L,M]\{i\} \qquad (3.8)$$

Transforming {i} with $[C_A]$ and $[C_B]$ to give the d-q currents then (3.8) becomes:

$$T = (1/2)\{i_{dq}\}^T [C_B]^T [C_A]^T (d/d\theta)[L,M][C_A][C_B]\{i_{dq}\}. \qquad (3.9)$$

From Jones[21], $(d/d\theta)[L,M]$ is

$$-M_m \begin{vmatrix} 0 & 0 & 0 & \sin\theta & \sin\theta & \sin\theta \\ 0 & 0 & 0 & \sin\theta & \sin\theta^2 & \sin\theta^3 \\ 0 & 0 & 0 & \sin\theta^4 & \sin\theta^2 & \sin\theta^2 \\ \sin\theta & \sin\theta & \sin\theta & 0 & 0 & 0 \\ \sin\theta & \sin\theta^4 & \sin\theta^2 & 0 & 0 & 0 \\ \sin\theta^2 & \sin\theta^3 & \sin\theta^4 & 0 & 0 & 0 \end{vmatrix}$$

where $\theta_2 = \theta + 2\pi/3$
$\theta_4 = \theta + 4\pi/3$
M_m is the mean value of the measured mutual inductance.

(3.10)

On substituting into (3.9):

$$T_M = M(i_q i_D + i_d i_Q)$$

where M is the value taken for the mutual inductance.

(3.11)

The currents for this equation are obtained from the d-q model given in equation (3.7) suitably manipulated to make the derivatives of current explicit, ready for numerical integration.

$$\begin{Bmatrix} Di_D \\ Di_Q \\ Di_q \\ Di_d \end{Bmatrix} = \frac{1}{(L_1 L_2 - M^2)} \left\{ \begin{Bmatrix} L_2 v_D \\ L_2 v_Q \\ -M v_q \\ -M v_d \end{Bmatrix} + \begin{bmatrix} -L_2 R_S & M^2\omega & ML_2\omega & MR_R \\ -M^2\omega & -L_2 R_S & MR_R & -ML_2\omega \\ ML_1\omega & MR_S & -L_1 R_R & L_1 L_2 \omega \\ MR_S & -ML_1\omega & -L_1 L_2 \omega & -L_1 R_R \end{bmatrix} * \begin{Bmatrix} i_D \\ i_Q \\ i_q \\ i_d \end{Bmatrix} \right\}.$$

(3.12)

3.3.2 The transmission chain

3.3.2.1 Motor to Drive Shaft

The drive shaft is assumed to be isotropic and homogeneous therefore is given a characteristic constant scalar torsional stiffness. The torque applied to the shaft causes an angular displacement of its ends, a twist, in reaction. This is

$$T_{SH} = K_{SH}(\theta_{SP} - \theta_{SM}).$$

(3.11)

The frictional and windage torques for the drive

shaft and the motor rotor are lumped and measured together. A cubic approximation angular velocity is used to model this drag.

$$T_{f1} = c_1 + c_2 D\theta + c_3 (D\theta)^2 + c_4 (D\theta)^3 \qquad (3.12)$$

The equation governing the motion at the motor to shaft coupling, hence the velocity of the motor's rotor and the displacement of this end of the shaft is:-

$$D^2\theta_{SM} = (T_M - T_{SH} - T_{f1})/I_1. \qquad (3.13)$$

3.3.2.2 Drive Shaft to Pulley

Similar to the above the equation of motion of the pulley end of the shaft is given by

$$D^2\theta_{SP} = (T_{SH} - T_B)/I_2. \qquad (3.14)$$

3.3.2.3 The belt transmission[22]

This requires a different approach from the shaft transmission. A satisfactory has been derived from a consideration of three aspects of the belt's behaviour.

(i) The fractional speed loss between the pulleys; due to the normal slipping of the belt against the pulley surfaces while transmitting torque.

(ii) Torque loss - the difference in the torque applied at the driving pulley and that sensed at

---

[22] A diagram of the belt and pulley is provided to help comprehension. Figure 10.

the following. this is taken as due to the frictional losses at the belts entry and exit points to the pulleys.

(iii) The global slip limit - The point at which the belt ceases to transmit torque in proportion to that applied because it slides over the entire surface of one or other pulley.

The model makes assumptions about the belt and pulley system that have been demonstrated to be inaccurate by Cowburn[23]. The model is not an accurate portrayal of the belts but gives a simulation of the transmission characteristics when embedded in the larger model. The short periods over which the model is solved allow the following approximations.

Creep theory[24], where the belt is replaced by a thin elastic member passed over flat pulleys, is the basis of the model. The effects that are considered the most import to model are detailed below.

Speed loss

The elastic belt stretches in proportion to the

---

[23]Cowburn, David; **The mechanical performance of automotive V-belts;** PhD. Thesis, University of Bradford; 1984

[24]Gerbert, B. G.; "Force and slip behaviour in V-belts"; **Acta Polytechnica Scandinavia** Mechanical Engineering Series No. 67; 1972

tension set up within it. However, when transmitting torque there is a difference between the tensions in the two arms of the belt. This difference causes a torques on the pulleys in reaction. Hence the belt arms are in different states of extension.

As the belt travels over the driving pulley it relaxes against the dynamic friction provided by the pulley surface. This friction supports the difference in tensions and the reaction torque. The change in extension causes the belt to have an exit speed lower than the pulley's circumference. This process is reversed on the following pulley.

In normal operation, the belt does not globally slip against the pulleys' surfaces. There is at least one point on each pulley where the belt is held by static friction and moves at the same speed as the surface. This point is at (or near) the first place of contact of belt and pulley in the direction of the belt velocity. The slack arm of belt is travelling faster than the following pulley and the taut arm slower than the driving pulley. The following pulley has the drive pulley's belt exit speed and vice versa. So an output shaft rotates at a lower velocity than the input shaft. This is the speed loss.

Other effects operate on speed loss, the next most important being the radial compliance of the belt allowing it to ride out of the "V" groove used on this rig.

From Cowburn[23],

$$(D\theta_{GP}-D\theta_{SP})/D\theta_{SP} = q\{F_t-F_s\}, \quad (3.15)$$

$$q = (1/c + g/R). \quad (3.16)$$

Torque loss

There is some loss of the transmitted torque due to some slipping at the entry and exit points where the belt is accelerated to the shape of the pulley, not all of the bending moment required at entry is recovered at exit. The balance is torque lost in friction. These and other effects are estimated to be, by Cowburn[23]:

$$T_{diff} = 0.01\{1+0.33\ln[10^5 EI/R^4 k]\}(F_t+F_s)R$$

for $\mu \leq 0.4$,

for $\mu > 0.4$ substitute 0.4 for μ. (3.17)

The torque loss acts to reduce the torque in the belt seen by the following pulley only and does not reduce the torque acting on the belt by the driving pulley.

Global slip

The belt slips with no point fixed relative to the pulley surface when the ratio of the tensions in each

arm exceeds the limit given by the capstan formula:-

$$F_t/F_s =< T_{pre}\exp(\mu/\varphi). \qquad (3.18)$$

This may reduced to:-

$$(F_t-F_s)_{max} = 2T_{pre}\tanh\{\mu/2\varphi\}, \qquad (3.19)$$

where $(F_t-F_s)_{max}$ is the greatest difference in tensions tenable between the two belt's arms before global slippage.

Model Equations

From equation (3.19), the difference in tensions may be written explicitly dependent on the instantaneous angular speeds of the driving and following,

$$(F_t-F_s)_{max}=\{1/q\}*\{D\theta_{dp} - D\theta_{fd}\}/(|D\theta_{dp}|), \qquad (3.20)$$

3.3.3 DC generator

Following the analysis given by Jones, the torque supplied by the generator when loaded is given by

$$T_G= D\theta_G(n_G G|_F|_A+K|_A), \qquad (3.21)$$

with a correction for the remnant flux.

This torque acts with the torque applied from the pulley on the inertia for the generator rotor resulting in an angular acceleration,

$$D^2\theta_G = (T_{PG} - T_G - T_{f2})/I_3, \qquad (3.22)$$

where T_{f2} is the frictional torque formulated similarly to equation (3.12).

3.4 The rig model coefficients and parameters

The detailed testing of the parameters for use within the model is described by the references for the model. The methods used follow Jones[21] and Cowburn[23].

Induction motor

Electrical parameters

V_S	420	volts
R	4.5	ohms
L	0.597	henrys
M	0.565	henrys
Number poles	2	

Mechanical parameters

I_1	0.0421	kgm^2

for T_{f1}

c_1	2.86×10^{-3}
c_2	3.78×10^{-3}
c_3	-1.62×10^{-3}
c_4	3.47×10^{-3}

Shaft and Belt transmission

K_{SH}	525	radians$N^{-1}m^{-1}$
R	0.09	m
K_b	1.28×10^5	Nm^{-1}
I_2	0.0382	kgm^2

DC generator

Electrical parameters

V_B	neglected
K	0.14
Gn_G	5.21
R_A	1.25
No. poles	1
I_F	0.25 amps

Mechanical parameters

I_3	0.2239	kgm^2

for T_{f2}

c_5	5.73×10^{-3}
c_6	1.30×10^{-4}
c_7	2.56×10^{-3}
c_8	-7.84×10^{-4}
μ	1.4

3.5 The Model Equations in Summary

$$T_M = M(i_q i_D + i_d i_Q),$$

where M is the value taken for the mutual inductance. (3.11)

$$\begin{Bmatrix} Di_D \\ Di_Q \\ Di_q \\ Di_d \end{Bmatrix} = \frac{1}{(L_1 L_2 - M^2)} \begin{bmatrix} \{L_2 v_D\} & \vert -L_2 R_S & M^2\omega & ML_2\omega & MR_R & \vert & \{i_D\} \\ \vert L_2 v_Q \vert + & \vert -M^2\omega & -L_2 R_S & MR_R & -ML_2\omega & \vert \cdot & \vert i_Q \vert \\ \vert -Mv_q \vert & \vert ML_1\omega & MR_S & -L_1 R_R & L_1 L_2 \omega & \vert & \vert i_q \vert \\ \{-Mv_d\} & \vert MR_S & -ML_1\omega & -L_1 L_2 \omega & -L_1 R_R & \vert & \{i_d\} \end{bmatrix}$$

(3.12)

$$T_{SH} = k_{SH}(\theta_{SP} - \theta_{SM}).$$

(3.11)

$$T_{f1} = c_1 + c_2 D\theta + c_3 (D\theta)^2 + c_4 (D\theta)^3.$$

(3.12)

$$D^2\theta_{SM} = (T_M - T_{SH} - T_{f1})/I_1.$$

(3.13)

$$D^2\theta_{SP} = (T_{SH} - T_B)/I_2.$$

(3.14)

$$DT = 0.01 \{1 + 0.33 \ln[10^5 EI/R^4 K_i]\}(F_t + F_s)R,$$

for $\mu \leq 0.4$,

for $\mu > 0.4$ substitute 0.4 for μ.

$$(F_t - F_s)_{max} = \{1/q\} * \{D\theta_{dp} - D\theta_{fd}\}/(\vert D\theta_{dp} \vert).$$

(3.20)

$$(F_t - F_s)_{max} = 2T_{pre} \tanh\{\mu/2\varphi\}.$$

(3.19)

$$D^2\theta_G = (T_{PG} - T_G - T_{f2})/I_3.$$

(3.22)

3.6 Computer solution of the model

The equations in section 3.3 are solved by a fourth order Runge-Kutta technique.

$$G_{1,r}=Hf_r(t, \quad x_1, \quad x_2, \quad \ldots, x_n)$$
$$G_{2,r}=Hf_r(t+H/2, \quad x_1+G_{1,1}/2, \quad x_2+G_{1,2}/2, \quad \ldots, x_n+G_{1,n}/2)$$
$$G_{3,r}=Hf_r(t+H/2, \quad x_1+G_{2,1}/2, \quad x_2+G_{2,2}/2, \quad \ldots, x_n+G_{2,n}/2)$$
$$G_{4,r}=Hf_r(t+H, \quad x_1+G_{3,1}, \quad x_2+G_{3,2}, \quad \ldots, x_n+G_{3,n})$$

and

$$x_r(\text{at } T+H)=x_r+[G_{r,1}+2\{G_{2,r}+G_{3,r}\}+G_{4,r}]/6,$$

where f_r is the equation of the differential coefficient of x_r in terms of the state variables and time.[25]

3.7 The computer control of the rig

Experiments will be carried out on the states of twist that occur normally and due to 'faults' such as start-up, star-delta switching, fast bus transfer and various types of loading conditions. For repeatability and flexibility the switching of the rig is controlled by thyristors signalled by computer.

3.7.1 Three Phase Supply Control

The induction motor has two configurations of its stator windings to the three phases of the supply. These are 'star' and 'delta'. The thyristor control is able to

---

[25] Fully anotated flow diagrams are displayed in the appendices listings for the Acorn BBC Master Turbo are available in BASIC IV and ISO-Pascal, a listing in BASIC V and ARM assembler for the Acorn Archimedes is also available

effect these two configurations and allow switching from one to the other[26]. The selection a particular configuration and switching transients reduces to that of the control of the sets of thyristors for each phase. This control is provided by the firing circuits and the signals sent to the same from the computer interface[27].

3.7.2 Generator Load

Experiments highlight the effects of loading variations on the angle of twist. The load on the generator is set by microcomputer by switching gate turn off thyristors (GTOs) that lie in parallel resistive circuits loading the generator armature[28]. The resistances are chosen to draw from 0 to 15.75 amperes from the generator in steps of 0.25A. The control of the GTOs is carried out by an interfaced firing circuit[29].

3.7.3 Software Control

Control of the motor switching and loading of the generator is written for the Archimedes only which has the capability of interacting in real time while

---

[26] See Figure 11, Star/Delta windings of an induction motor

[27] See Circuits 2, The thyristor firing circuit; and 3, The computer interface.

[28] See Circuit 4, Load the DC generator

[29] See Circuit 6, Interface to computer.

collecting data. All routines are written in RISC assembler code in the form of operating system primitives in a 'relocatable module'[30] to be used in higher level programs.

[30] Acorn Computers, **Archimedes Progrmmer's Guide**, 1988

Chapter 4

Outline of experimentation

The experiments carried out on the rig described above have two aims: the development of the software and mechanism of the twist detector to retrieve better grades of information and the analysis of the effects of the various modes of operation of the rig in terms of the state of twist of the transmission shaft. These two aims coincide in the goal of continuous monitoring of this system from the twist signals.

4.1 The start up transient

This transient, which generates some of the severe torsional vibrations, is used to configure the torsion meter and the supporting software.

The initial results are compared to the expected result from the time domain model of the rig. Any differences are carefully noted and the software inspected and improved.

4.2 Other tests

To discover parameters that distinguish between different transient and continuous modes of the system operation records will be taken of the state of twist for each of the cases. These will be analysed in both time

and frequency domains for significant identifying features.

Comparisons will be made with the models to determine the nature of the parameters discovered.

Chapter 5

The Results, Graphs from the Meter and Model

Below are the results obtained from the torsion meter and the models of the rig. These are intended to be a clear example of the meter's capabilities by a comparison of the values obtained with the theoretically predicted.

These results have been collected by the Mark I interface on a BBC Master microcomputer.

The final sections of the chapter explain the nature of the errors that are corrected by and remain after the current data processing.

5.1 Comparison between the experimental and theoretical[31]

A visual inspection of the closeness of fit between the model and the experimental results.

A number of the electrical and mechanical aspects of the rig were monitored to gauge the accuracy of the lumped parameter model. These are presented as graphs 14 to 21 and represent the unloaded and electromagnetically loaded start up transient.

---

[31] The graphs are drawn after the other figures

5.2 Errors demonstrated by the time domain graphs

5.2.1 Faithless recording of low speed transients

The frequency resolution of the encoding discs is directly proportional to the speed. At full speed each encoding disc samples the velocity at approximately 500Hz. This gives a maximum transient frequency of 250Hz recorded. However, at low speeds, 100rpm, the fastest recorded transient frequency becomes 17Hz. The resonant frequency of the rig is about 22Hz, as is seen in the graphs. Compare Graphs 10 and 11. The first three cycles of twist are lost and the vibration is not clear until the encoding discs speed up.

5.2.2 Zones of doubt and sensitivity.

There are two zones at the top and bottom of the angular displacement graphs where the system would have to cope with the simultaneous arrival of two interrupts. Due to the interrupt latency the computer fails to record accurate data. The inaccuracy stems from the nature of the timers. In the period between the VIA issuing and the CPU acknowledging an IRQ the timer continues to count down. This problem will be discussed at length in Chapter 7. It is this extension to the time recorded that causes the zones because the CPU would be delayed due to the immediately previous IRQ.

5.2.3 Variable interrupt servicing

This is a delay of between 0 and 4 microseconds on top of the time recorded due to the normal latency. The calculated error on the displacement record +/- 0.08 degrees.

The width of the variation in the tail of the displacement Graph 10 is measured at 0.15 degrees. It is proposed that this variation is due entirely to the variable delay in the interrupt service.

5.3 Frequency domain graphs

Only a limited amount of analysis of the frequency domains of the velocity and twist signals has been carried out.[32] The fast Fourier algorithm demonstrates the limitation of the system by the Nyquist frequency to approximately 250Hz. This constraint is due to the use of 20 transitions per revolution for measurement.

Some significant components and there harmonics are apparent from the graph. These have been identified in frequency but have not been related sources in the rig or the processing.

---

[32] See graphs 12 and 13

5.2.3 Variable interrupt servicing

This is a delay of between 0 and 4 microseconds on top of the time recorded due to the normal latency. The calculated error on the displacement record +/- 0.08 degrees.

The width of the variation in the tail of the displacement Graph 10 is measured at 0.15 degrees. It is proposed that this variation is due entirely to the variable delay in the interrupt service.

5.3 Frequency domain graphs

Only a limited amount of analysis of the frequency domains of the velocity and twist signals has been carried out.[32] The fast Fourier algorithm demonstrates the limitation of the system by the Nyquist frequency to approximately 250Hz. This constraint is due to the use of 20 transitions per revolution for measurement.

Some significant components and there harmonics are apparent from the graph. These have been identified in frequency but have not been related sources in the rig or the processing.

---

[32] See graphs 12 and 13

Chapter 6

Concluding discussion

Even at this stage when much experimentation and analysis needs yet to be completed, signals, after elementary processing, are generated from the twist of the shaft that are sufficient sensitive and accurate for the purpose of deducing the state of the machine. There are strong indications that the frequency analysis will reveal a signature that gives indication of the torque signature and the mechanical transfer to the detector.

As mentioned these conclusions are as yet poorly founded and the remainder of the work will develop the technique and explore the signals from the rig under different operating conditions.

The work is expected to be continued to explore the application of this technique to more general and complex structures, for example a crankshaft.

The basis of the thesis for the degree of Doctor of Philosophy will be developed from data collected from a crankshaft. There will be an exploration of the feasibility to determine the operating condition of an internal combustion engine by the signals from an encoder, as described here, attached to is crankshaft.

Appendix 1

Selected Routines in Pascal Cc

```
procedure getbits;
{recover data from the sideways ram for processing}
constsraccess=66;
osword  =&fff1;
type word = 0..65535;
fudgerec = packed record
                case boolean of
                false: (addr:^byte);
                true : (int :word )
                end;

var dummy:integer;

function peek(address:word):byte;
{emulates PEEK to inspect a memory location
from Acornsoft guide to ISO-Pascal on BBC microcomputer}
var fudge:fudgerec;
     begin
          fudge.int:=address;
          peek:=fudge.addr^
     end{peek};

function samplereturn:integer;{turn data into an integer}
var databyte, datavalue, j:integer;
     begin
     datavalue:=0;
     for j:=0 to 2 do
         begin
         databyte:=((-peek(data+j)-1)
                              + 256)MOD &100;
         datavalue:=(datavalue)*256
                              +databyte;
         end;
     samplereturn:=datavalue;
     end{samplereturn};

procedure bits;{get data from sideways ram}
var dummy:integer;
     begin
     params[9]:=readsample mod &100;
     params[10]:=(readsample div &100) mod &100;
     dummy:=code1(osword,sraccess,params);
```

```
      number:=number+1;
      readsample:=readsample+3;
end;{bits}

      begin{body of getbits}
      bits;
      period:=samplereturn/1E6;
      bits;
      sample:=samplereturn/1E6;
      if (number=2)and(sample>period) then
      begin
            period:=sample;
            bits;
            sample:=samplereturn/1e6
      end;
end;{getbits}


procedure ratios;
var i,j:integer;
begin
      for i:=0 to 1
      begin
            for j:=0 to 20
            begin
                  zone[i,j]:=0;
                  if ratiob then zone[i,j]=1;
            end;
      end;
      if ratiob then
      begin
            readsample:=12000;
            repeat
            begin
                  for i:=1 to 20
                  begin
                        getbits;
                        daterror;
                        process;
                        zone[0,0]:=zone[0,0]+period;
                        zone[0,i]:=zone[0,i]+period;
                        zone[1,0]:=zone[0,1]+sample;
                        zone[1,i]:=zone[1,i]+sample;
                  end;
            end
            until readsample>=36000;
            for i:=0 to 20
            begin
                  zone[0,i]=zone[0,i]/zone[0,0]/5
                  zone[1,i]=zone[1,i]/zone[1,0]/5
```

```
            end;
            readsample:=0
            numberofsamples:=0 .
      end;
end{ratios};


procedure daterror;
{compensates for some hardware errors}
begin
if number>20 then
      begin
      if sample<oldsample[1]/8 then
            sample:=sample+oldperiod[1];
      if (period>1.6*AVperiod) and (period<2.2*AVperiod)
            then
            begin
                  period:=period/2;
                  runtime:=runtime
            end;
      if period>AVperiod+150 then period:=period-256;
      if sample>AVsample+150 then sample:=sample-256;
end;{daterror}


procedure process;
{turn the integer times into velocity and twist}
var j:integer;
begin
      if ratiob else
      begin
            sample:=sample*zone[1,
                  (numberofsamples/2+offset)mod20 +1]
            period:=period*zone[0,
                  (numberofsamples/2+offset)mod20 +1]
      end;
      for j:=3 downto 1 do
      begin
            oldsamples[j+1]:=oldsamples[j];
            AVsample       :=AVsample+oldsamples[j];
            oldperiods[j+1]:=oldperiods[j];
            AVperiod       :=AVperiod+oldperiods[j]
      end;
      oldsamples[1]:=sample;
      oldperiods[1]:=period;
      AVsample:=(AVsample+sample)/4;
      AVperiod:=(AVperiod+period)/4;
      if AVprocB then
      begin
            period:=AVperiod;
```

```
            sample:=AVsample
        end;
        velocity:=60/period/stripe;
        runtime:=runtime+period;
        twist:=sample/period
end;{process}
```

Figure 1, Code disc location

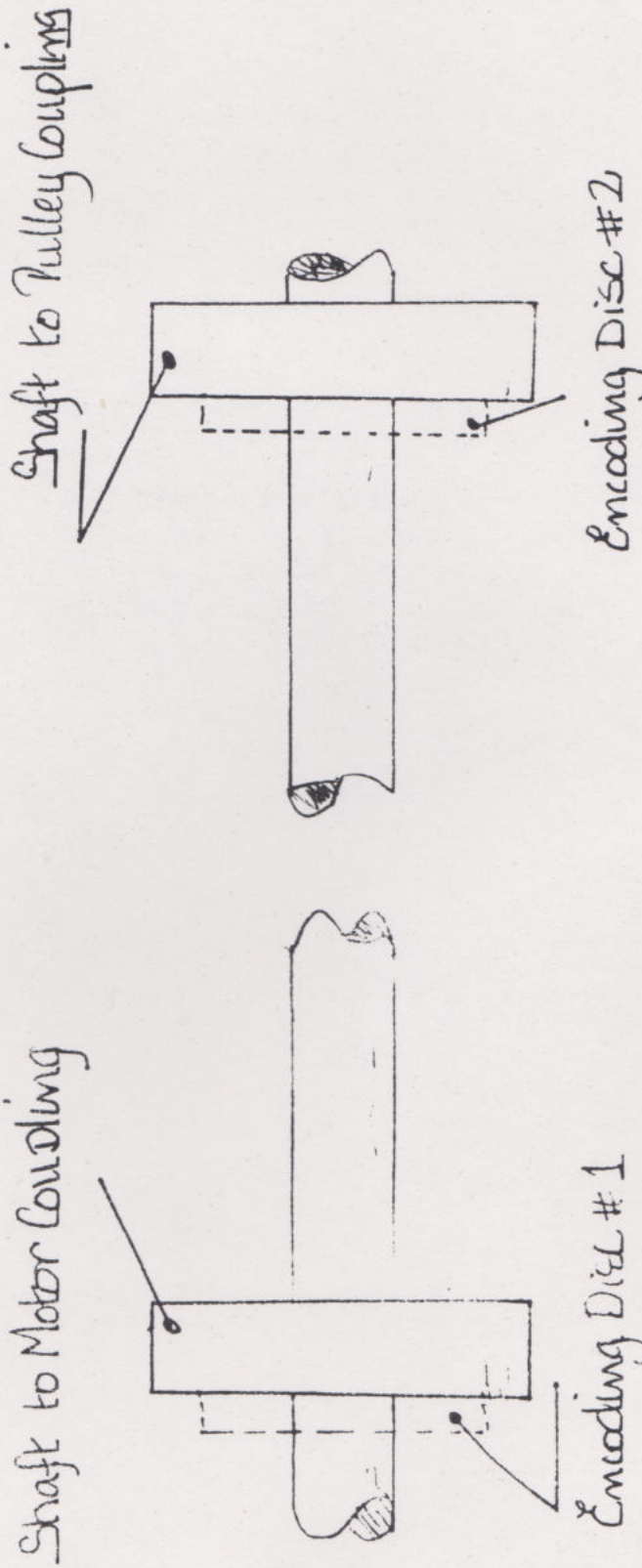

Figure 2, Code disc construction

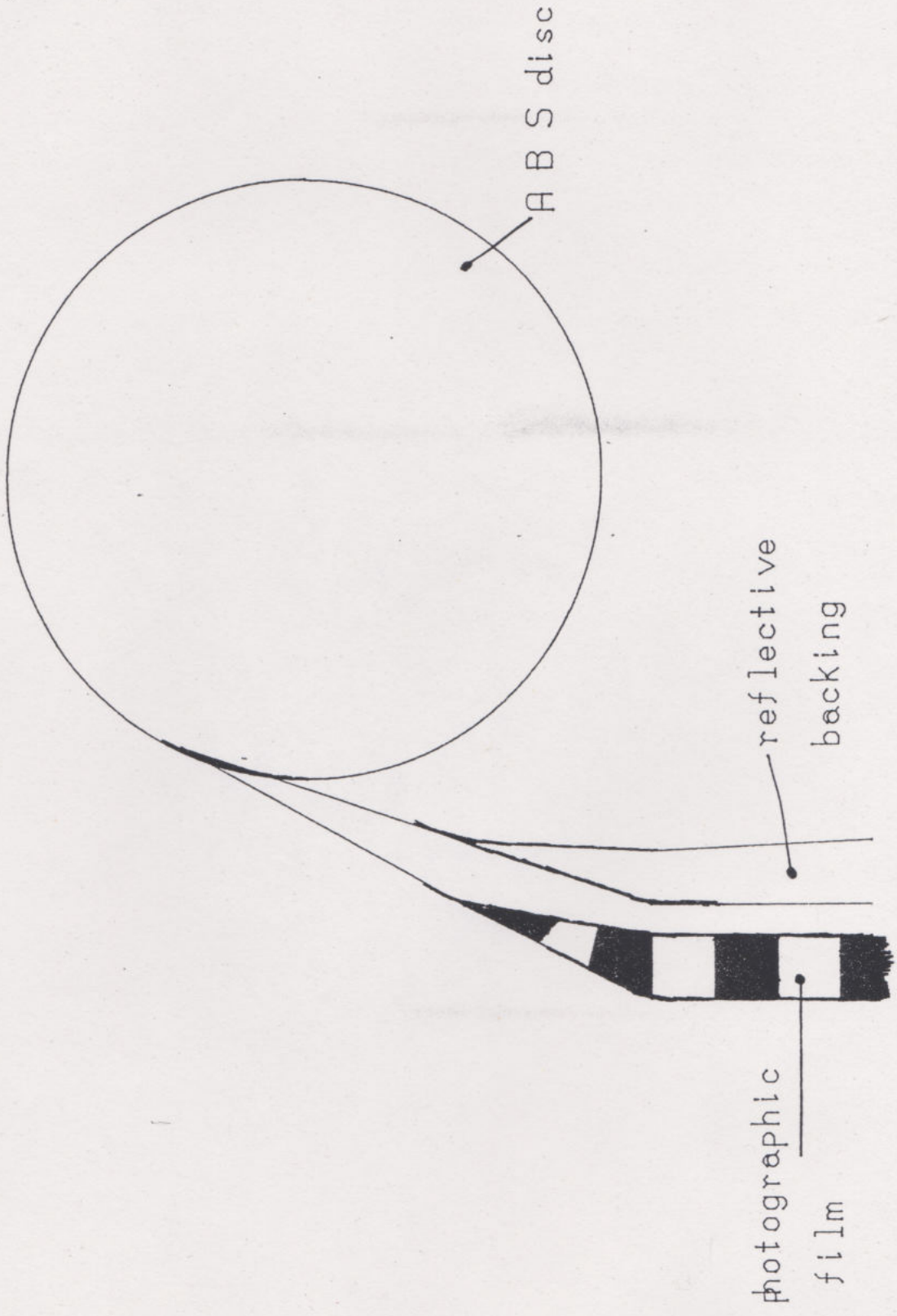

Figure 3, Light signal

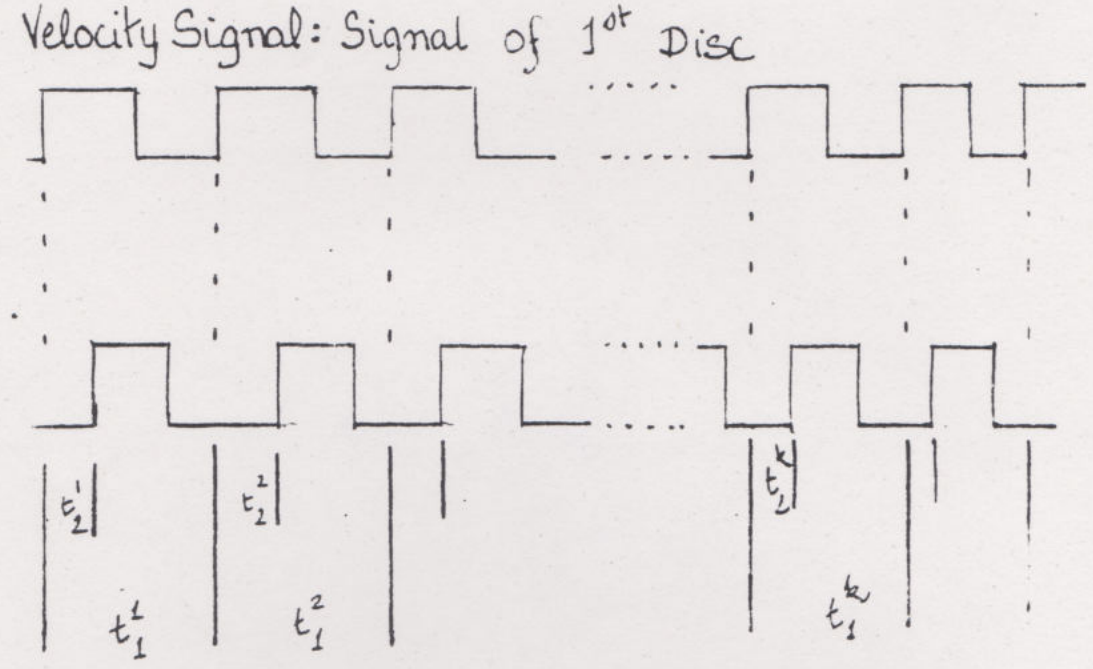

Figure 4, Signal Compensation

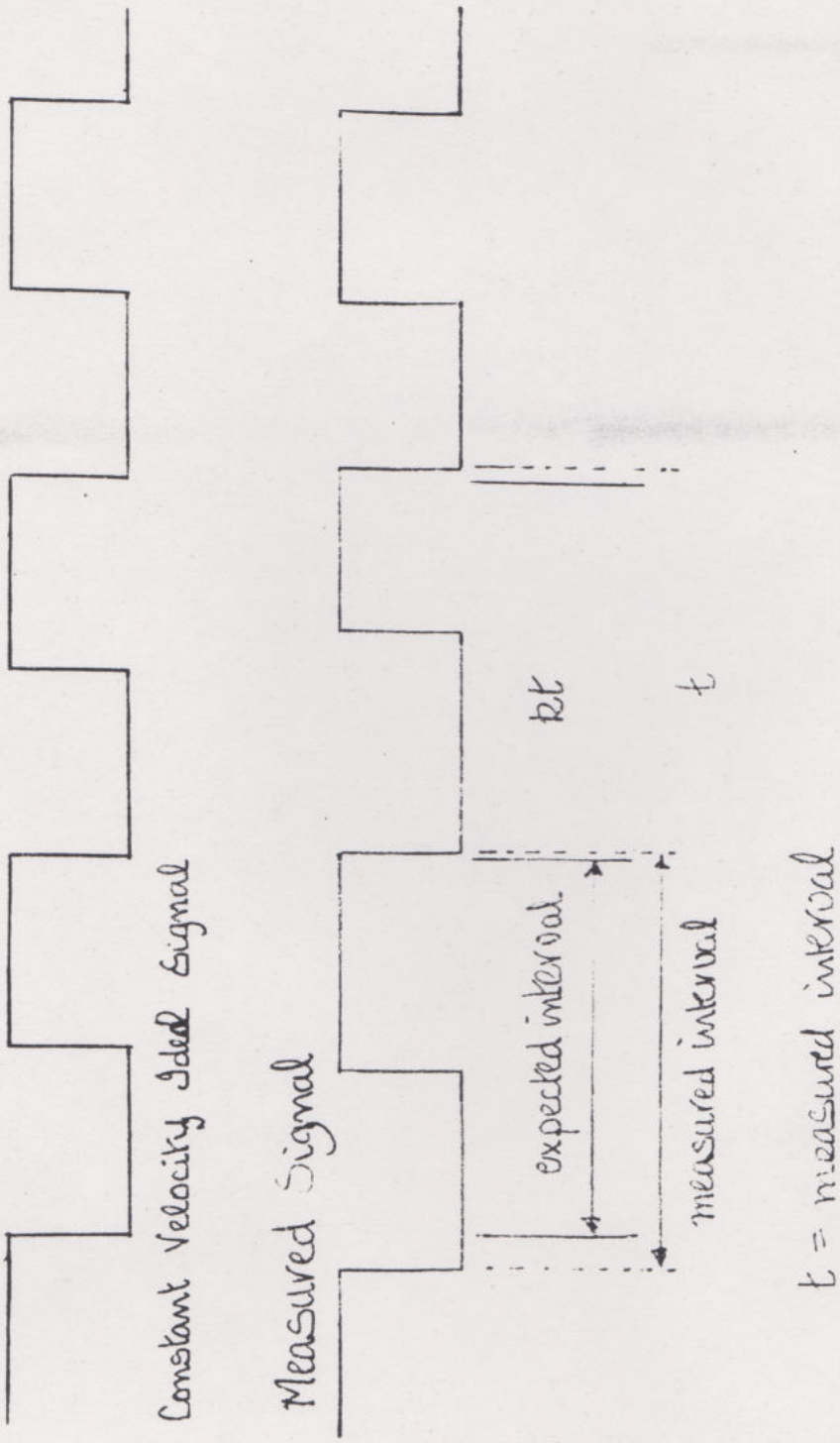

Figure 5, Interrupt servicing

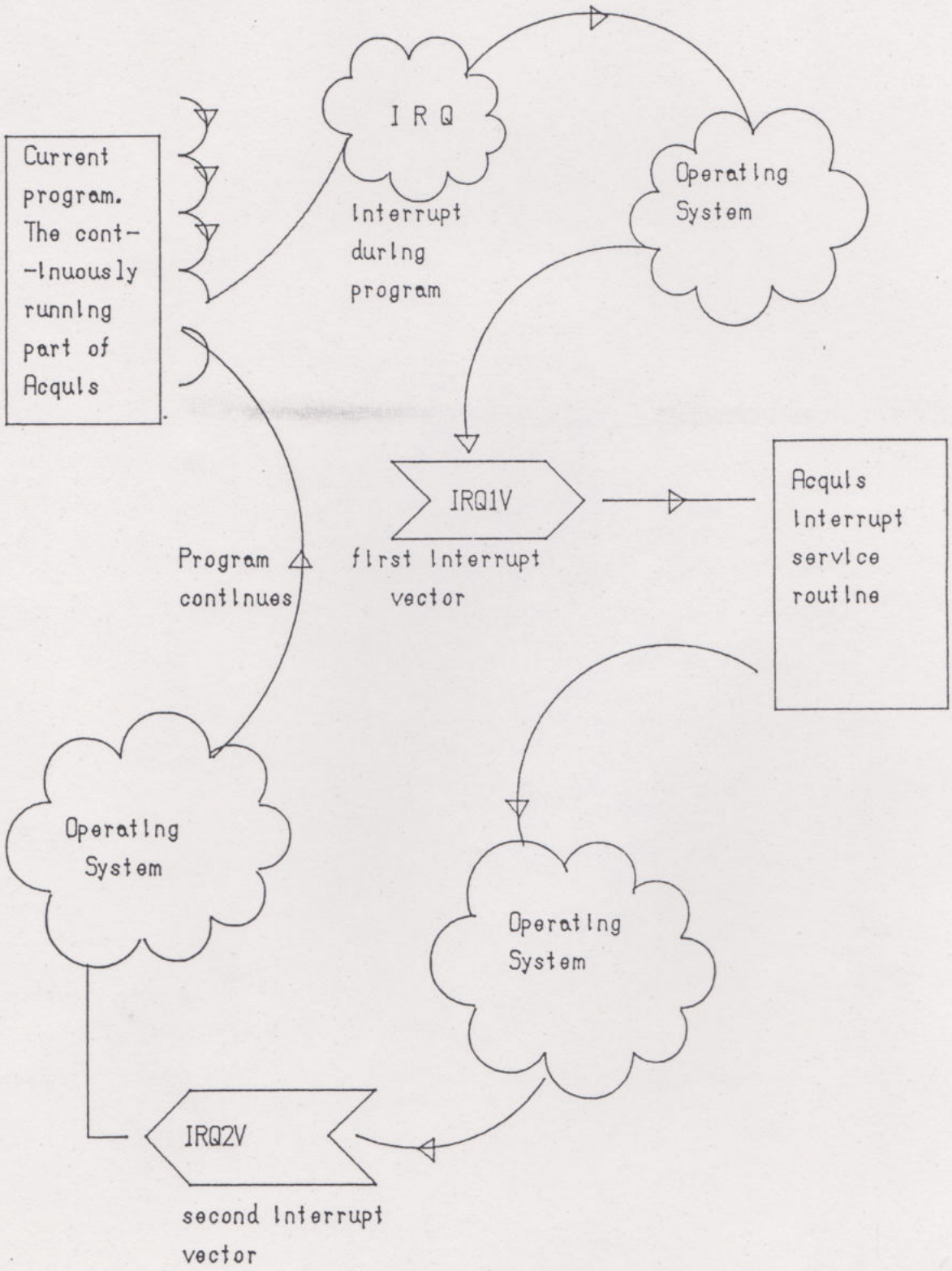

Adapted from Colin Ople; Interfacing the BBC

jt1300988

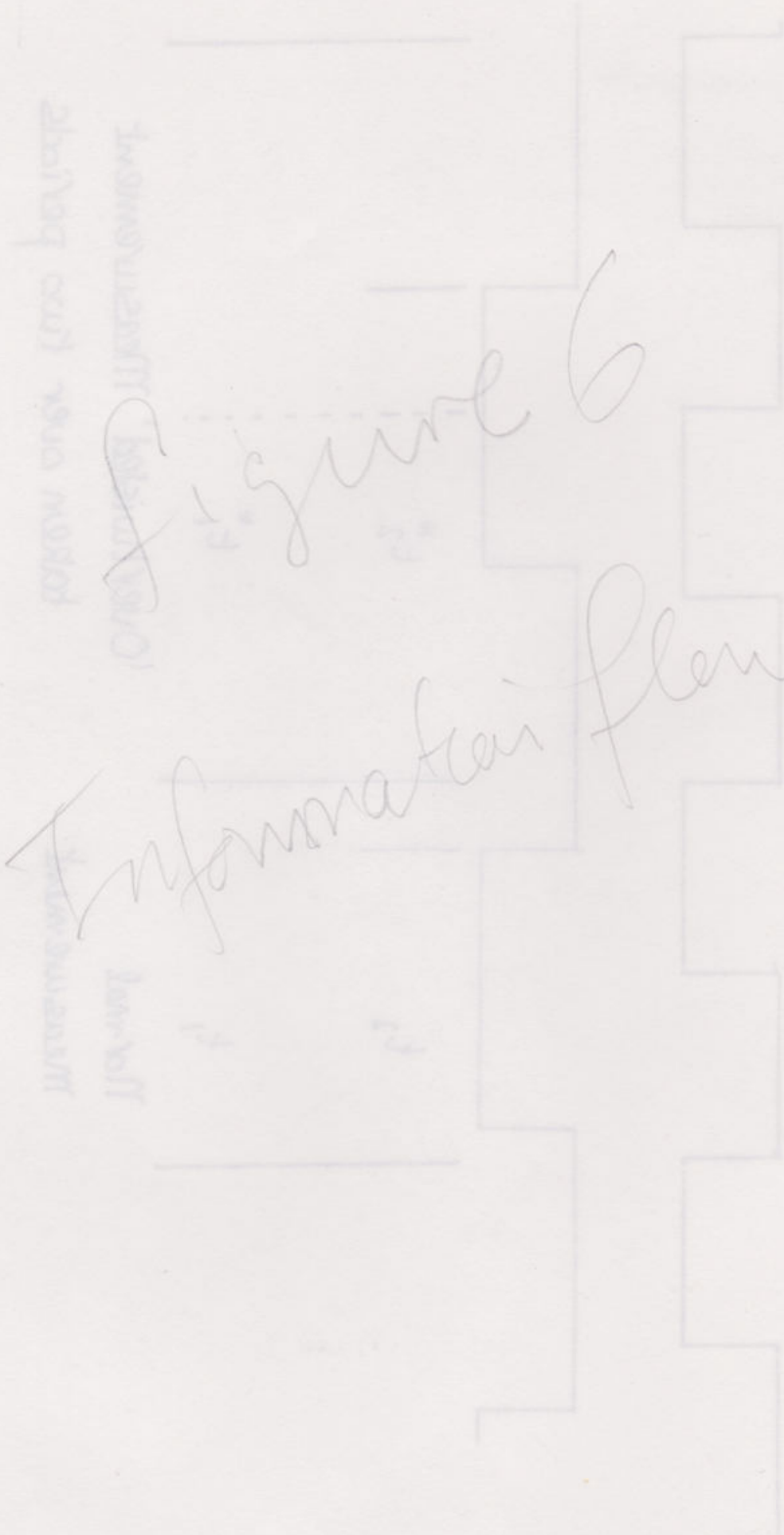

Figure 6

Information flow

Figure 7, Over twist of encoder

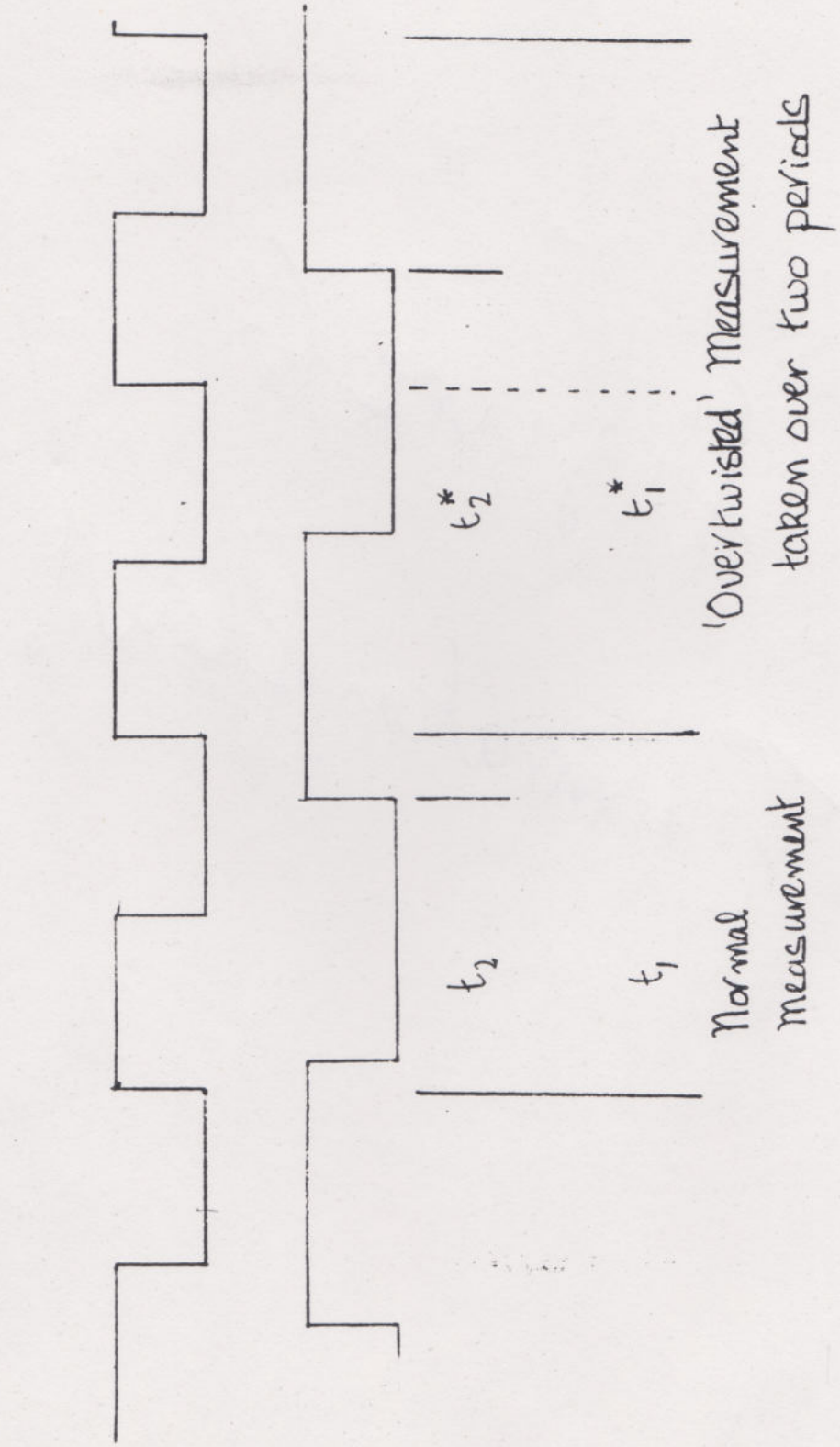

Figure 8, Photograph of rig

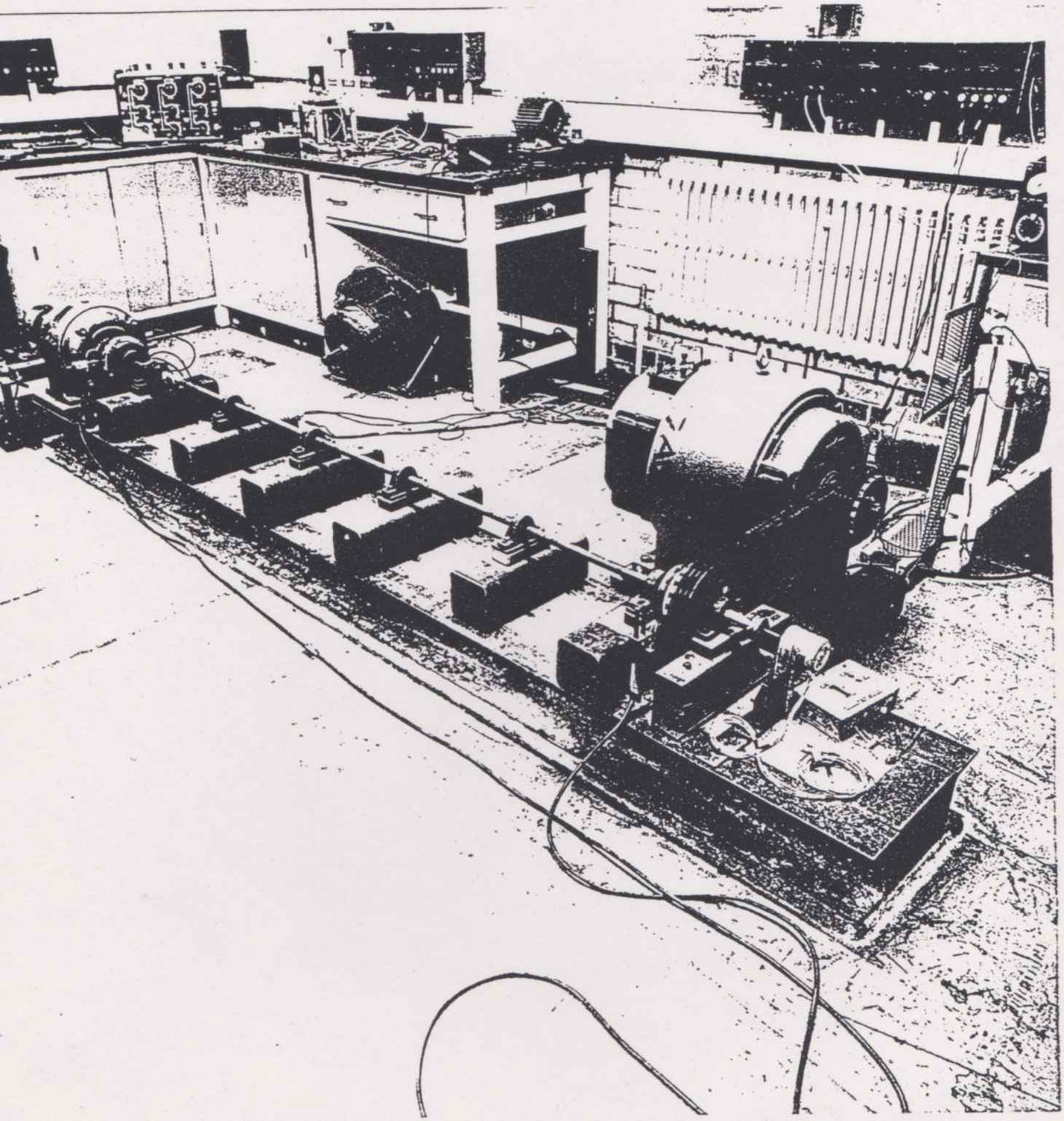

Figure 9, Schematic of rig

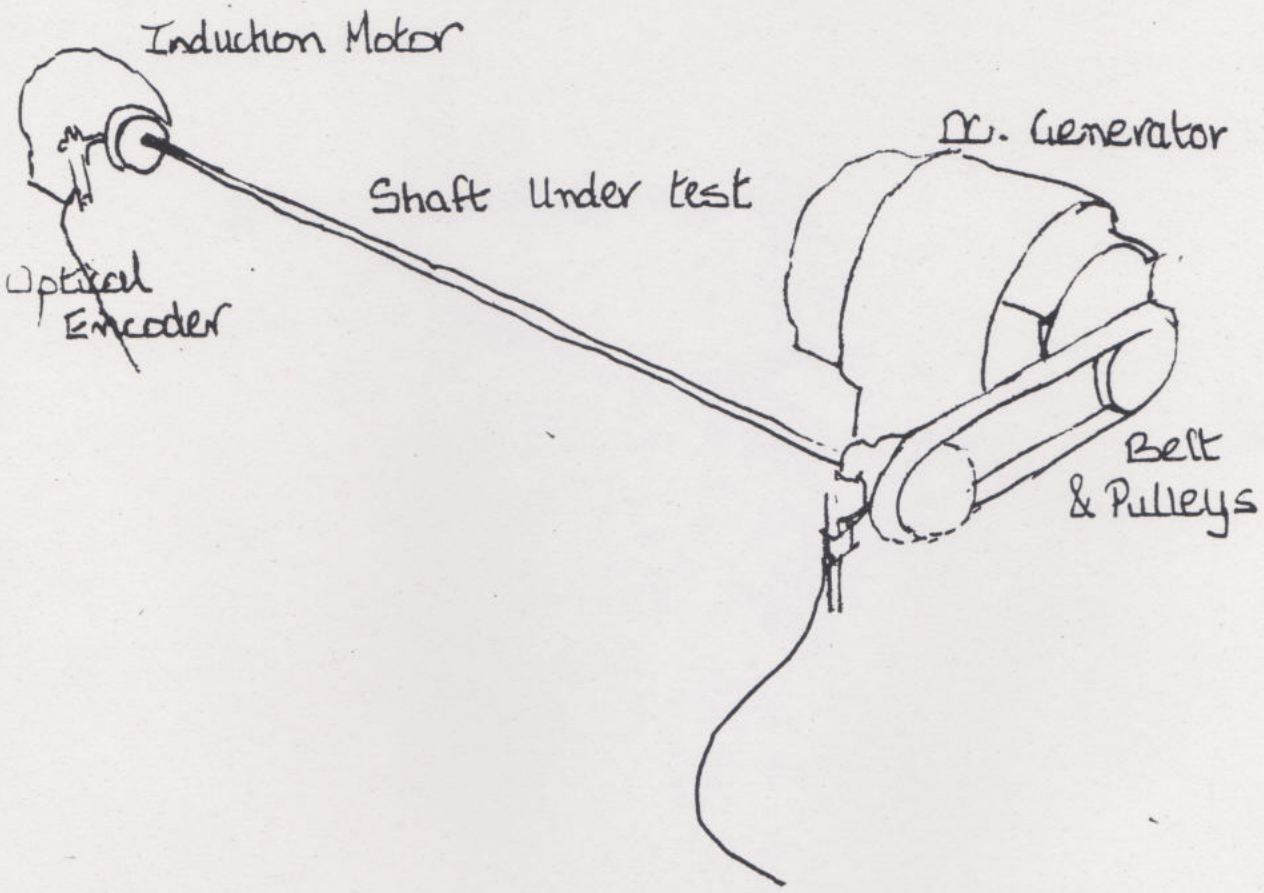

Figure 10, Belt and pulleys

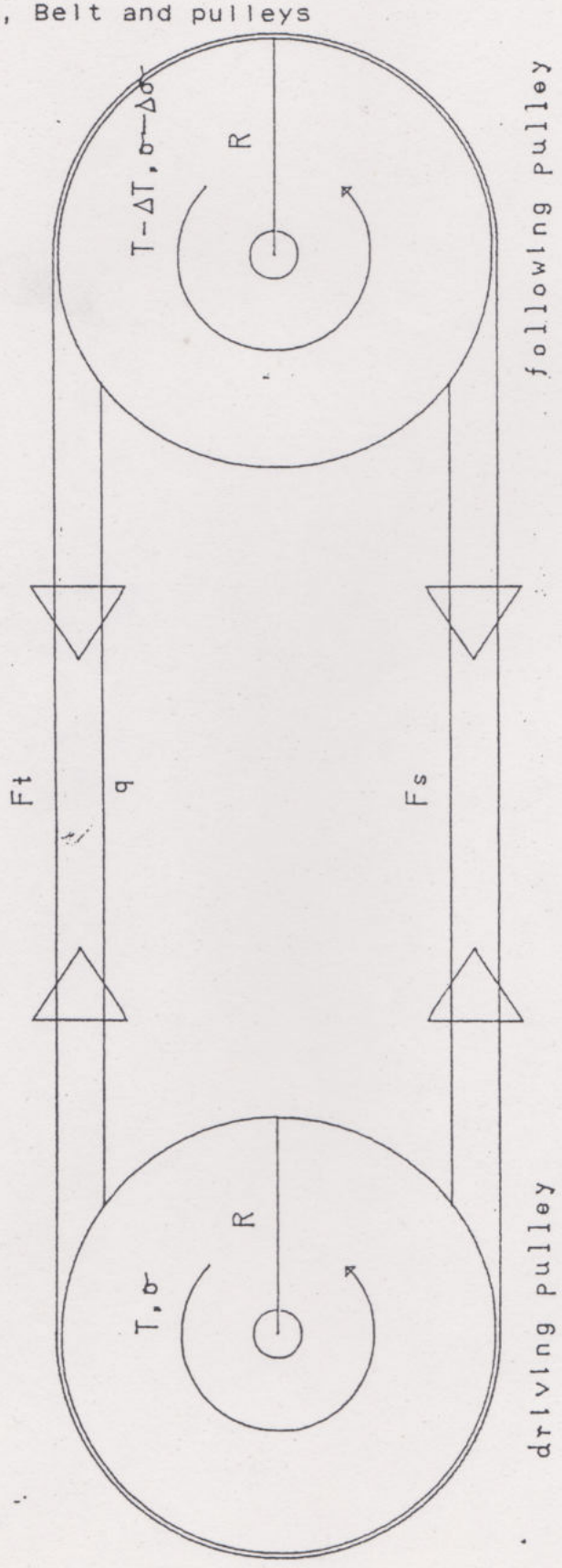

BELT AND PULLEY SYSTEM

Figure 11, Star/delta connection of motor

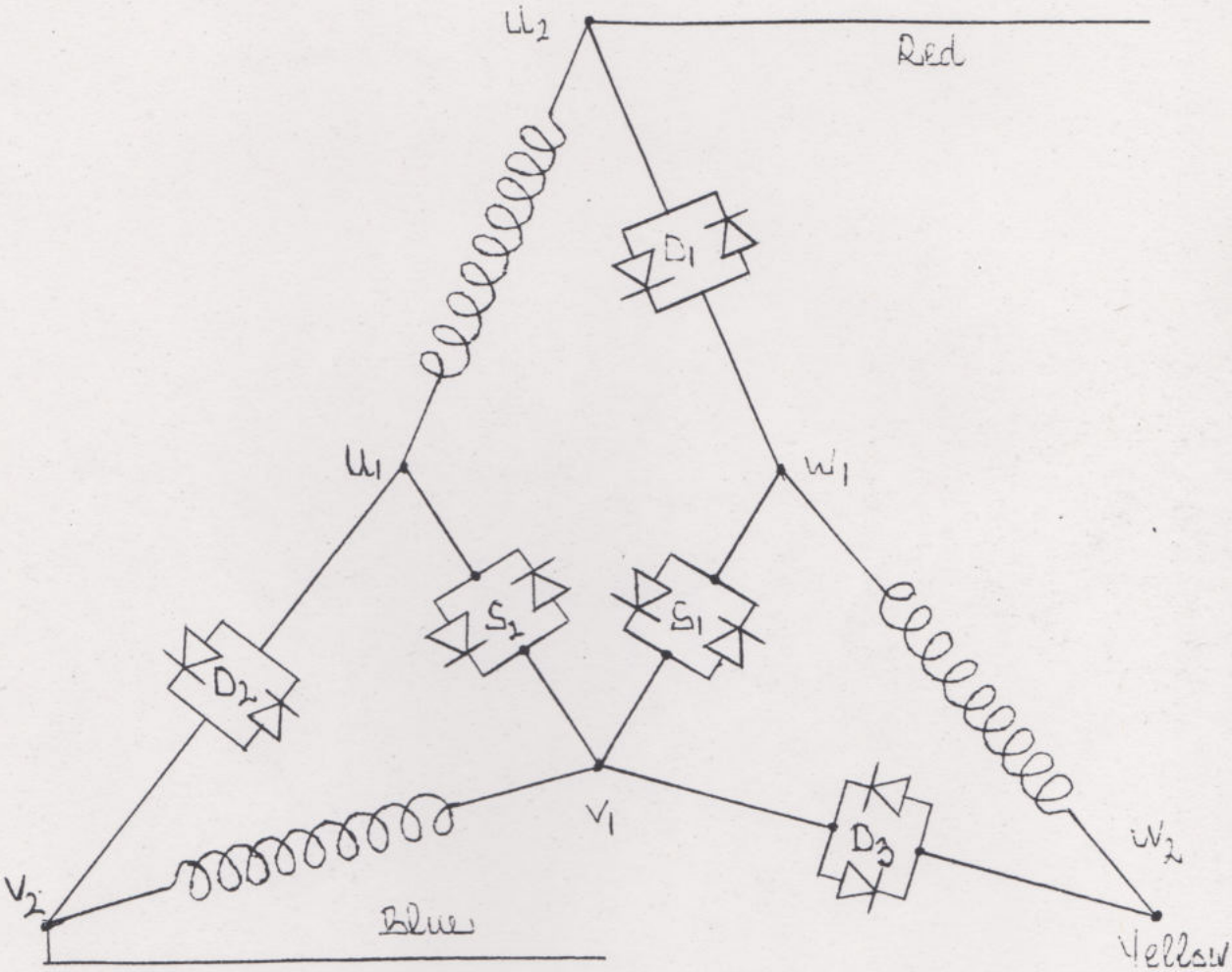

6 thyristors only - for Star connection
D thyristors only - for Delta connection

General flow diagram of acquis

Gereral flow diagram for ACQUIS, the data acquistion program
Interrupt service routines.

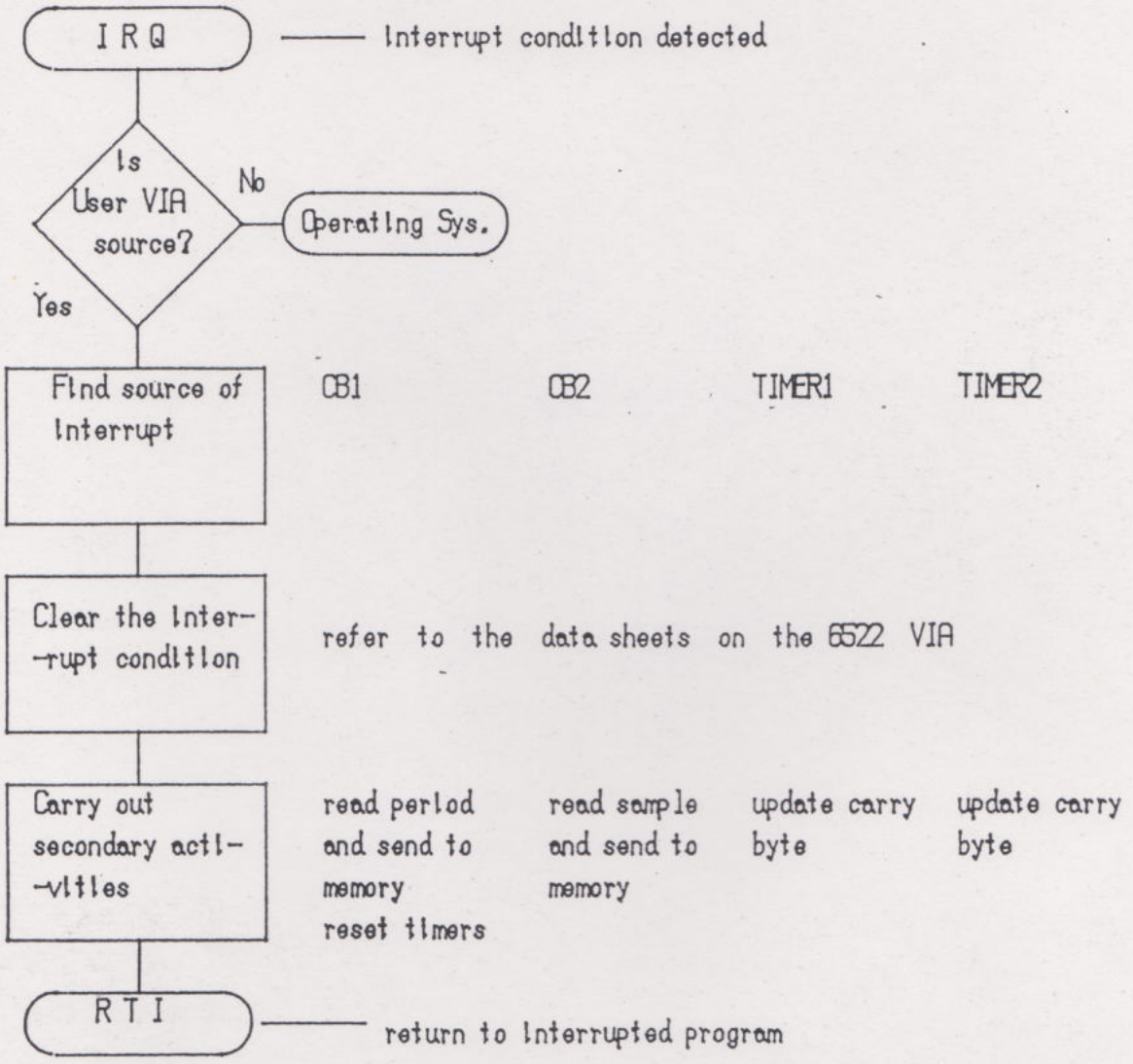

Flow of information

Information transfer through system

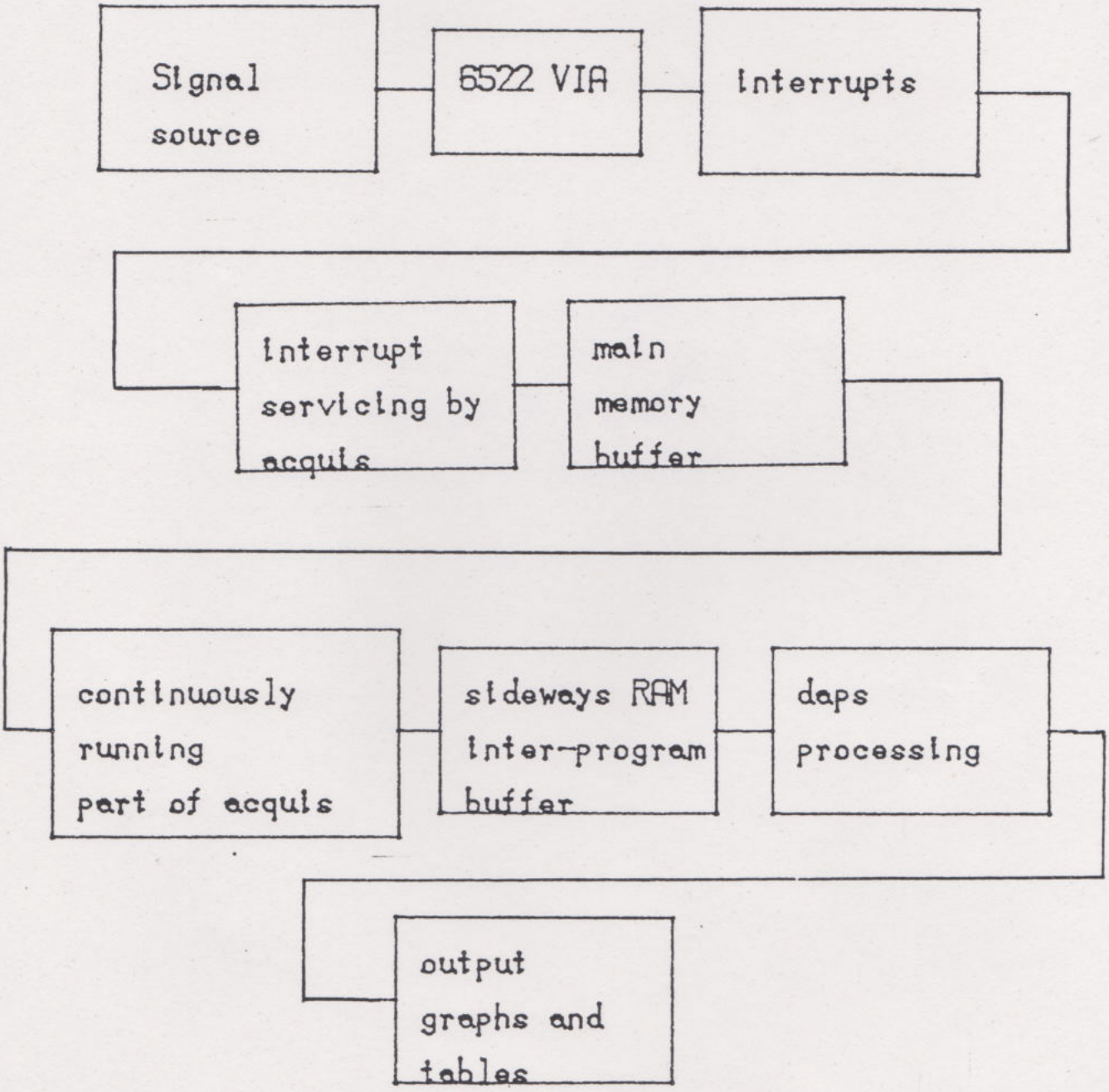

Circuit 1 - Opto-switch to TTL interface

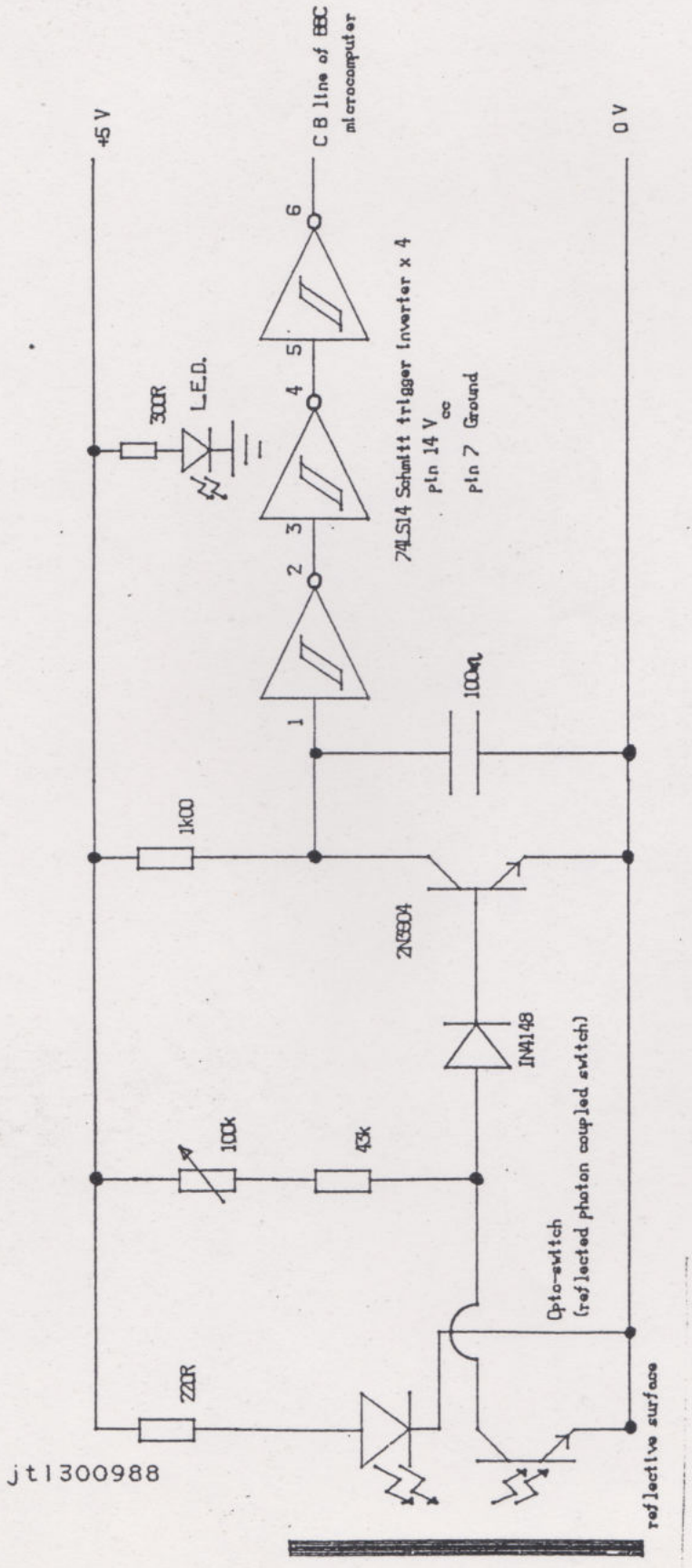

Circuit 2 - Thyristor firing circuit

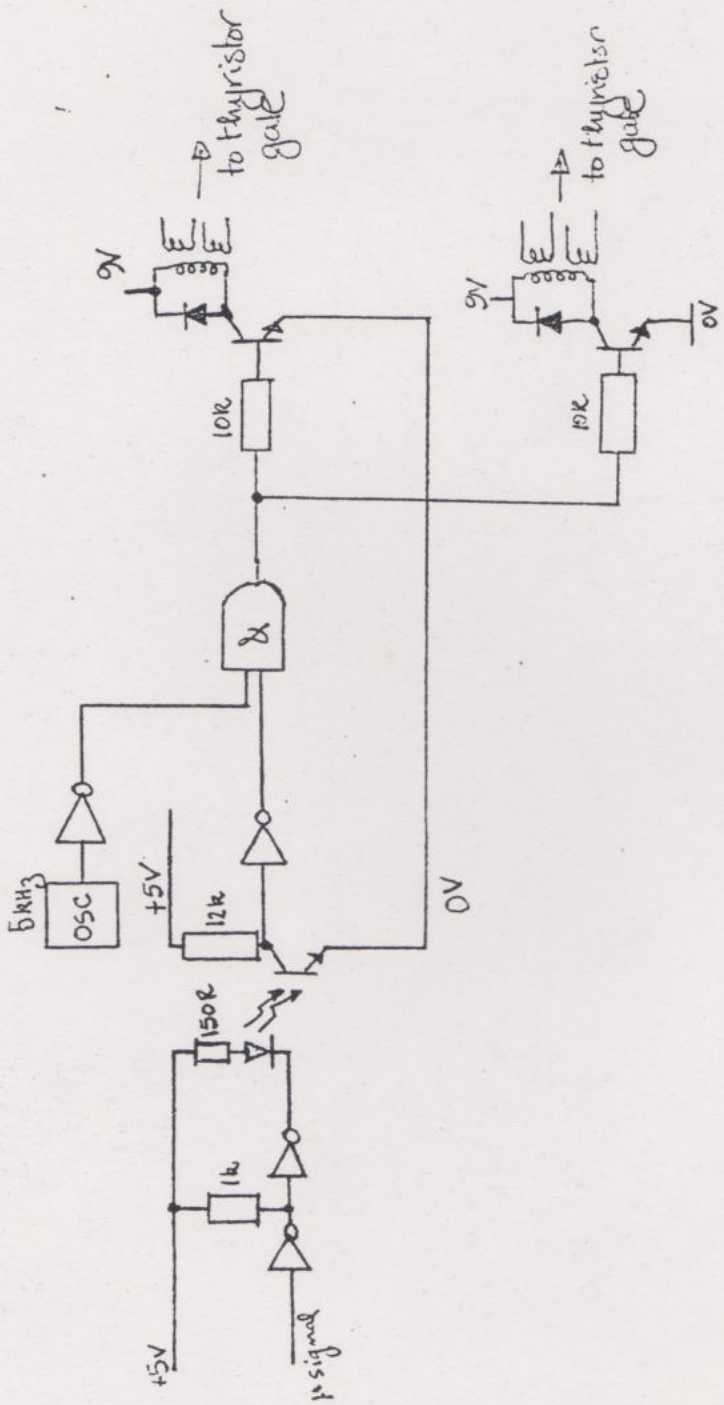

Circuit 4 - GTO controlled loading of the generator

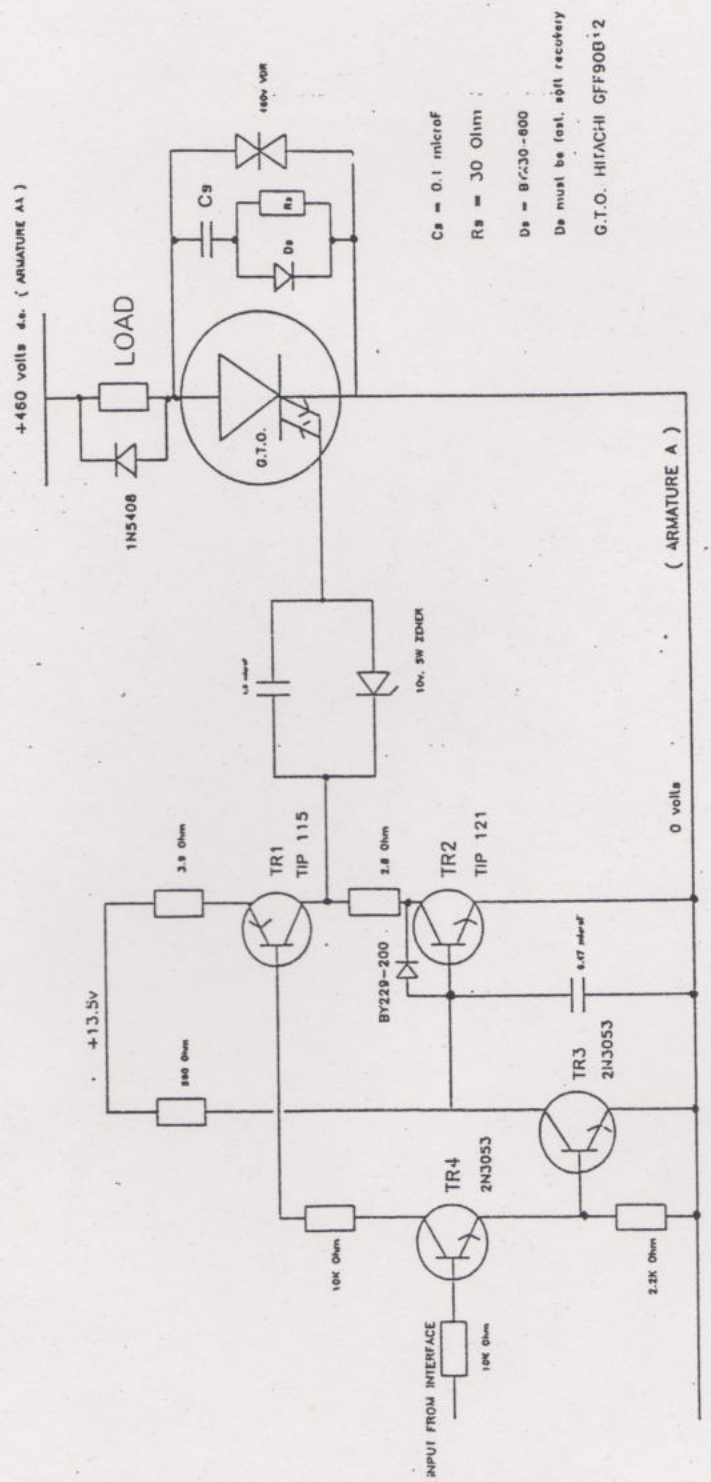

Circuit 5 - GTO interface to computer

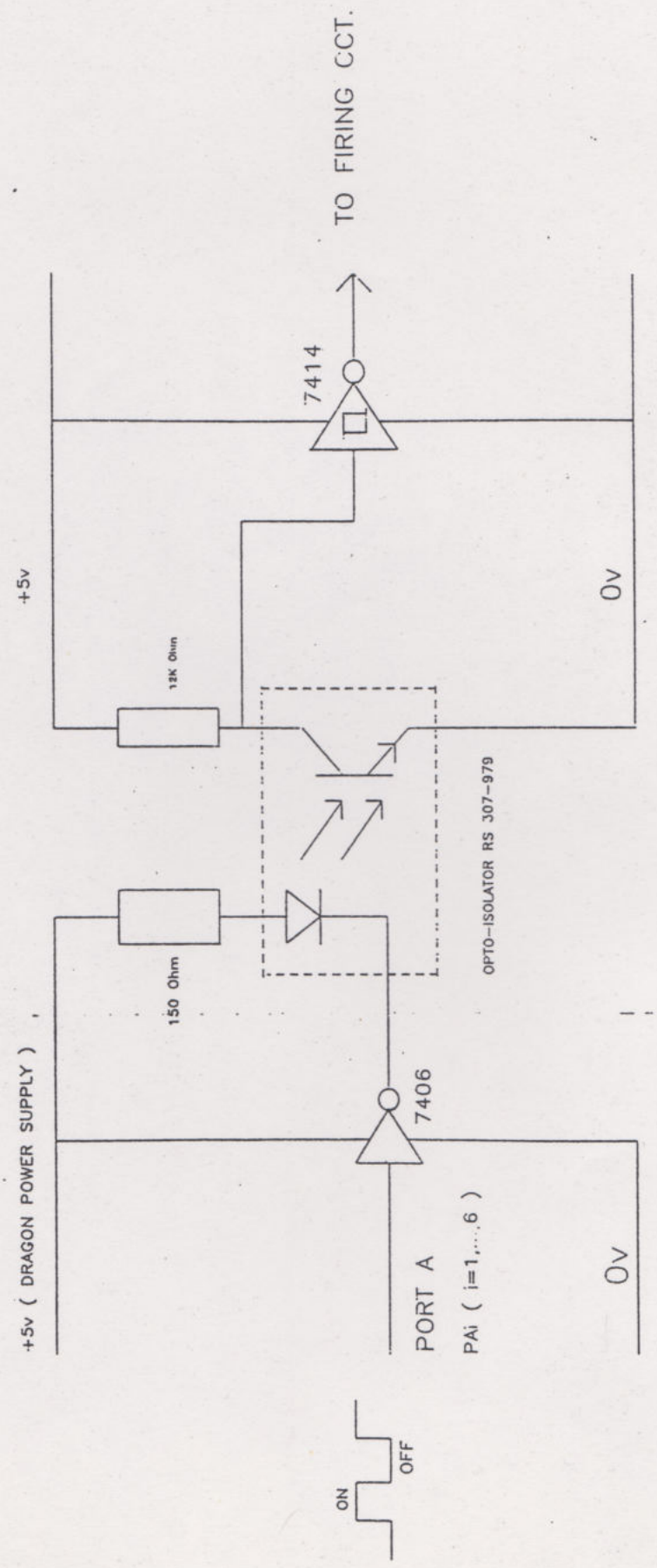

Graph 1: Velocity - raw data

No error detection and the minimum of calculation to reveal the velocity

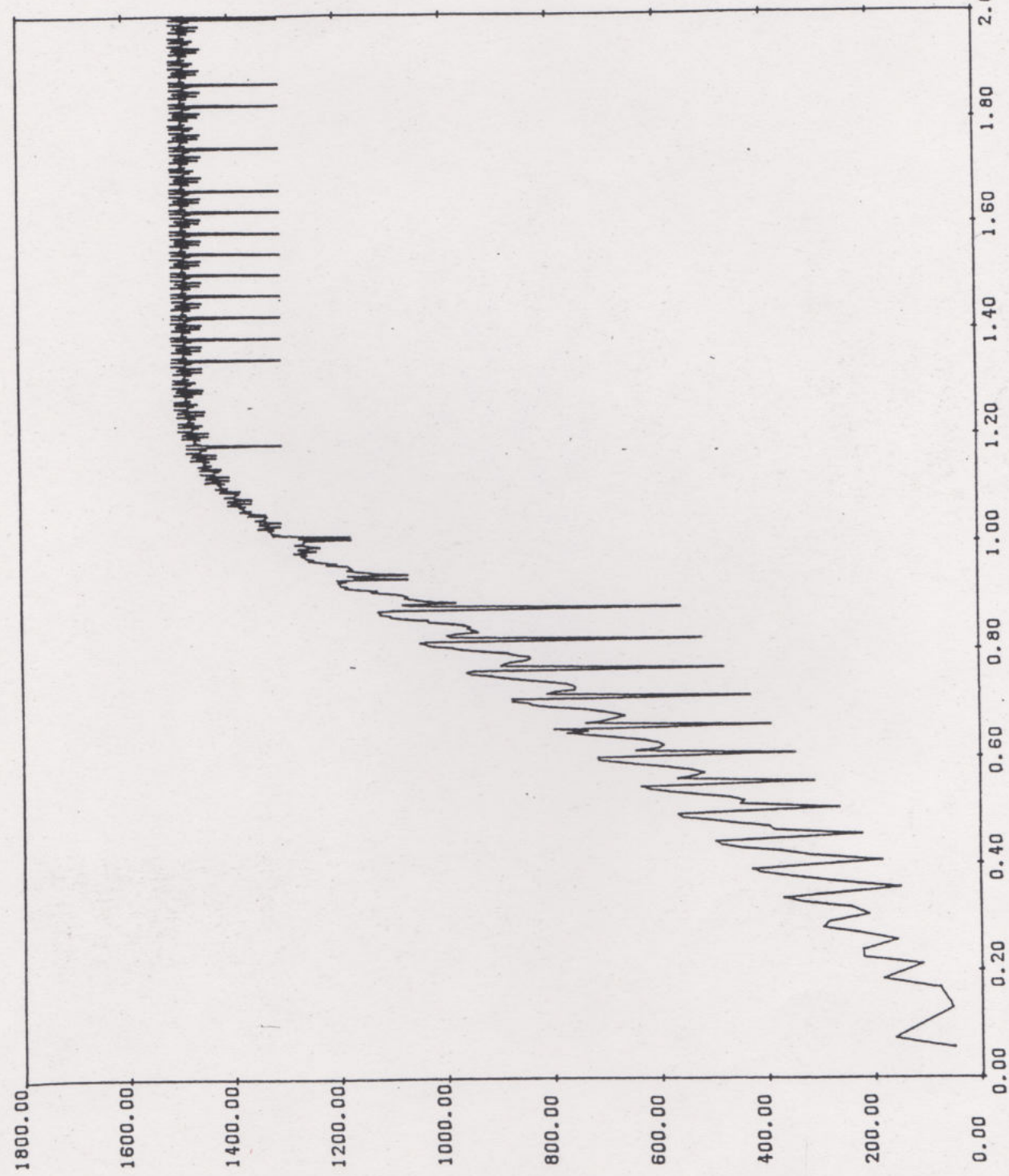

Speed

Graph 2: Velocity - no timer rollover

The routines for the detection and correction are applied to the data for graph 1

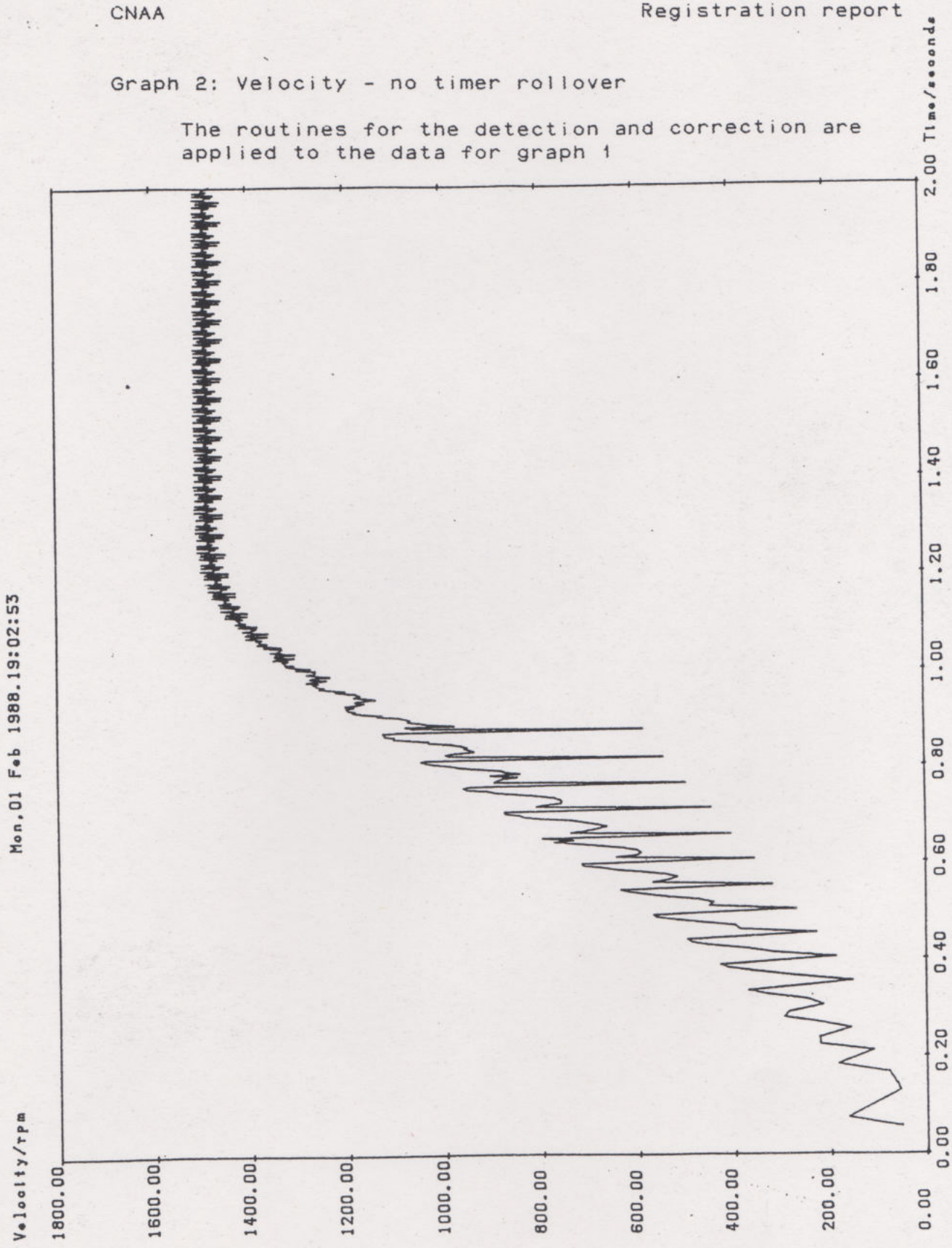

Graph 3: Velocity - as previous and no over-twist

The routines for the detection and correction of over twist are applied to the data

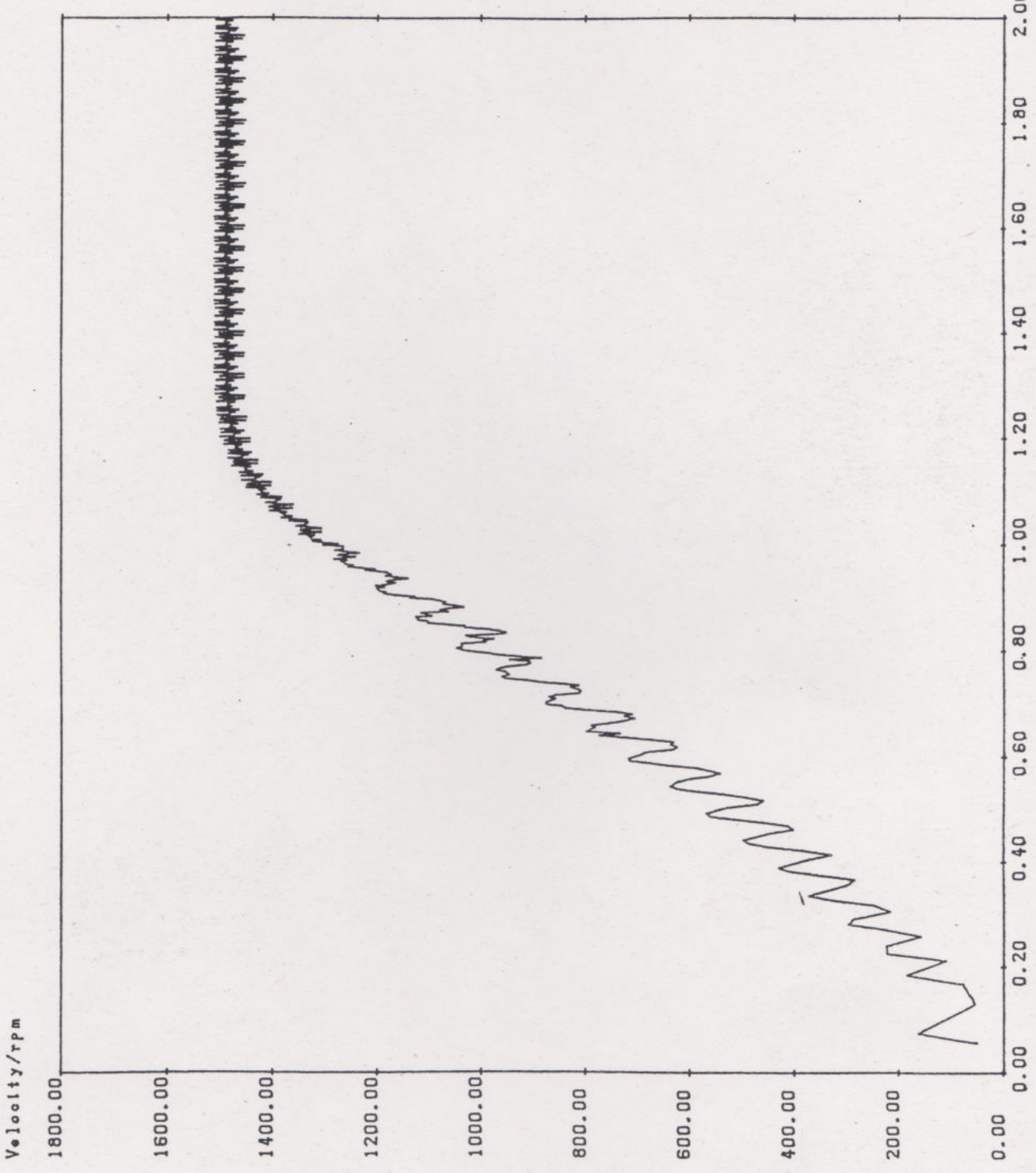

Graph 4: Velocity - as previous and encoding disc compensation

The routine for generating the scaling factors is applied to the data and those factors are used in the subsequent processing

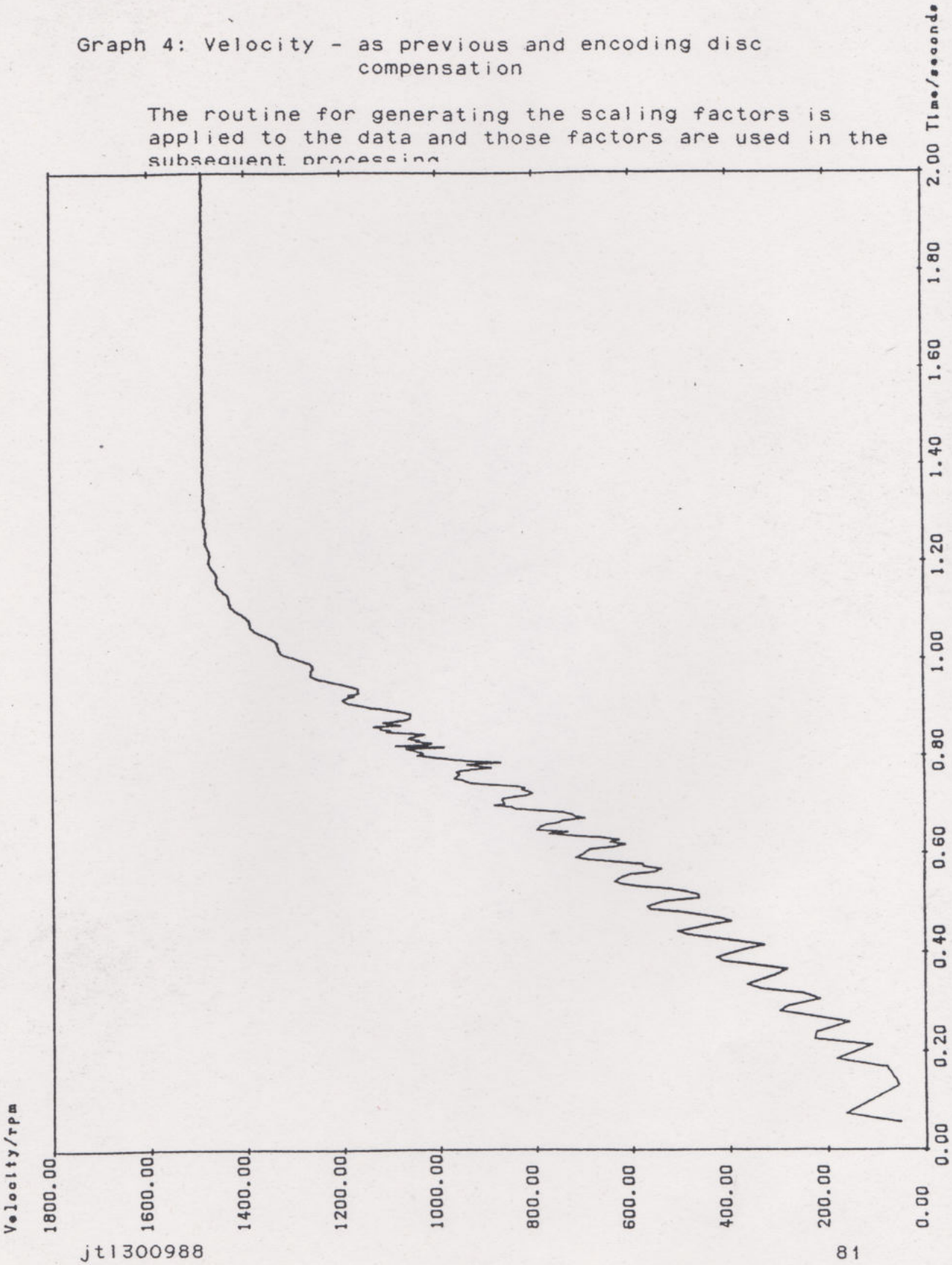

jt1300988

Graph 5: Velocity - Model

The velocity of the rig during the start up over the same period as the measurements

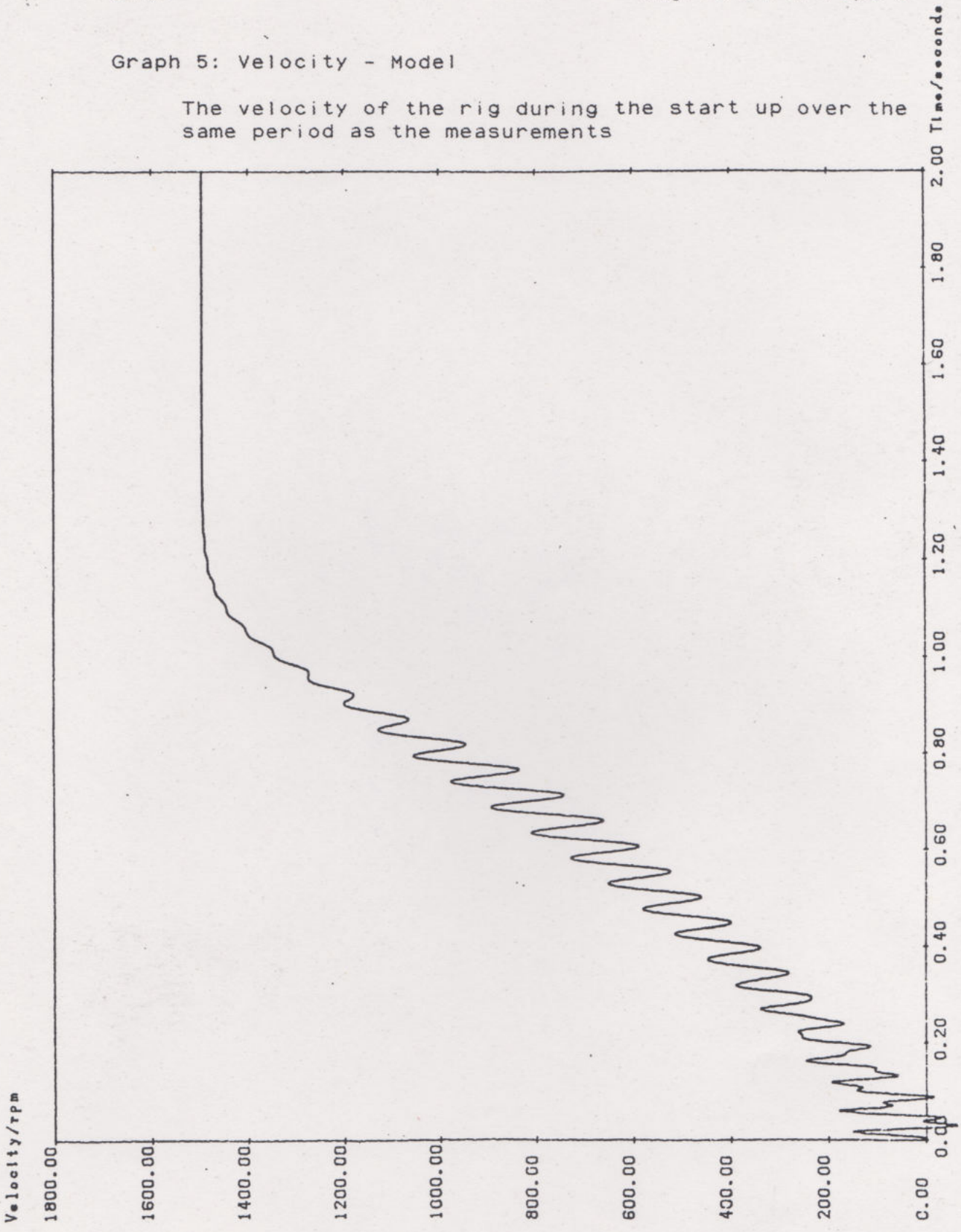

Graph 6: Zones of doubt

The areas of the graphs where interrupt latency interferes with the accuracy of the measurements

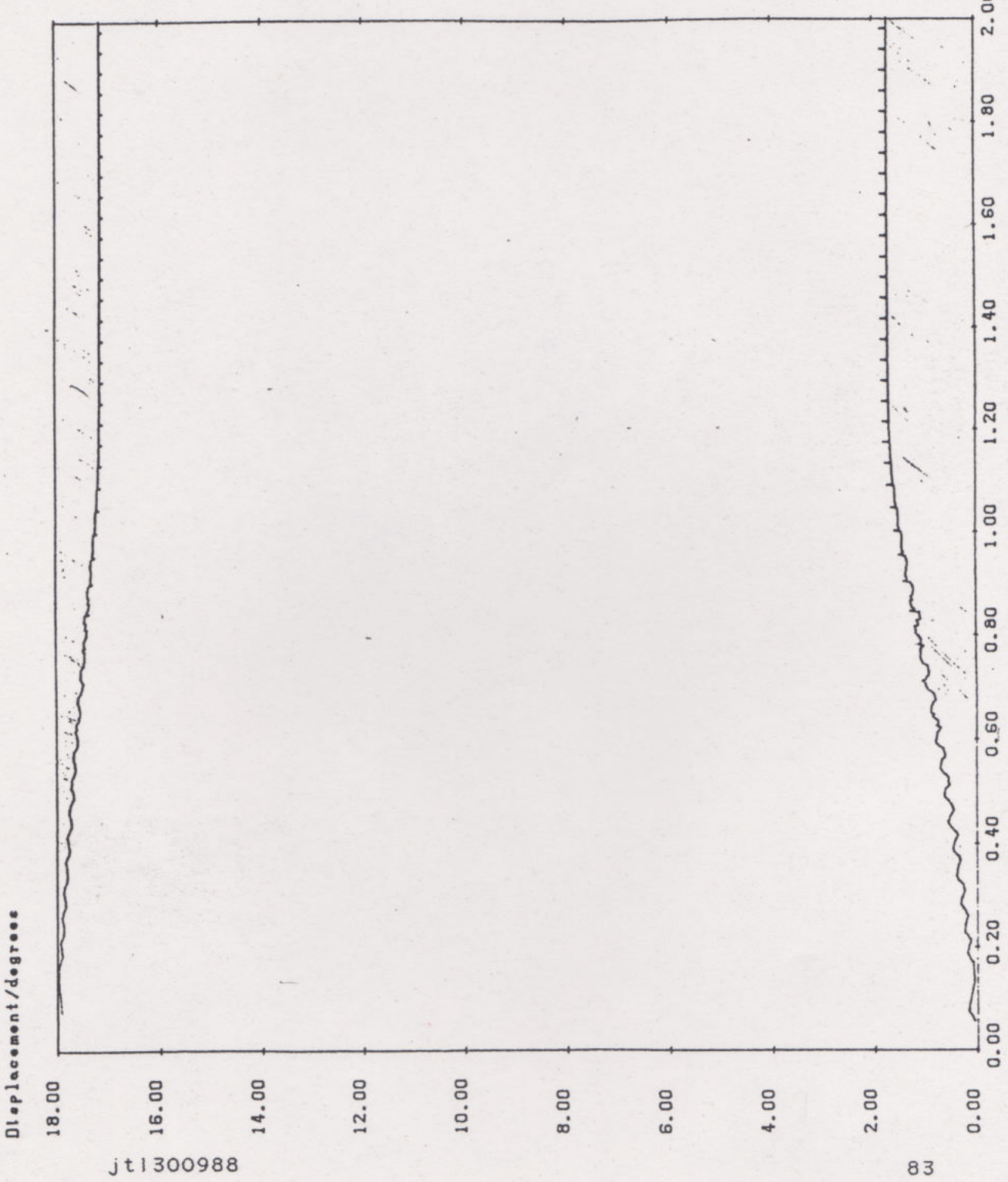

Graph 7:Angular Displacement - Raw Data

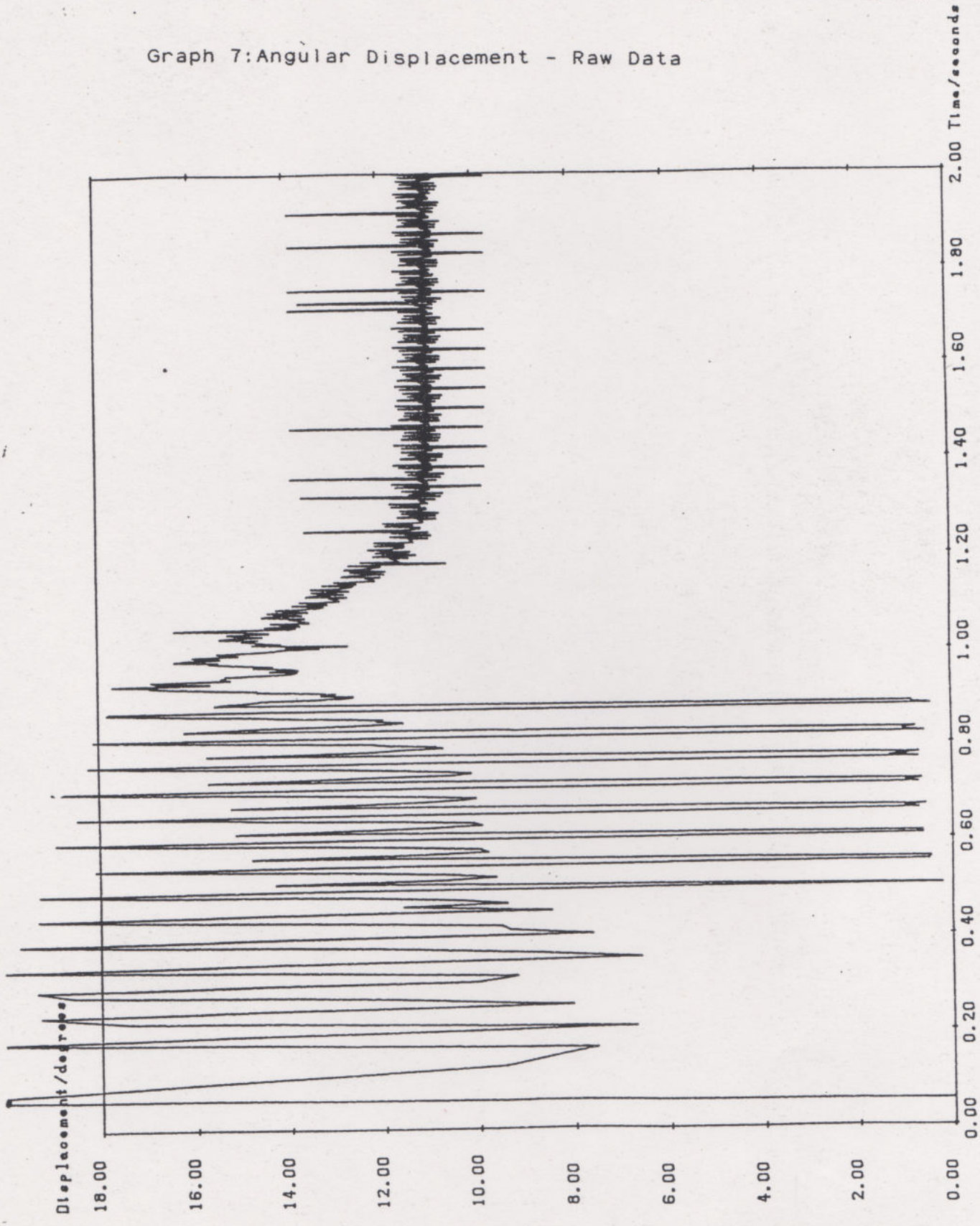

Graph 8:Angular Displacement - no timer rollover

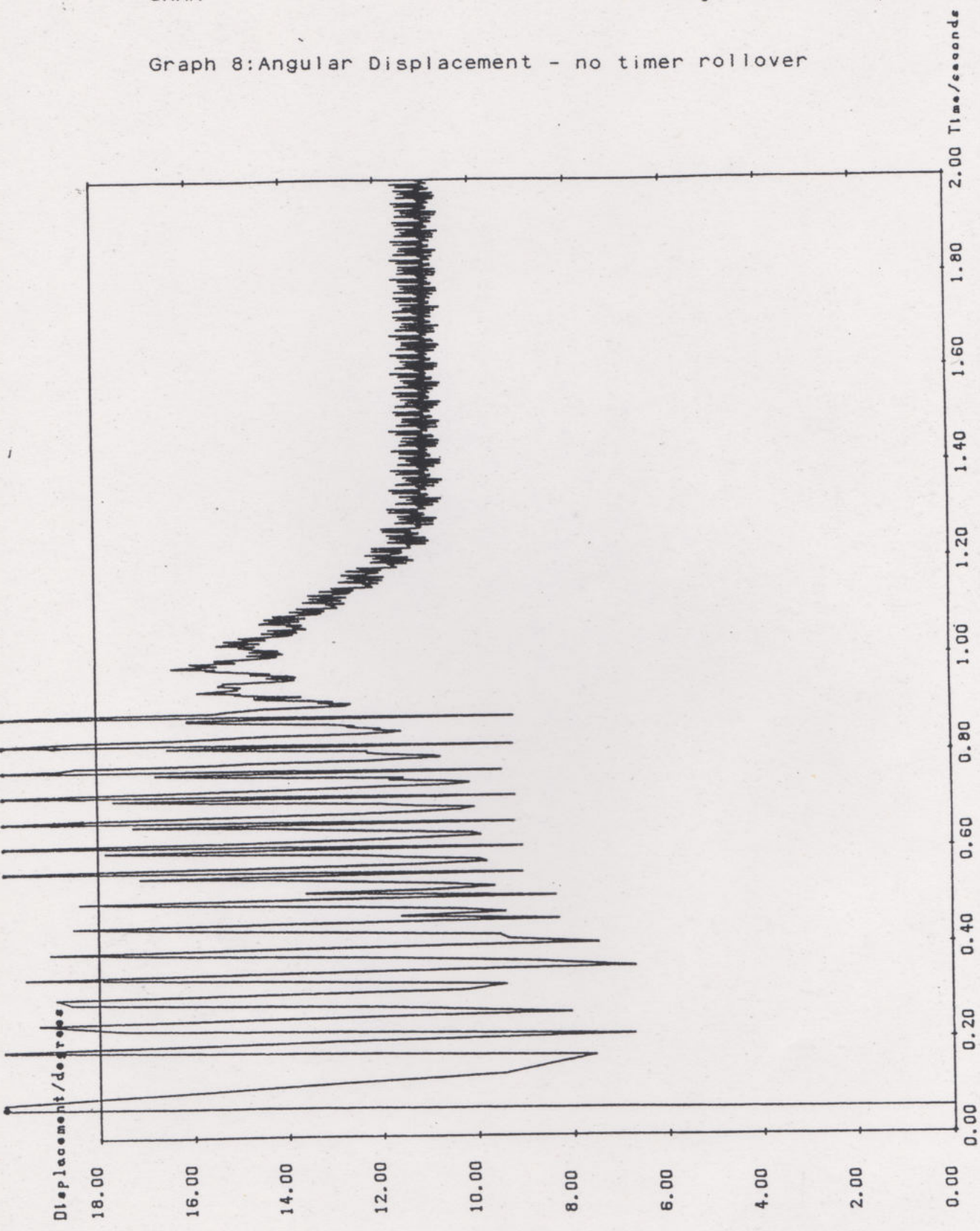

Graph 9:Angular Displacement - as previous and no over twist

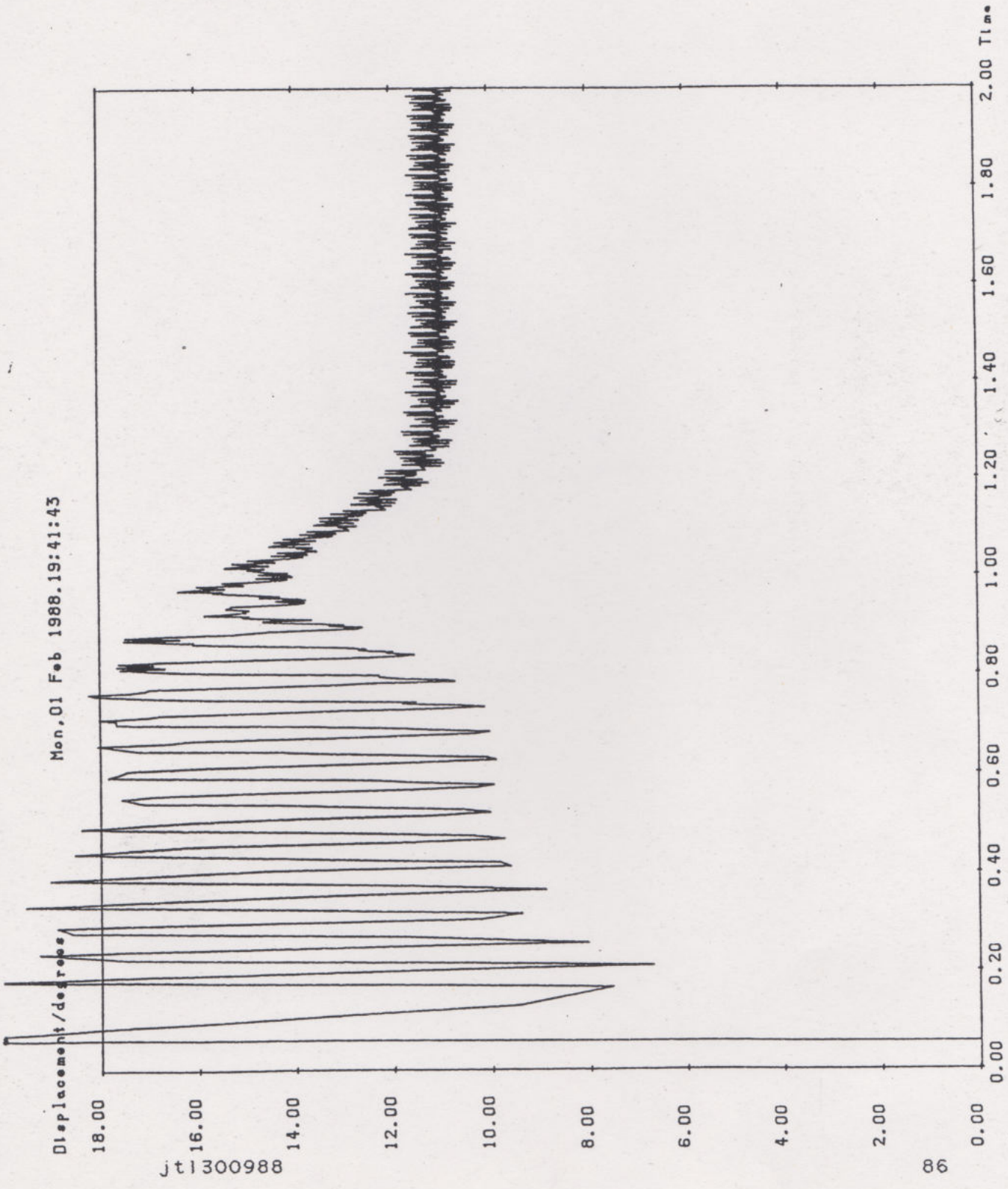

Graph 10:Angular Displacement - as previous and disc compensation

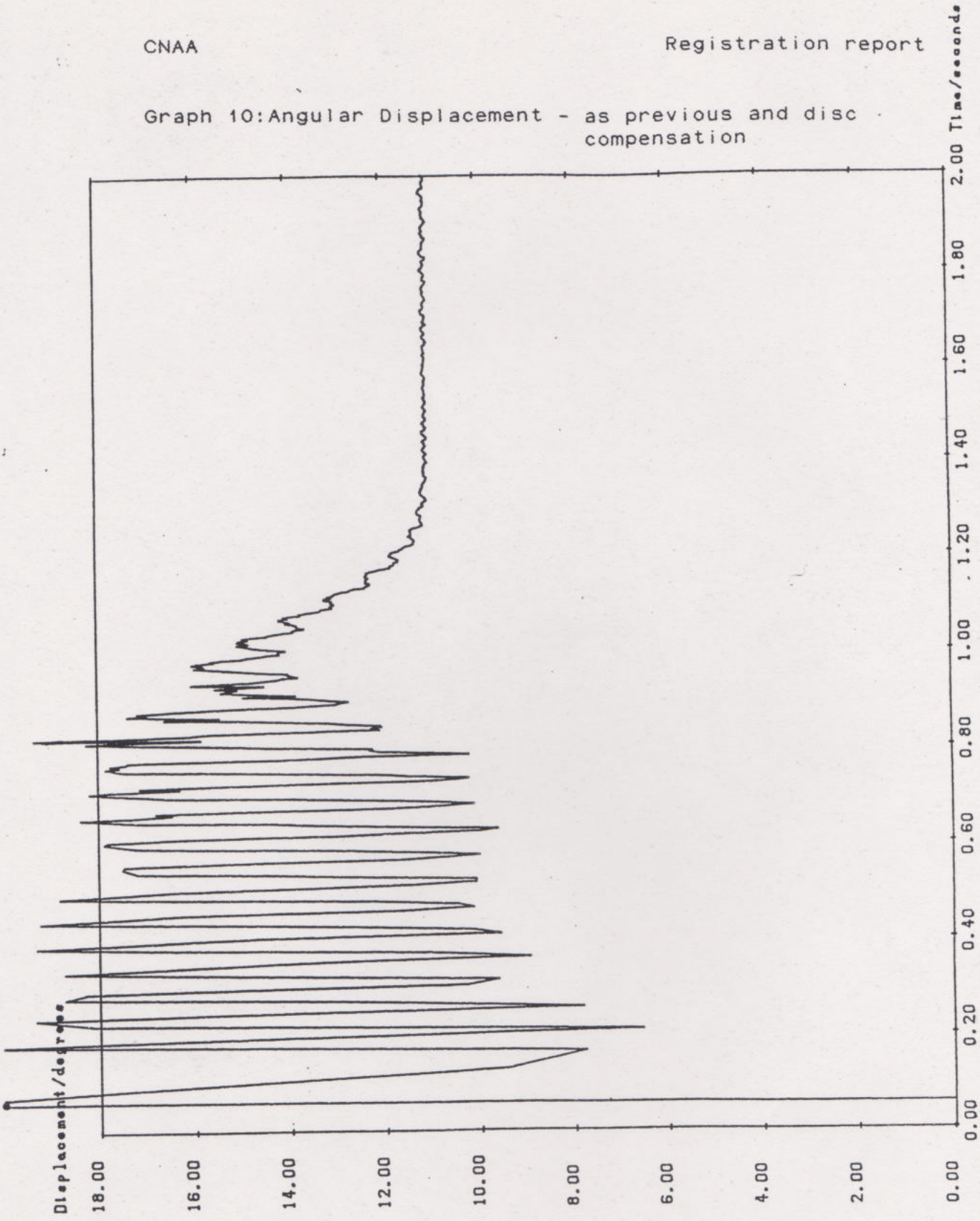

Graph 11:Angular Displacement - Model

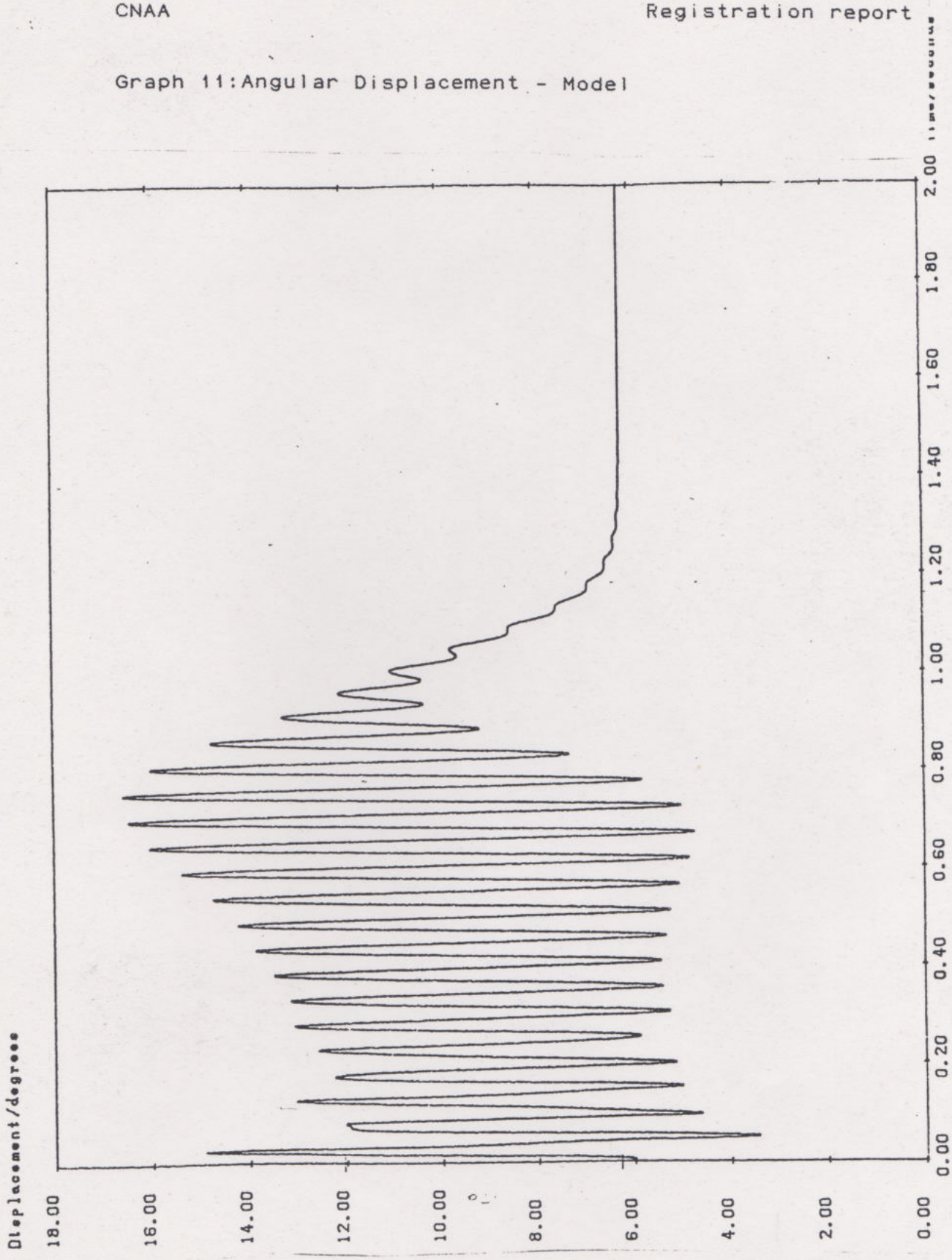

Graph 12:Frequency analysis - velocity, of the uniform velocity section

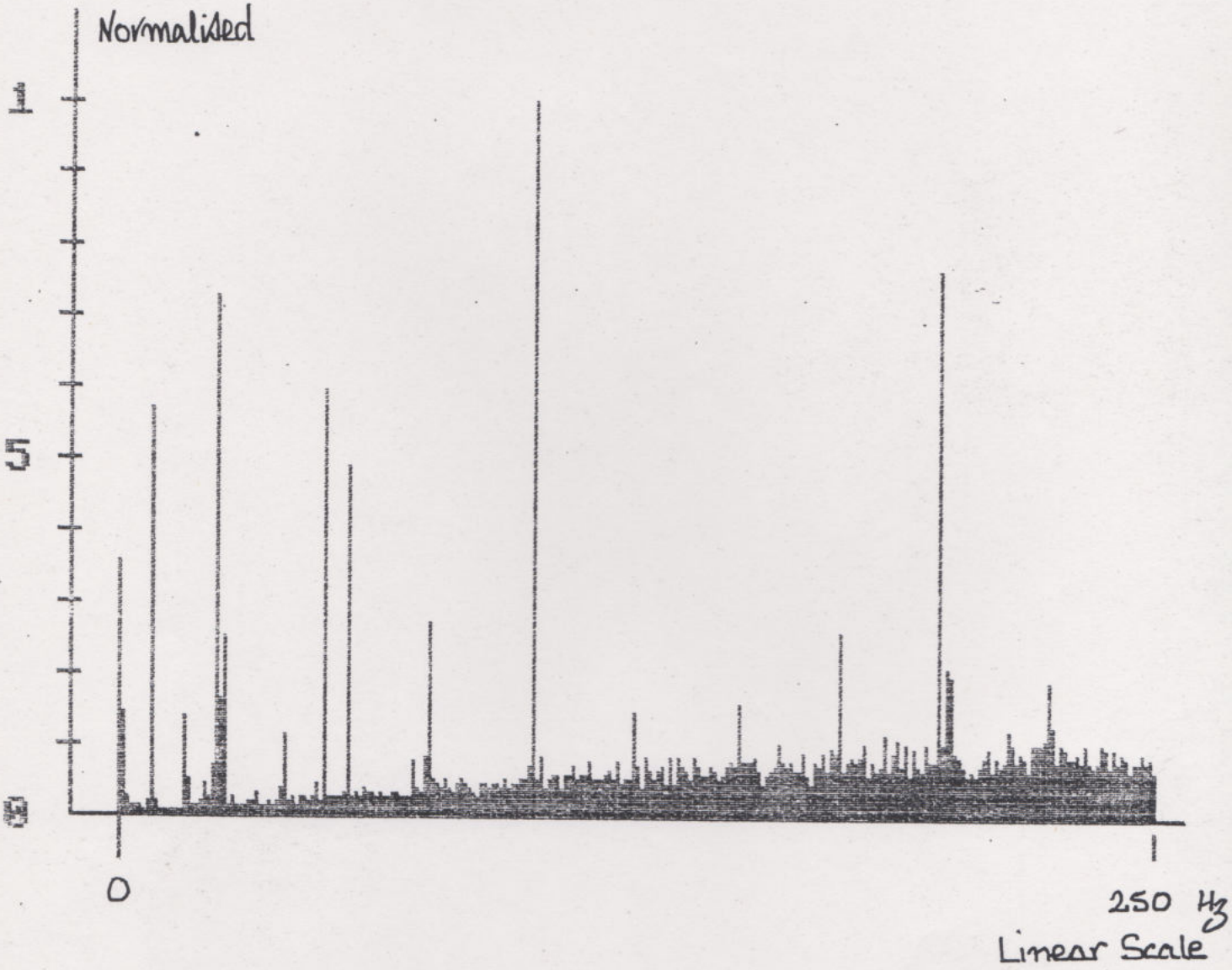

FFT of 8192 samples

Graph 13:Freq. analysis - twist, uniform velocity section

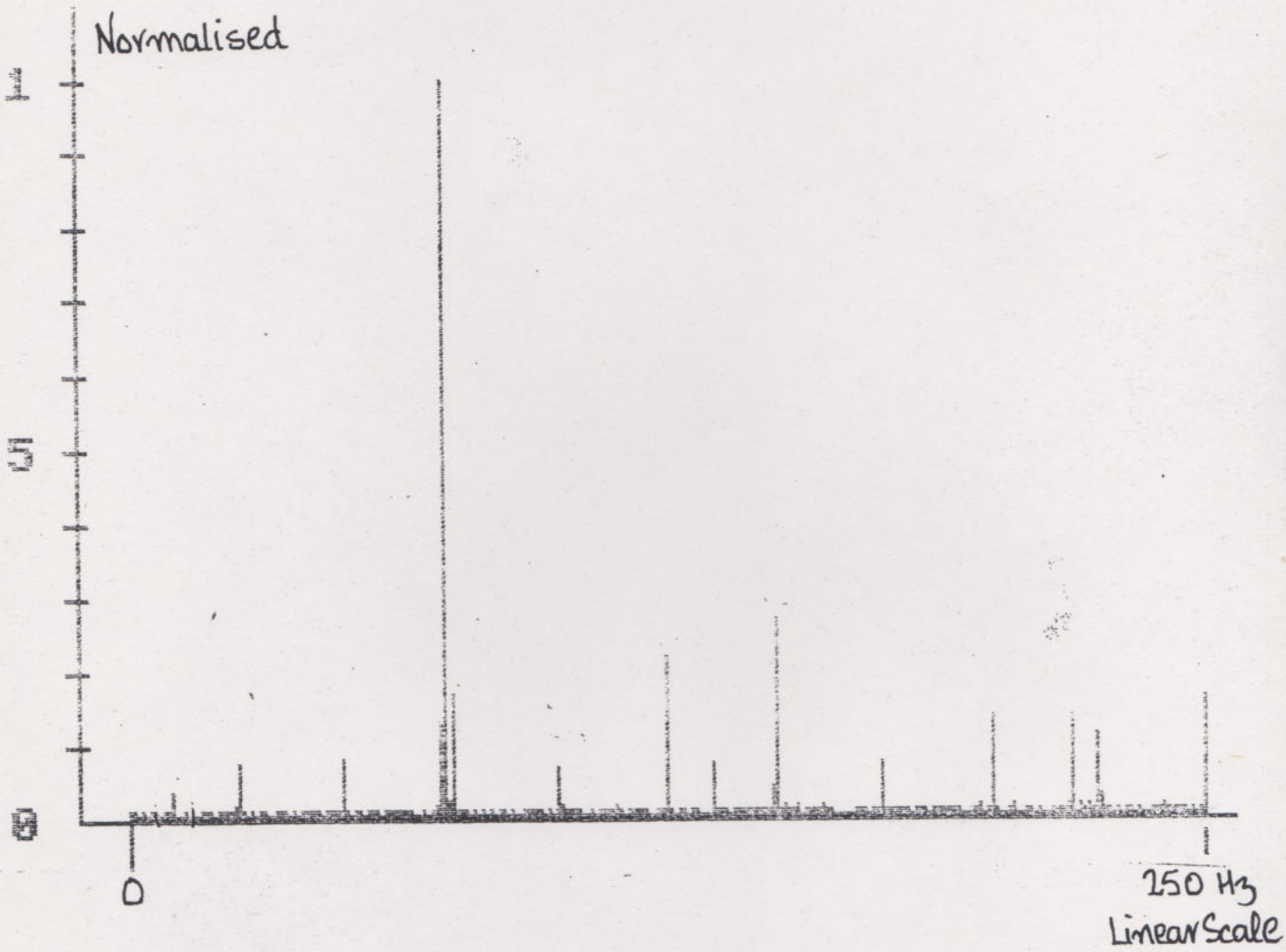

FFT of 8192 samples
Average value omitted

Graph 14:Verification of model - acceleration, motor, model

No load

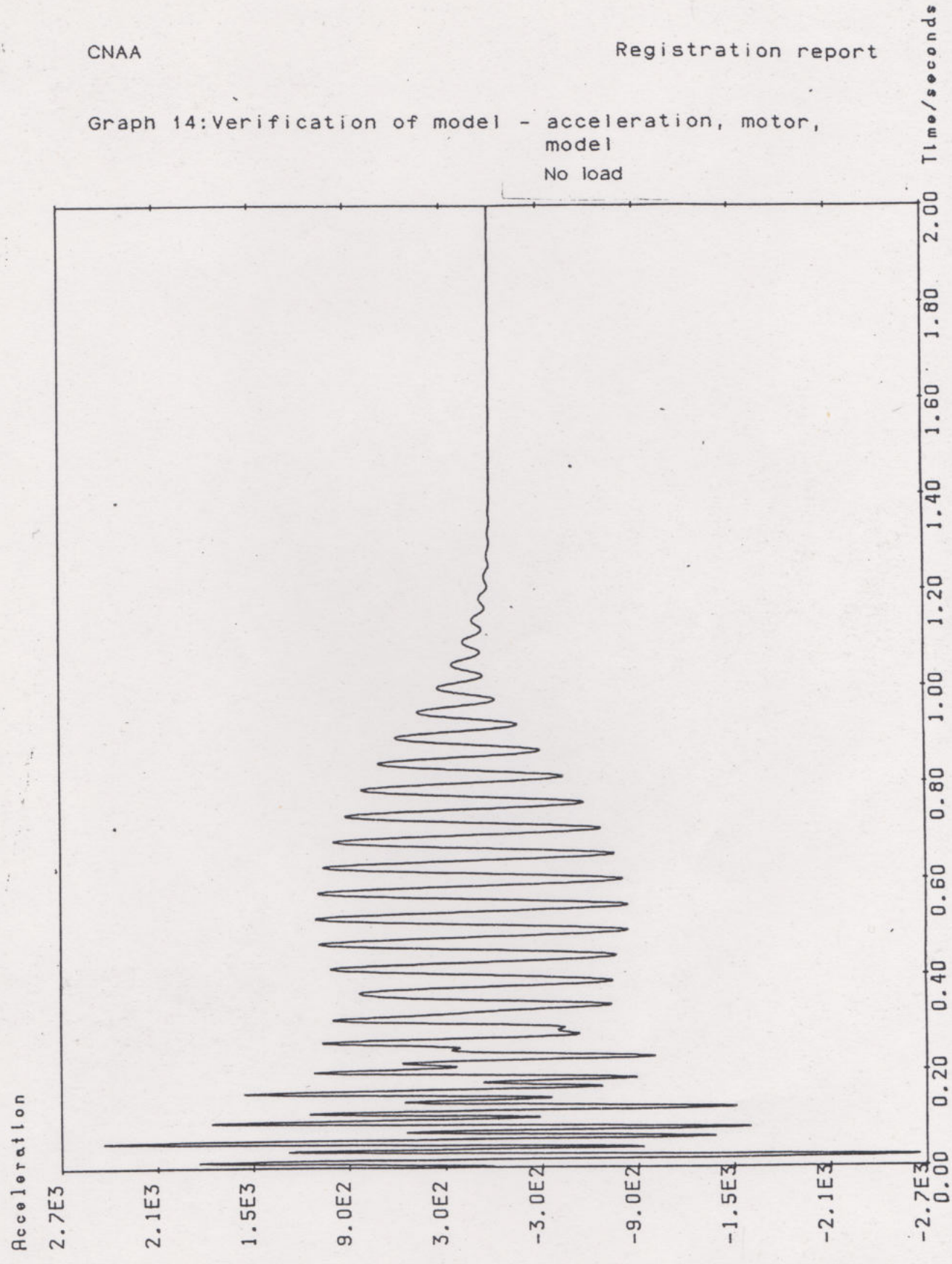

WATANABE INSTRUMENTS CORP.

Graph 14: Verification of model - acceleration, motor, model
Loaded electromagnetically

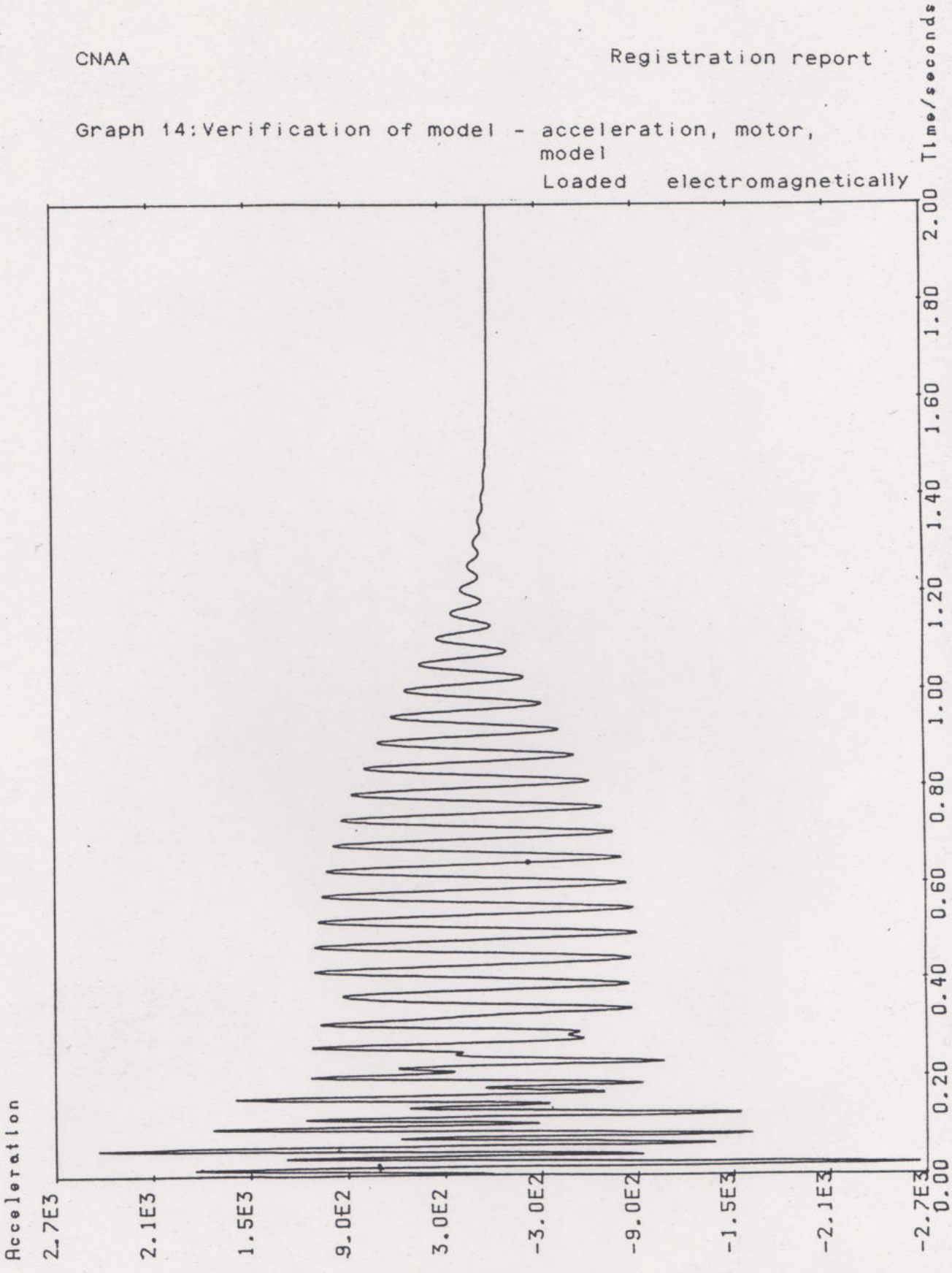

WATANABE INSTRUMENTS CORP

Graph 15:Verification of model - acceleration, motor, experiment

No load

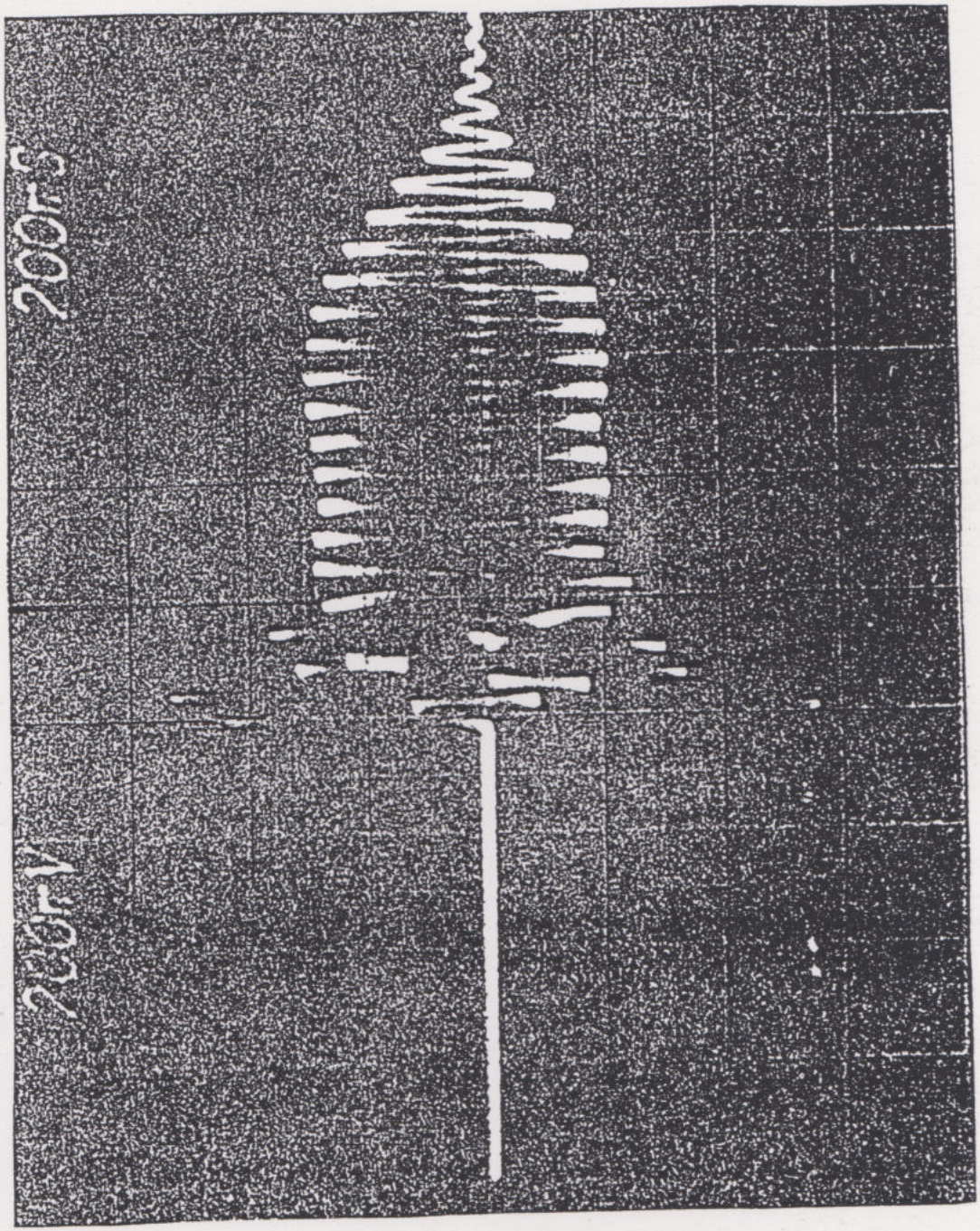

Scale: 950 radians^{-2}

Graph 15: Verification of model - acceleration, motor, experiment
Loaded electromagnetically

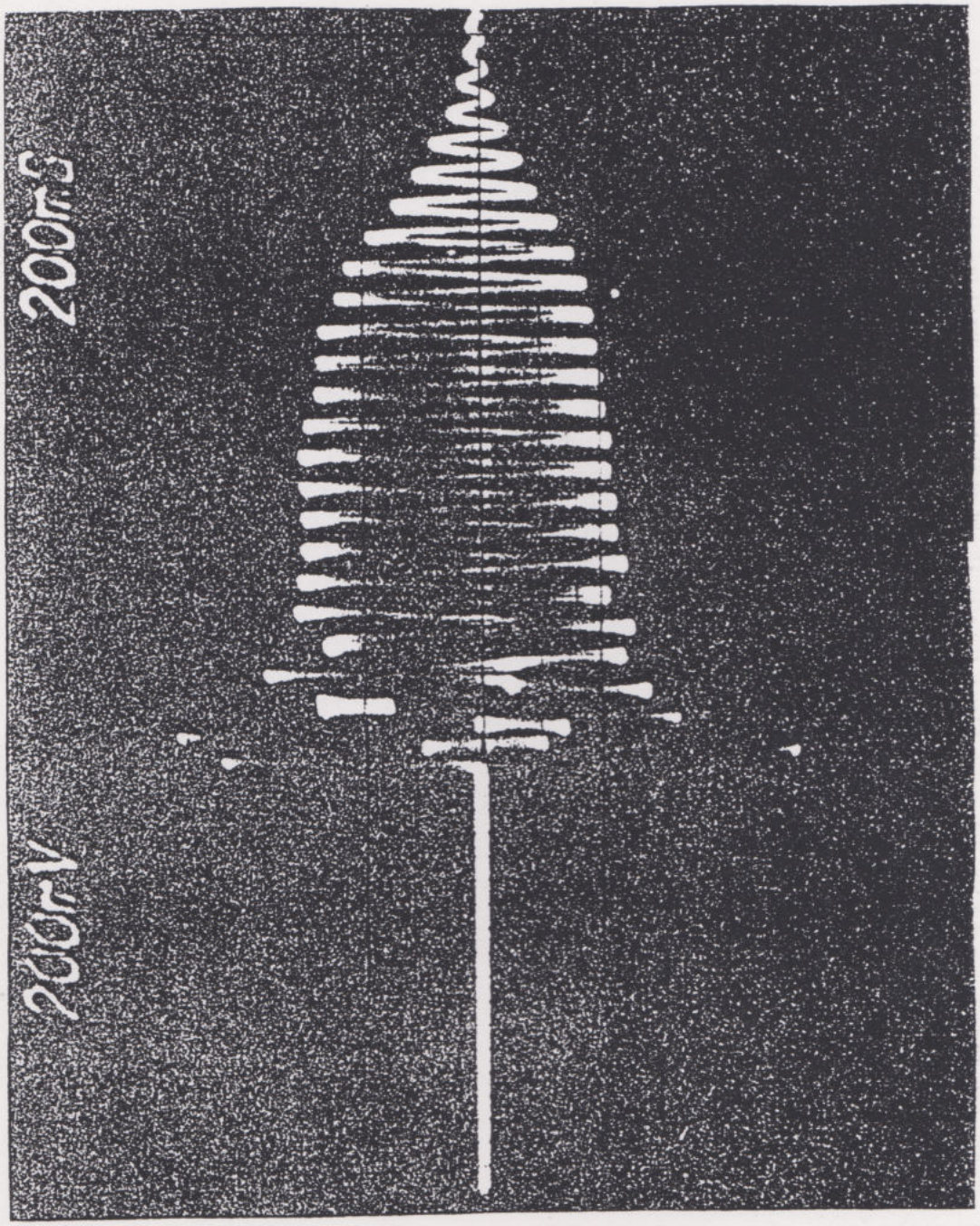

Scale: 950 radians^{-2}

Graph 16:Verification of model - velocity, motor, model

No load

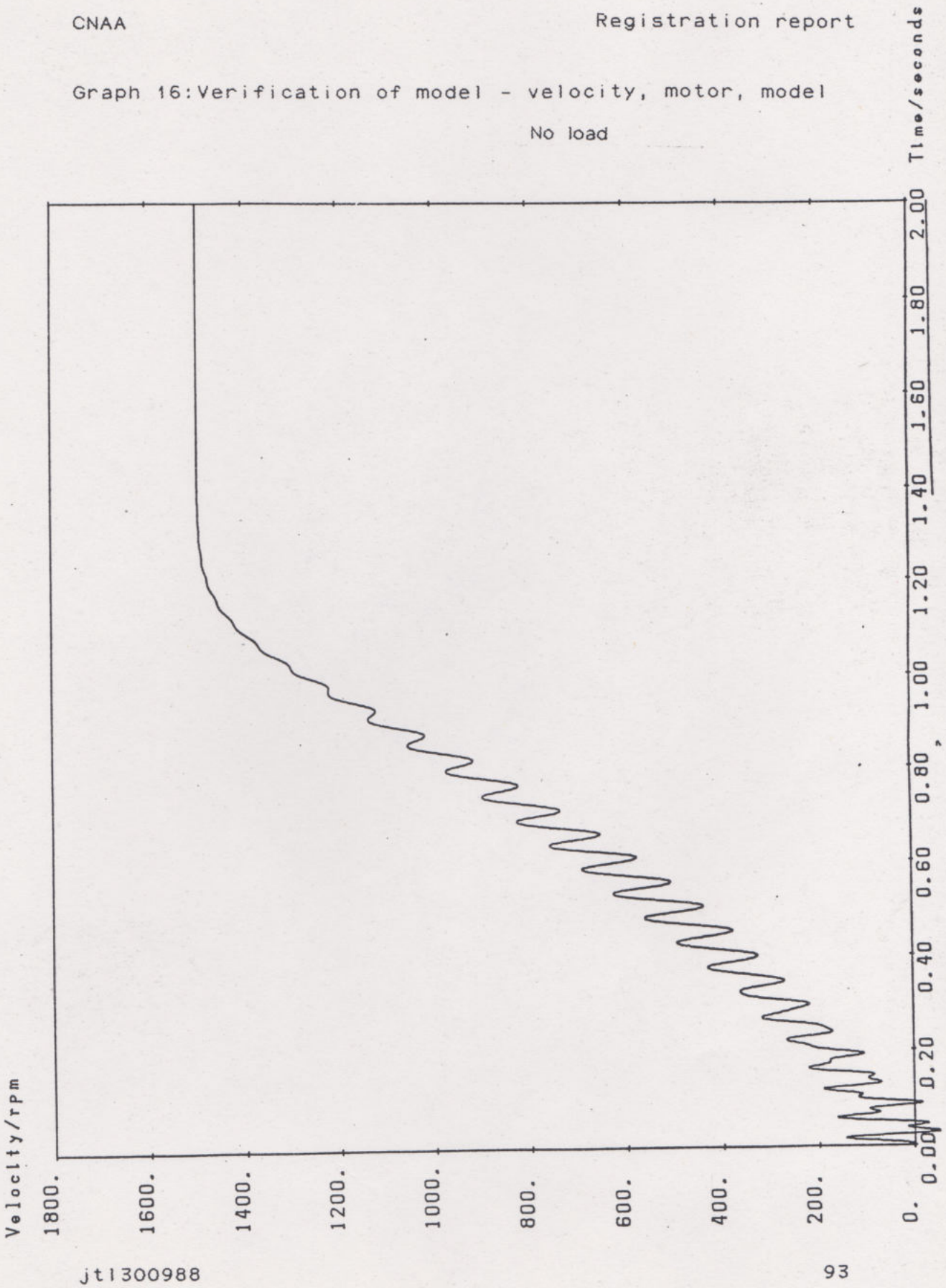

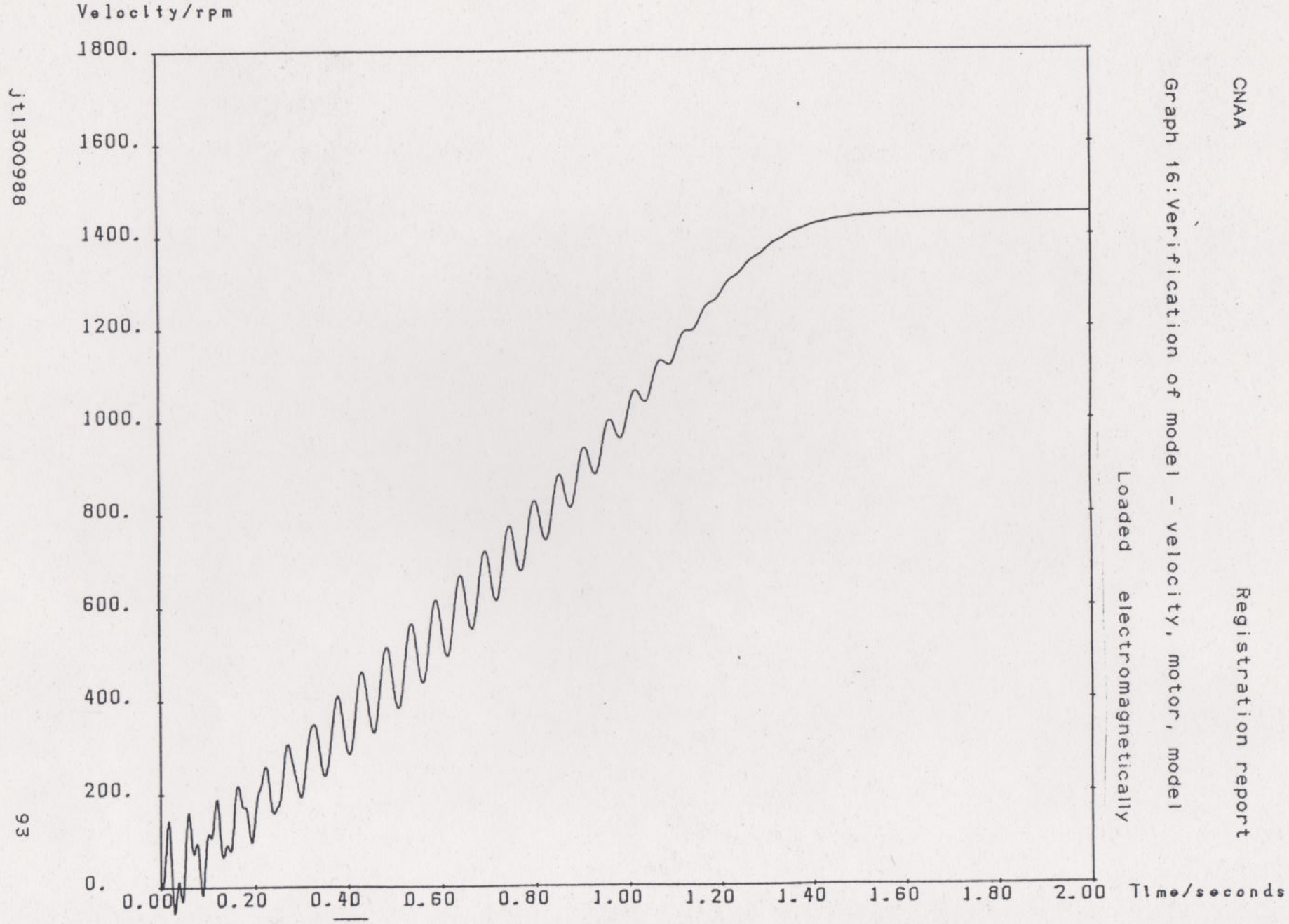

WATANABE INSTRUMENTS CORP.

Graph 17: Verification of model - velocity, motor, experiment

No load

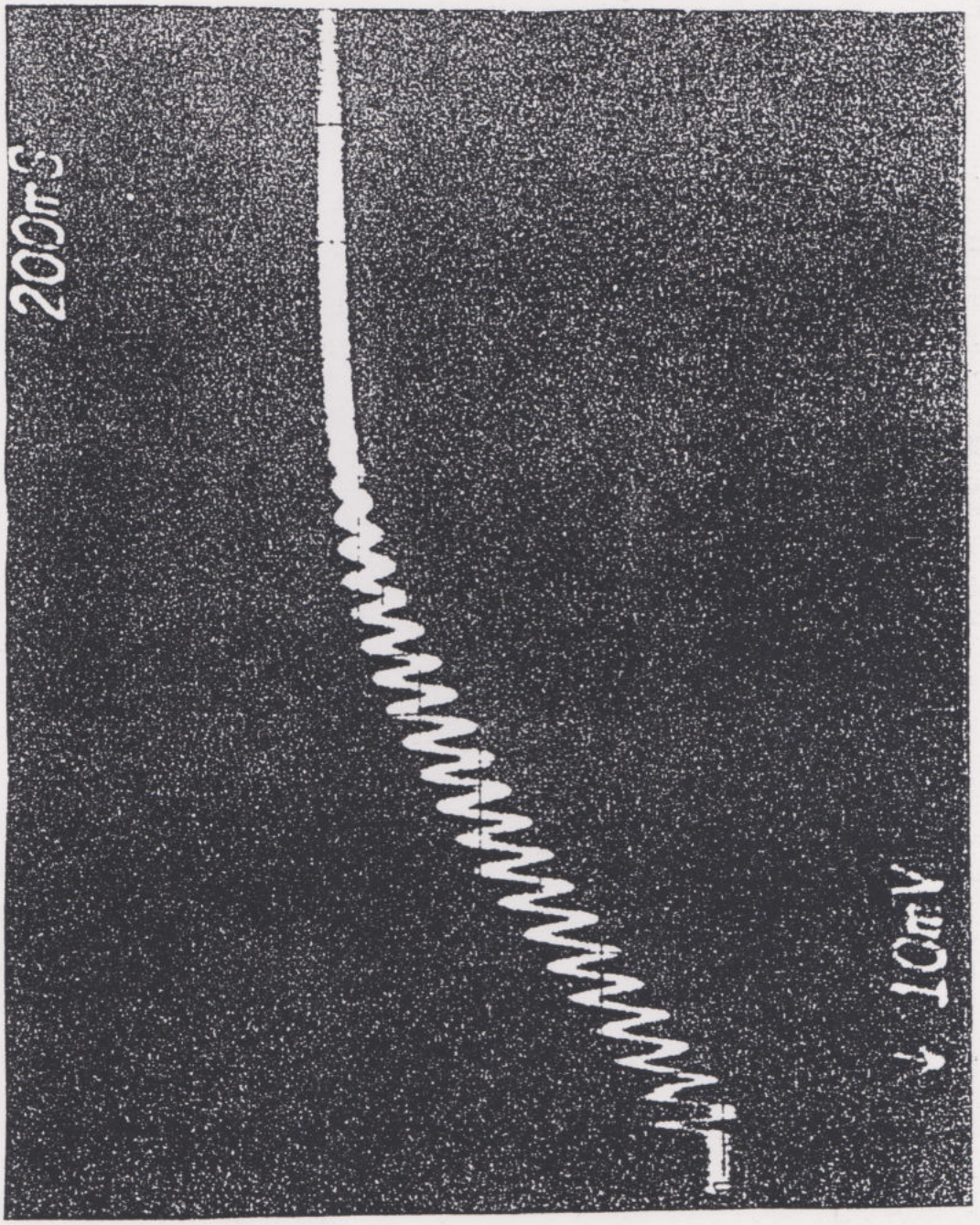

Scale: 462.5rpm per major division

Graph 17: Verification of model - velocity, motor, experiment

Loaded electromagnetically

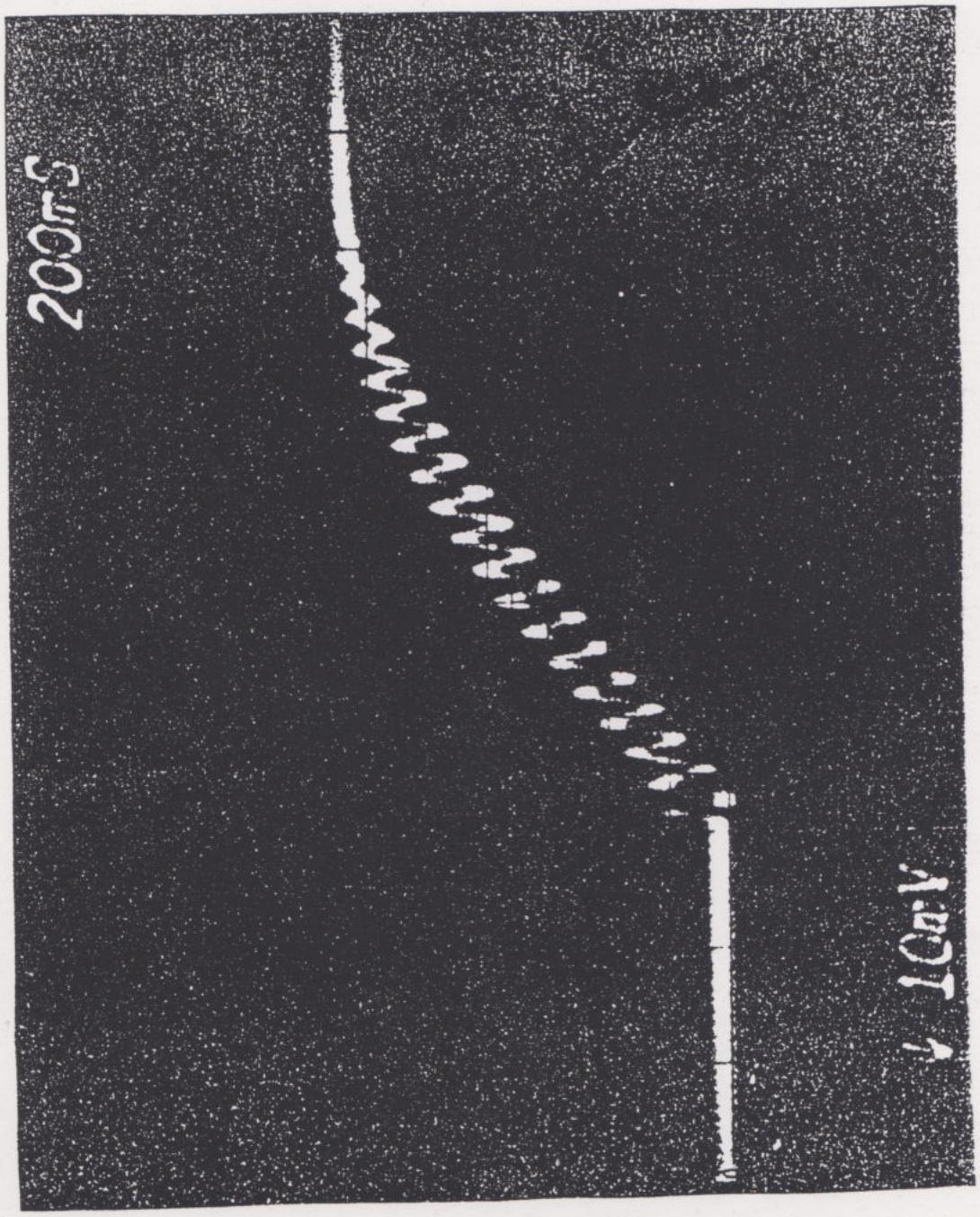

Scale: 462.5rpm per major division

Graph 18:Verification of model - current, motor, model

No load

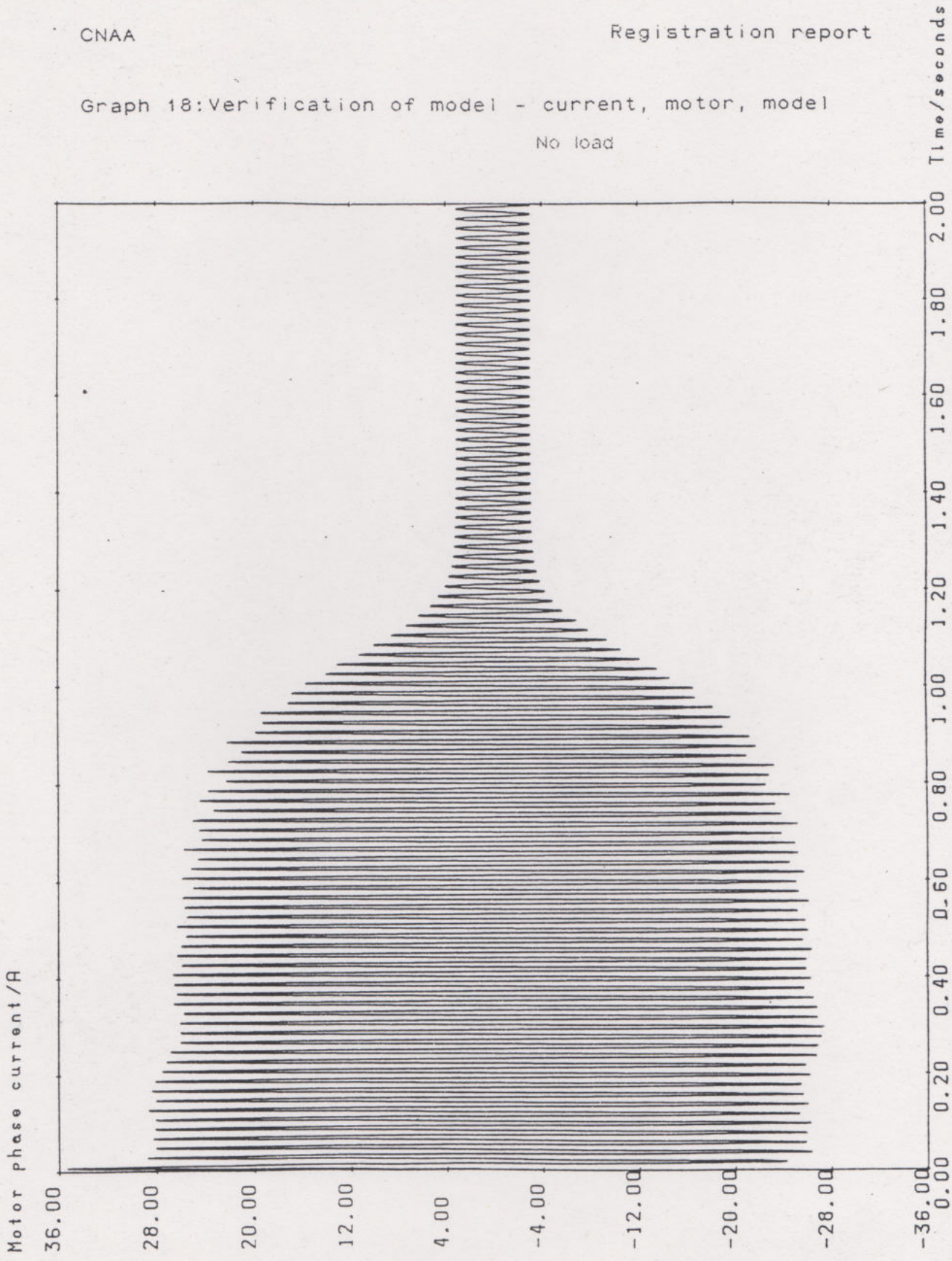

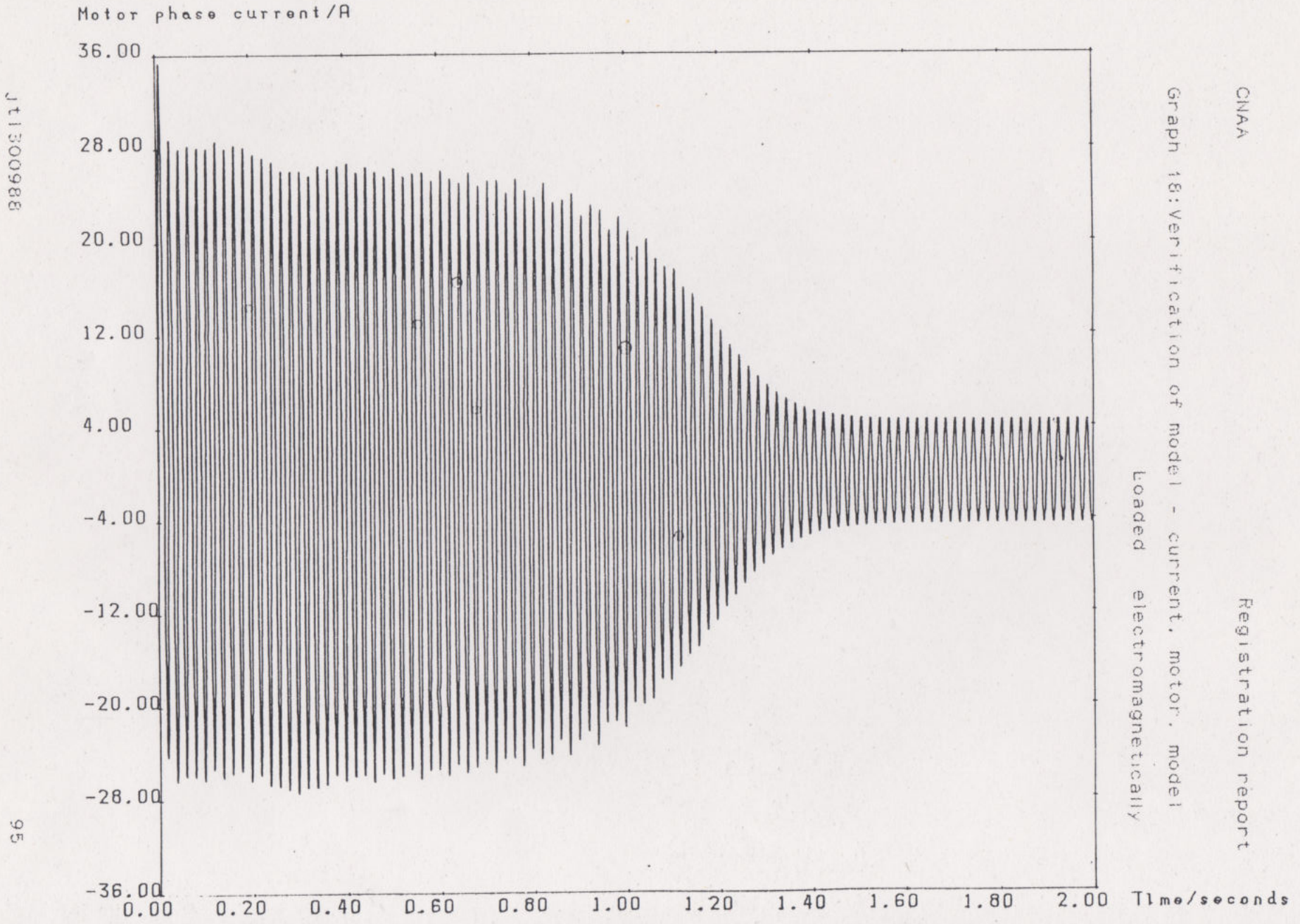

WATANABE INSTRUMENTS CORP.

Graph 19: Verification of model - current, motor, experiment

No load

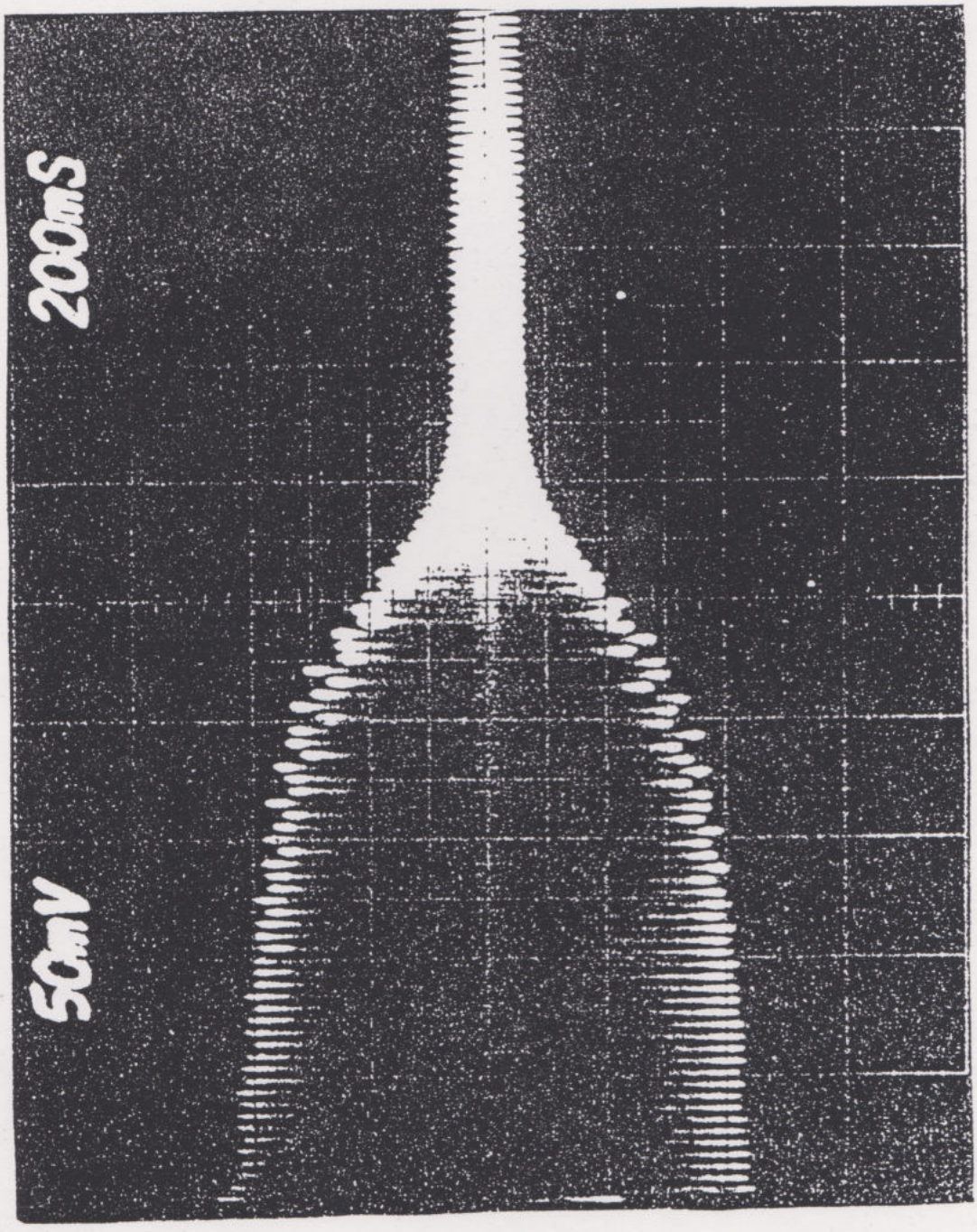

Scale: 10A per major division

Graph 19:Verification of model - current, motor, experiment

Loaded electromagnetically

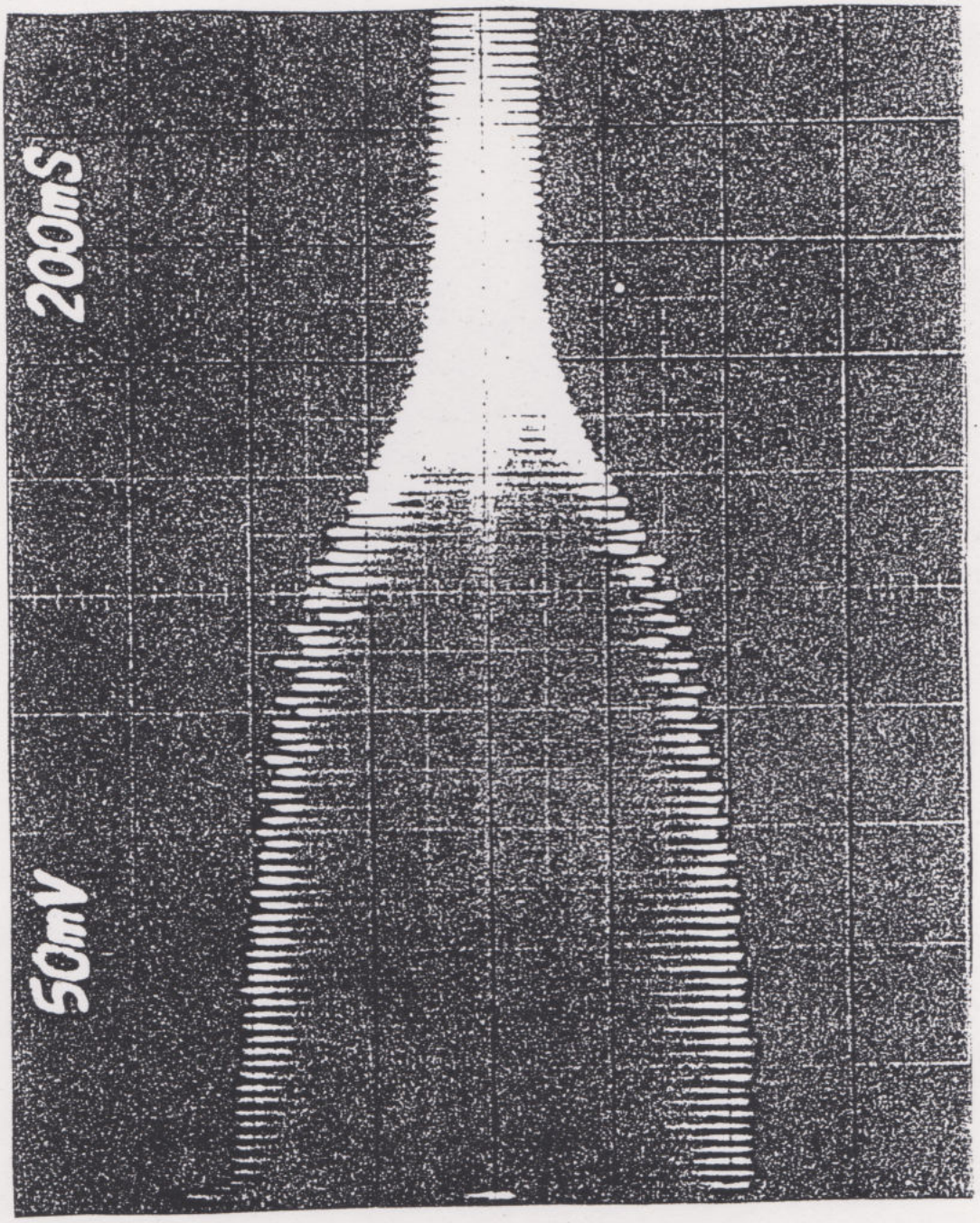

Scale: 10A per major division

Graph 20: Verification of model - current, generator, model

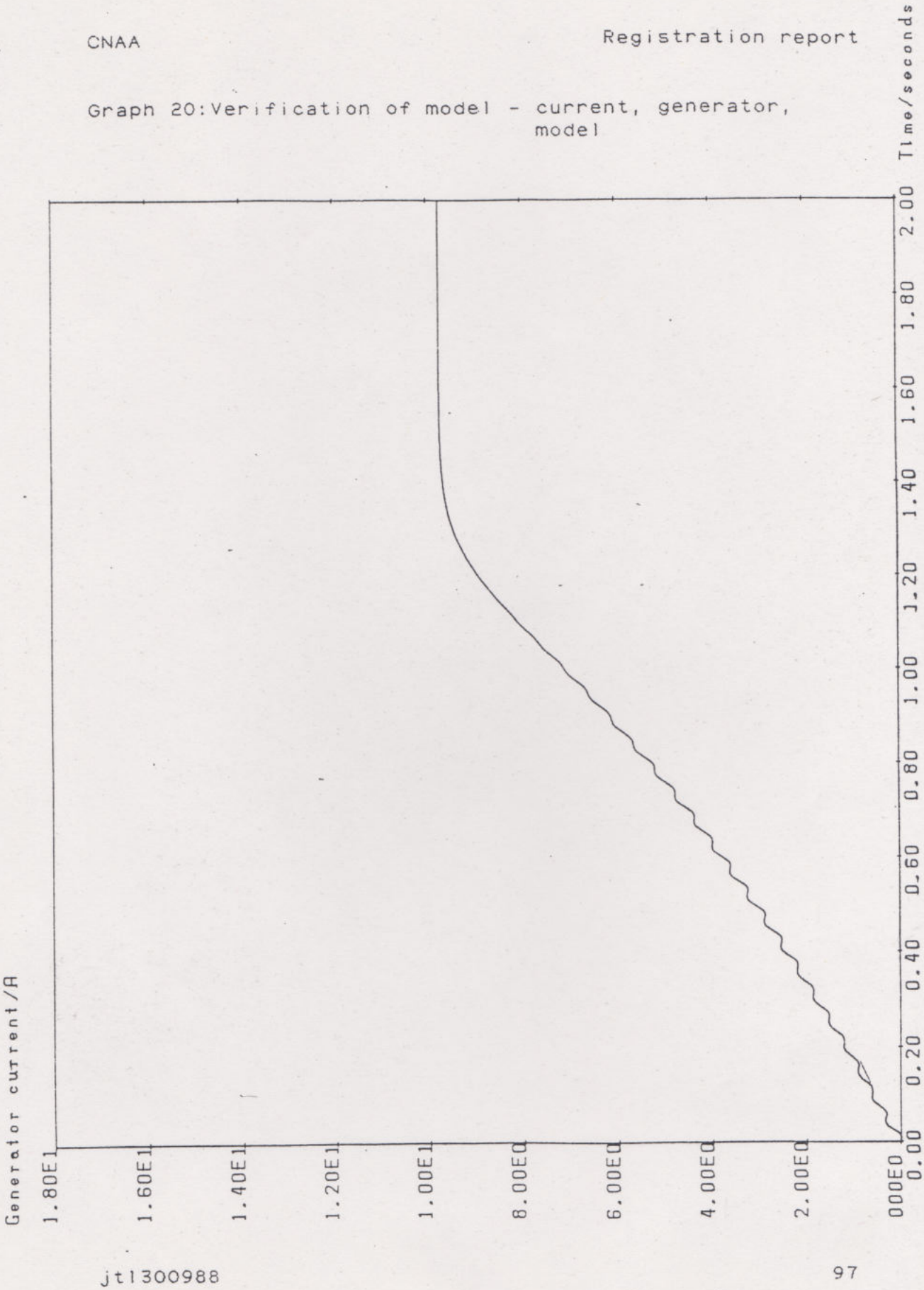

jt1300988

WATANABE INSTRUMENTS CORP.

Graph 21:Verification of model - current, generator, experiment

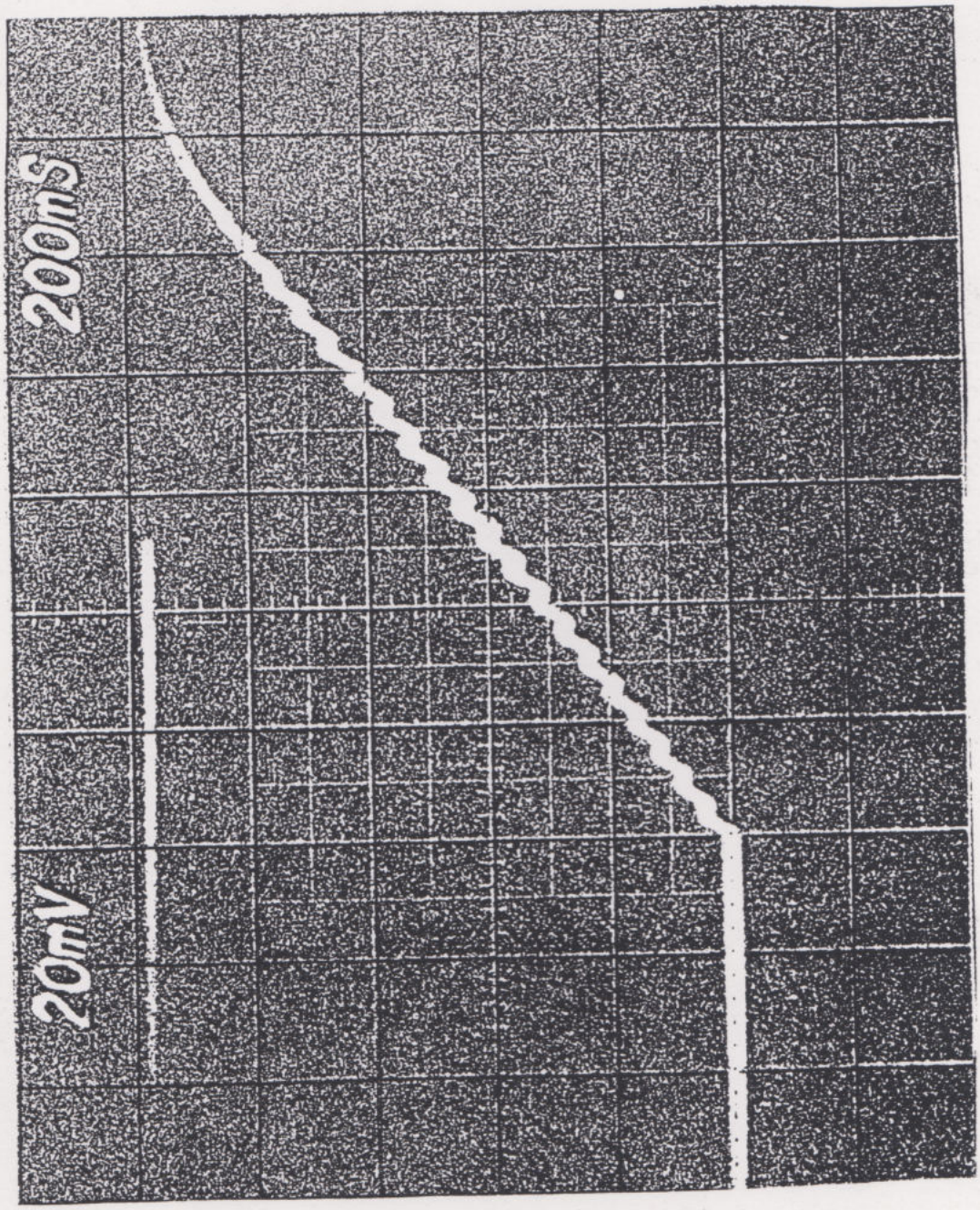

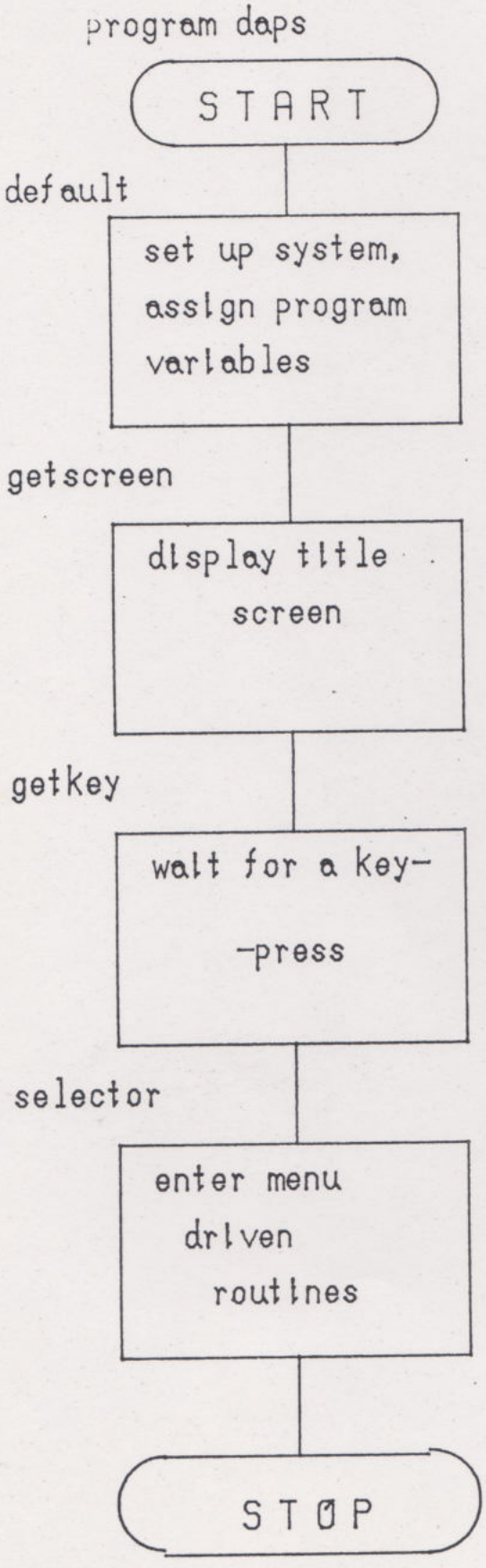
program daps
START
default
set up system,
assign program
variables
getscreen
display title
screen
getkey
wait for a key-
-press
selector
enter menu
driven
routines
STOP

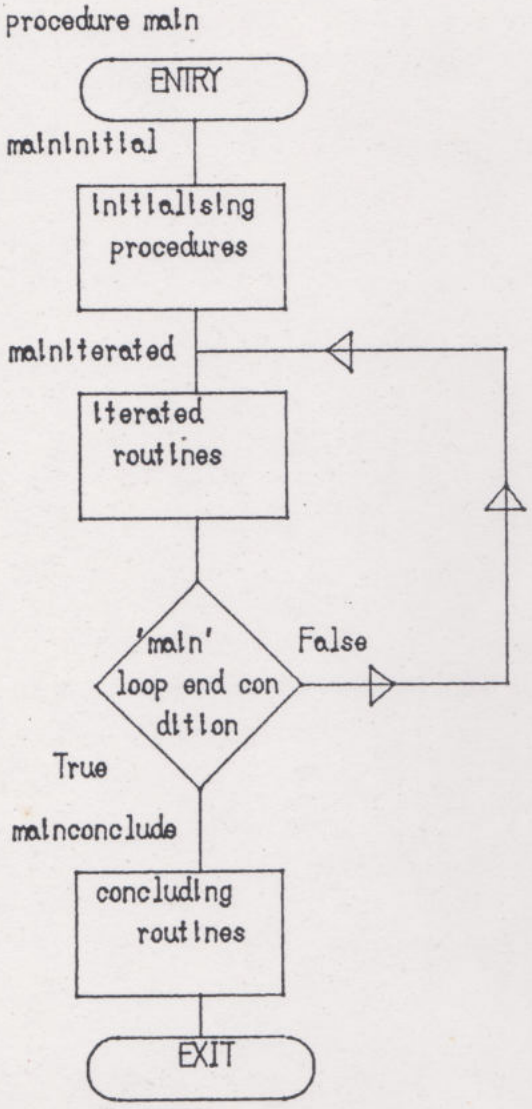
procedure main
ENTRY
mainInitial
Initialising procedures
mainIterated
Iterated routines
'main' loop end condition
False
True
mainconclude
concluding routines
EXIT

rocedure maininitial

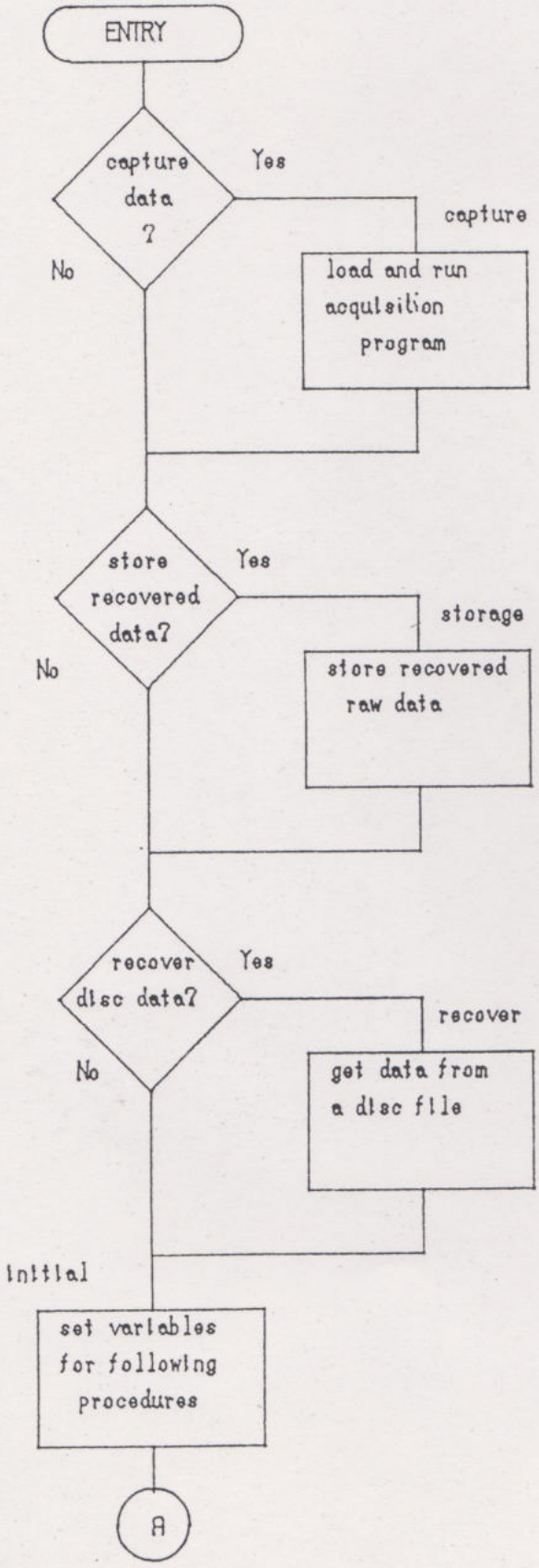

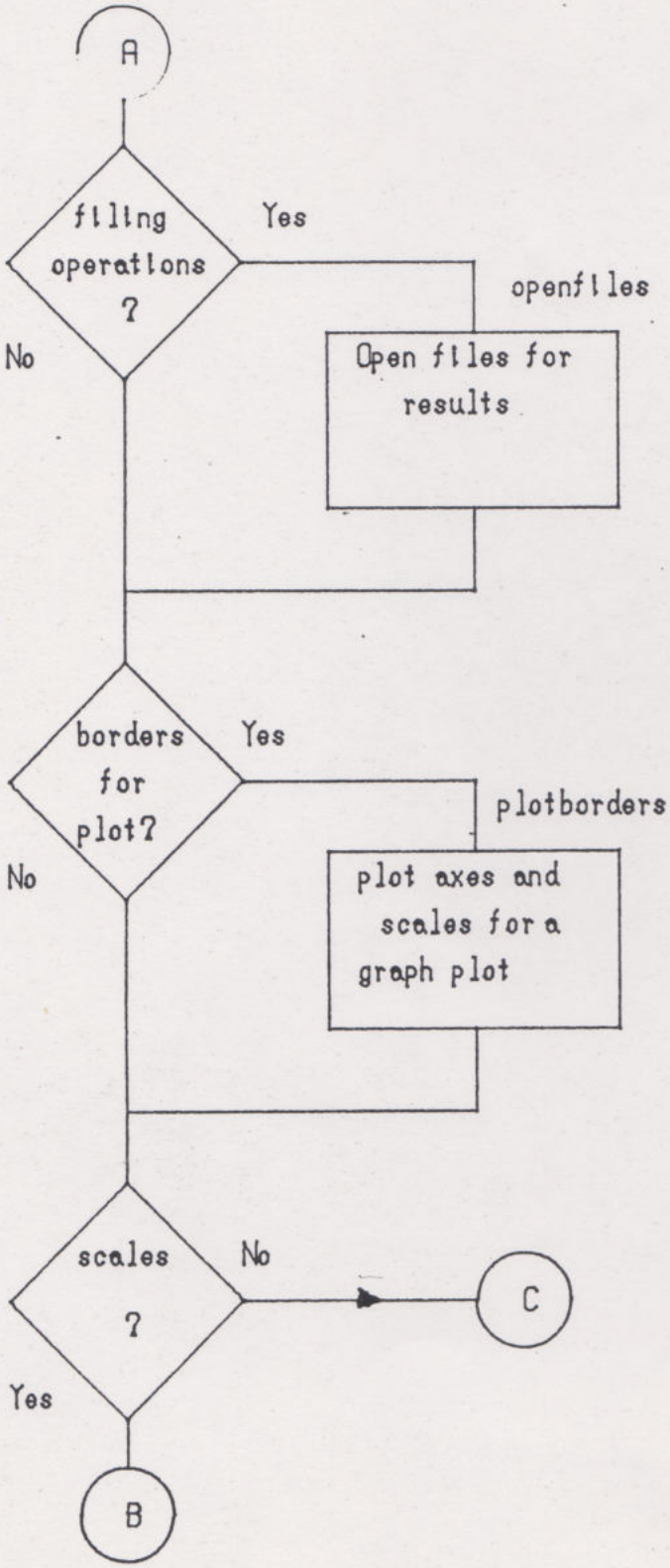
A
filing operations ?
Yes
openfiles
No
Open files for results
borders for plot?
Yes
plotborders
No
plot axes and scales for a graph plot
scales ?
No
C
Yes
B

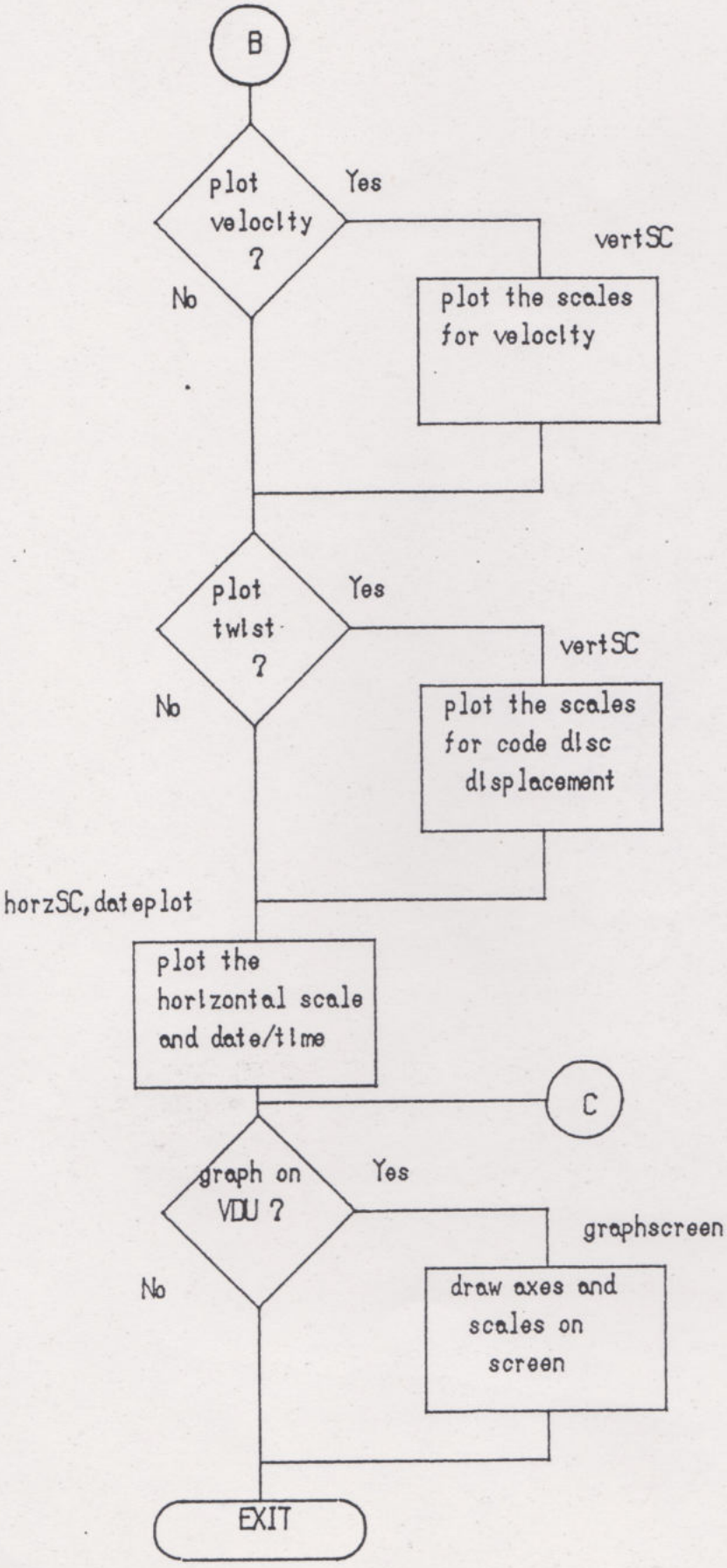
B
plot velocity ?
Yes
vertSC
No
plot the scales for velocity
plot twist ?
Yes
vertSC
No
plot the scales for code disc displacement
horzSC, dateplot
plot the horizontal scale and date/time
C
graph on VDU ?
Yes
graphscreen
No
draw axes and scales on screen
EXIT

procedure mainiterate

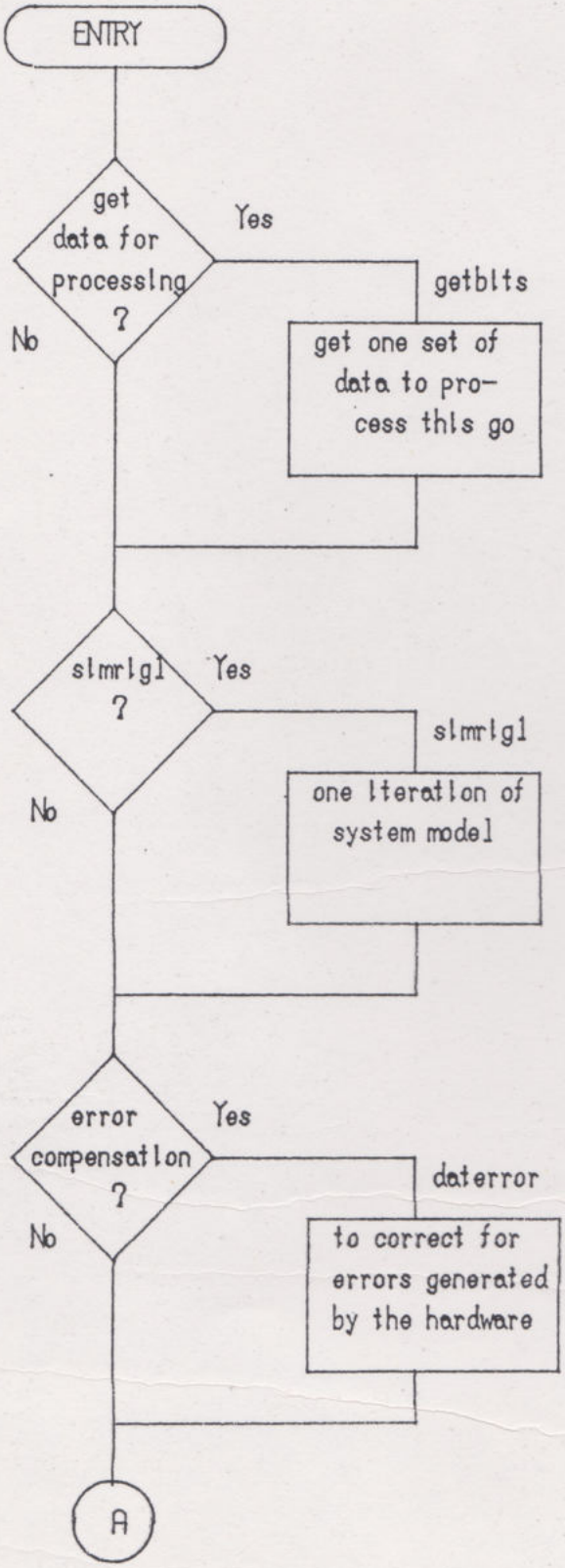

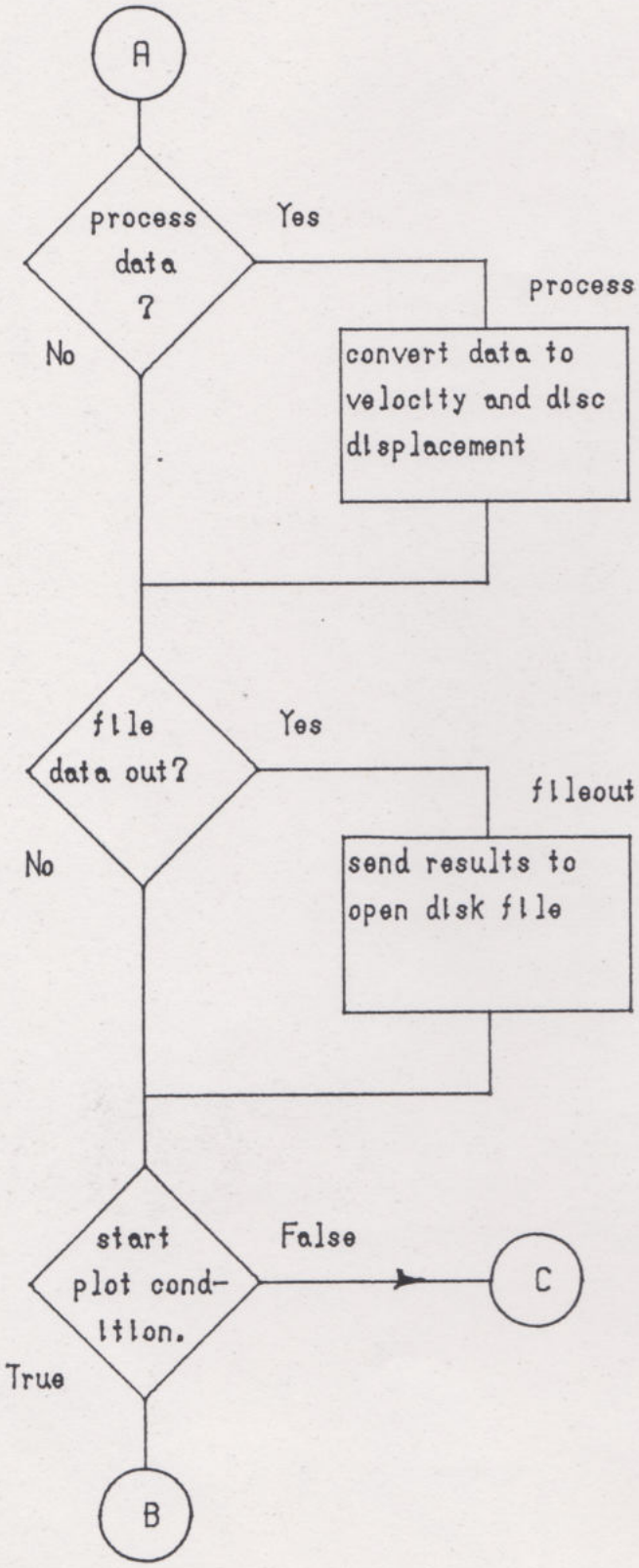
A
process data ?
Yes
process
convert data to velocity and disc displacement
No
file data out?
Yes
fileout
send results to open disk file
No
start plot condition.
False
C
True
B

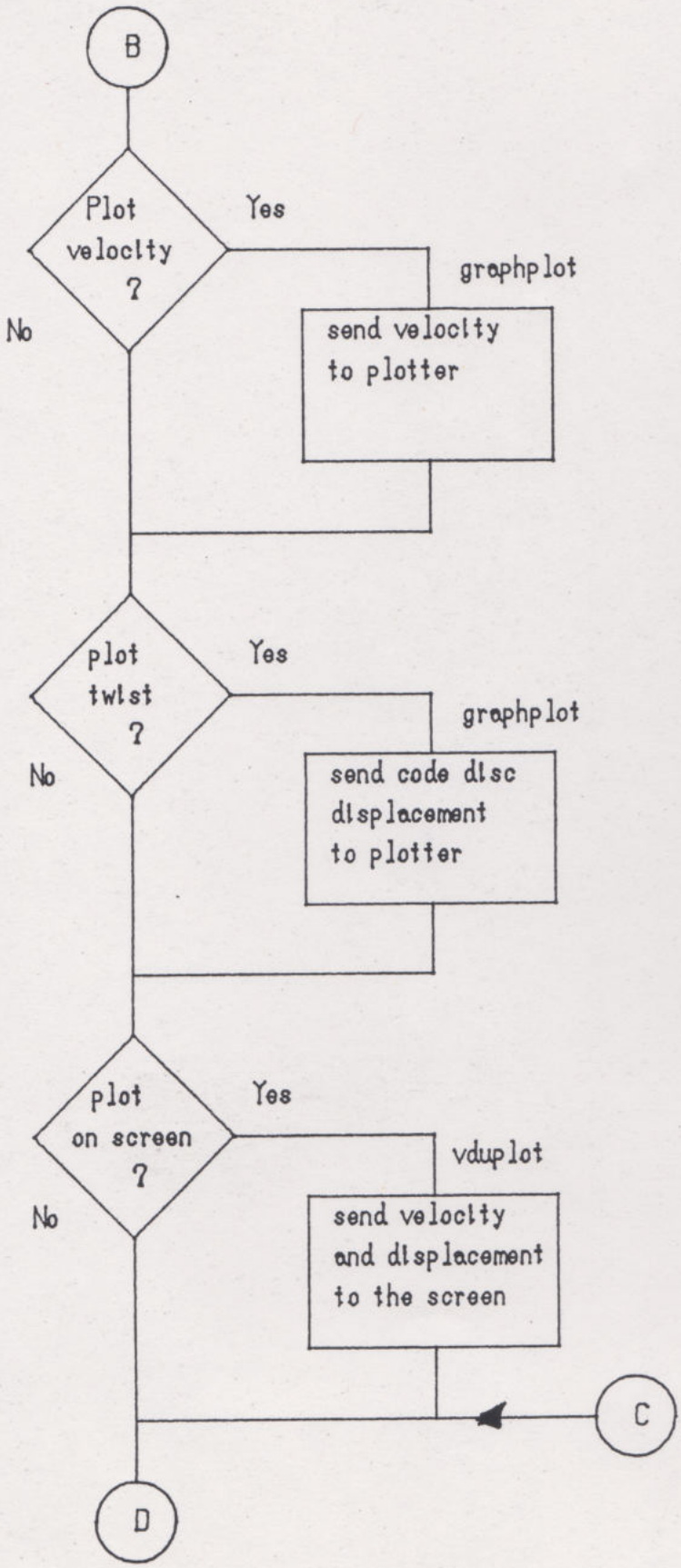
B
Plot velocity ?
Yes
graphplot
send velocity to plotter
No
plot twist ?
Yes
graphplot
send code disc displacement to plotter
No
plot on screen ?
Yes
vduplot
send velocity and displacement to the screen
No
C
D

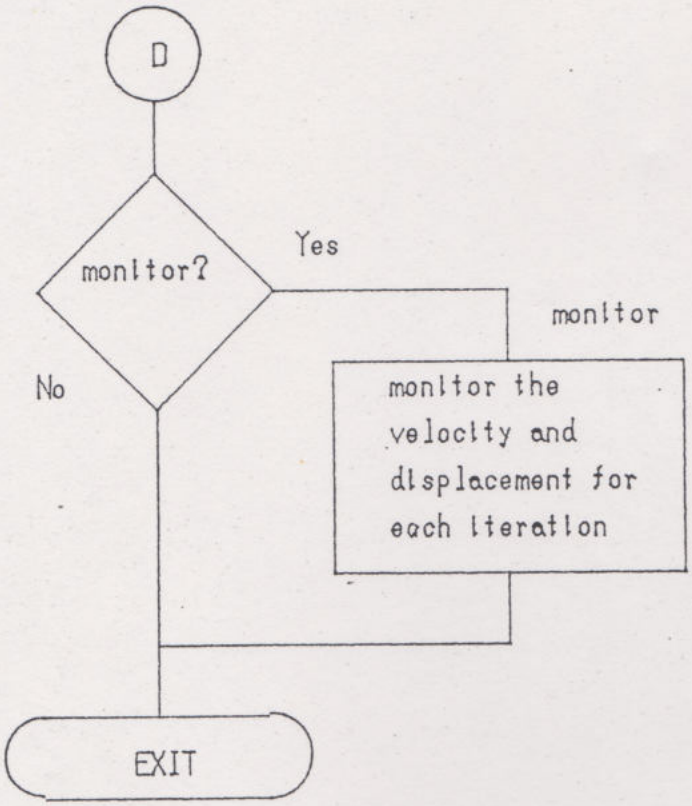
D
monitor?
Yes
monitor
No
monitor the
velocity and
displacement for
each iteration
EXIT

procedure mainconclude

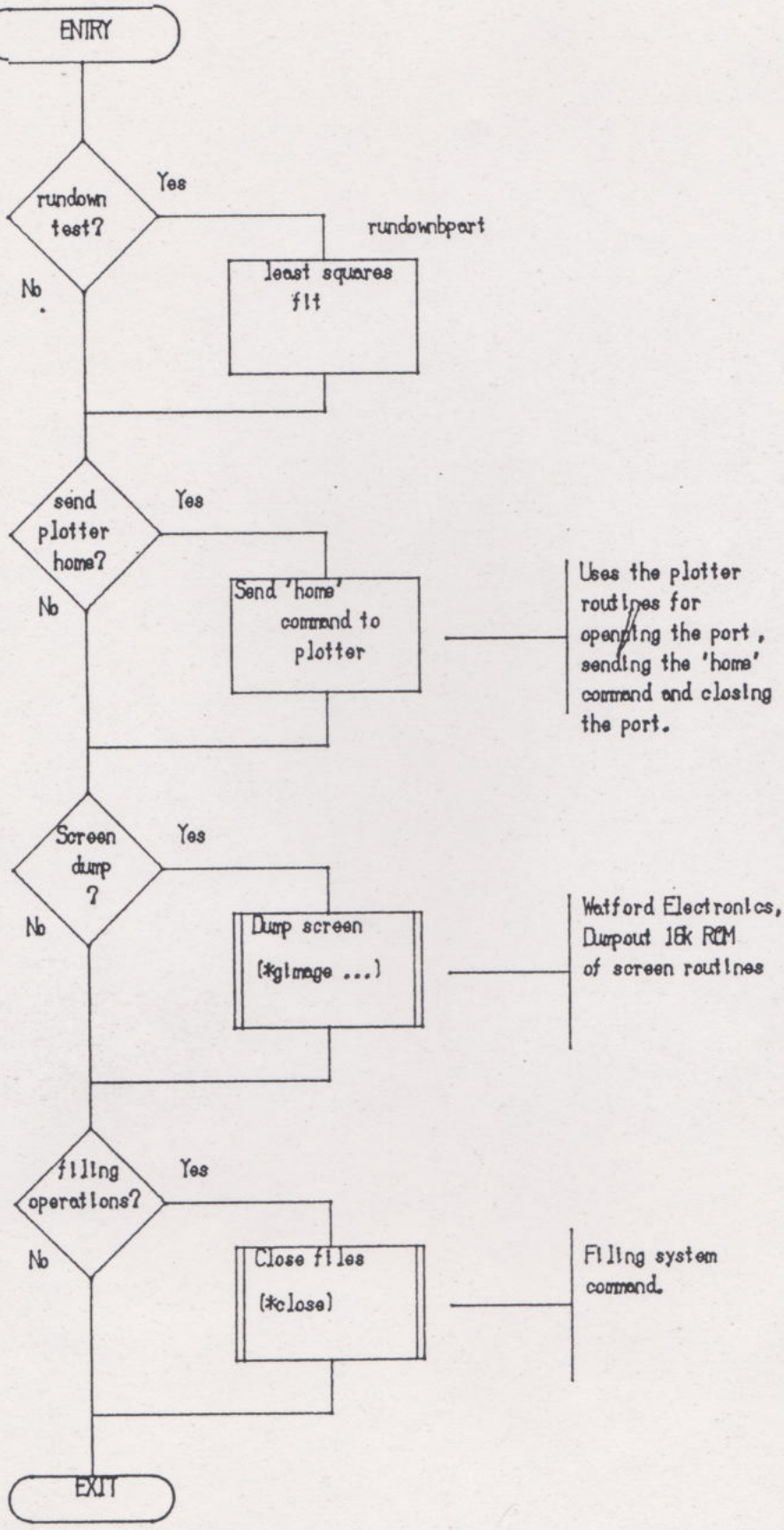

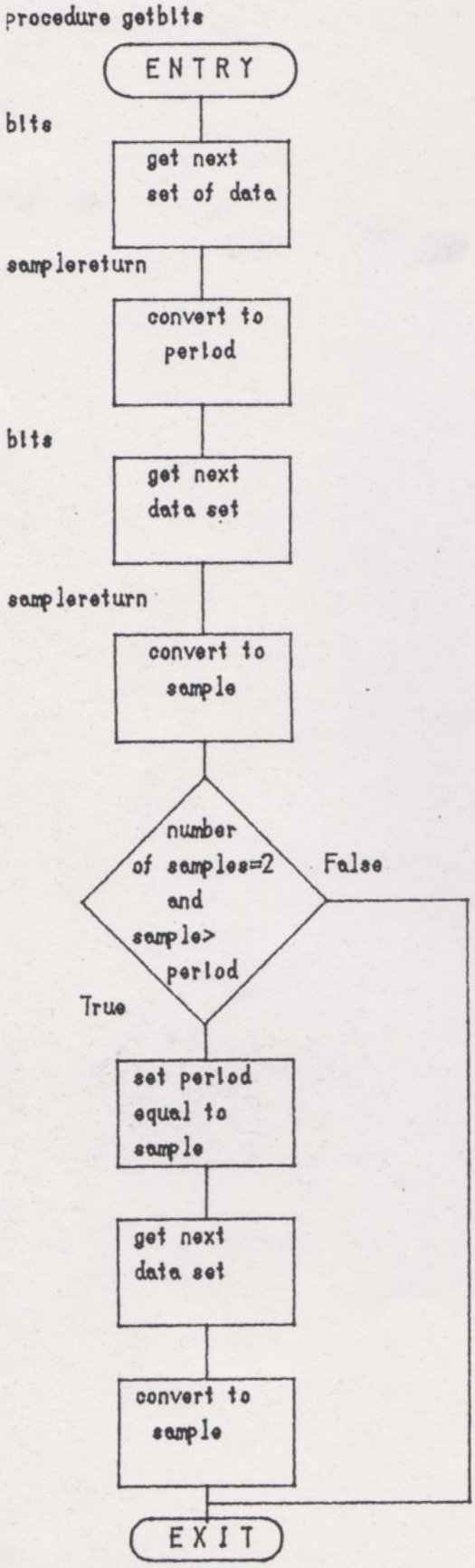
procedure getbits
ENTRY
bits
get next set of data
samplereturn
convert to period
bits
get next data set
samplereturn
convert to sample
number of samples=2 and sample> period
False
True
set period equal to sample
get next data set
convert to sample
EXIT